Evaluation of geo-physics methods to study the effects of land use on salinity in rice production systems in the Vietnam Mekong Delta

Dissertation to obtain the doctoral degree of Agricultural Sciences (Dr. sc. agr.)

Faculty of Agricultural Sciences

University of Hohenheim

Hans-Ruthenberg Institute for Tropical Agricultural Sciences

submitted by

Van Hong Nguyen

Ha Noi, Vietnam

2023

This thesis was accepted as a doctoral thesis (Dissertation) in fulfillment of the regulations to acquire the doctoral degree “Doktor der Agrarwissenschaften” by the Faculty of Agricultural Sciences at University of Hohenheim on December 14, 2023.

Date of the oral examination: December 14, 2023.

Examination Committee

Chairperson of the oral examination:	Prof. Dr. Uwe Ludewig
Supervisor and Reviewer:	Prof. Dr. Fokard Asch
Co-Reviewer:	Prof. Dr. Harro Stolpe
Additional examiner:	Prof. Dr. Thilo Streck

Acknowledgements

In order to get this far, I would like to thank the two most important men in my doctoral life, Prof. Dr. Folkard Asch and Dr. Jörn Germer. To my dear supervisor, Folkard Asch, I appreciate your patience and great support. You are the one who has inspired me the most and you have convinced me to believe in my abilities on the academic path. I would also like to express my deep gratitude to Jörn Germer, who has always supported me from the beginning stages of the fieldwork to the writing phase. Working alongside both of you has been an absolute pleasure, and I am grateful for the wonderful experiences we have had together.

This endeavor would not have been possible without the sponsoring from the Federal Ministry of Education and Research (Germany) and helping from our partners in Vietnam, Kien Giang University and An Giang University. My special thanks go to Dr. Duong Van Nha for his great assistance during my fieldwork in the Mekong Delta.

Many thanks to all my colleagues and friends, even though I cannot list them all here. You cheered me up when I was down, helped me stay mentally and physically healthy, and kept me in a positive mood by talking, exercising and hiking together. I have had many unforgettable moments with all of you in Hohenheim.

And I want to save my last words to express my love for my beloved family. Without their support, I could not follow my dream. Above all, I would like to thank Minh for his love and constant support. *Cảm ơn con trai nhỏ của mẹ, con thật mạnh mẽ khi không có mẹ bên cạnh. Con là động lực để mẹ có thể hoàn thành tốt công việc để sớm được về với con. Cảm ơn ông và bà của Tí luôn bên cạnh dạy dỗ Tí thật tốt. Cảm ơn các bác, Ngọc, Huyền, Mít, Xoài đã chăm sóc và chơi với Tí trong thời gian qua.*

Table of Contents

List of Abbreviations

Alternative Wetting and Drying Irrigation ..... AWD

Electrical Resistivity Tomography ..... ERT

Electromagnetic Induction ..... EMI

Gross Domestic Product ..... GDP

Ground Range Detected ..... GRD

Total Dissolved Salts ..... TDS

Universal Transverse Mercator ..... UTM

Vietnam Mekong Delta ..... VMD

Summary

In the Vietnam Mekong Delta (VMD), salinity is a major concern for rice production, which is highly susceptible to saltwater intrusion due to its proximity to the sea and tidal influences. Climate change induced sea level rise, reduced upstream freshwater flows and land subsidence are exacerbating the problem. As a result, saltwater intrudes into the rivers, canals and aquifers of the VMD, reducing the availability of freshwater for irrigation and agricultural use. As the world's largest rice exporter, the impacts of salinity on rice production in the VMD is significant and poses a serious threat to food security. Addressing the impact of salinity on rice production in the VMD requires a comprehensive approach to assess salinity from the topsoil to the subsoil layers. Therefore, this study was conducted to evaluate salinity issues in rice production systems and figure out the link between rice production systems in the VMD and salinity by applying geophysical methods. Geophysical methods were used in this study including Electromagnetic Induction (EMI) and Electrical Resistivity Tomography (ERT). EMI measures electrical conductivity, while ERT measures electrical resistivity, which is the inverse of conductivity and is closely related to soil salinity. ERT was employed to assess salinity of the subsurface to a depth of 40 m, while EMI was used to detect topsoil salinity up to 1.5 m depth. The case study, Tra Vinh province, in the VMD was chosen for the soil salinity investigation. Soil salinity measurement was conducted during dry season in different land-use types related to rice production systems in the VMD. The field measurements were carried out in two consecutive dry seasons, the dry season of 2019-2020 and dry season of 2020-2021. The first measurement was carried out at five case study sites with different cropping patterns to validate the ERT data and to compare the two methods to determine the best method for investigating soil salinity. Five boreholes were drilled to a depth of 40 m to validate the ERT measurement for subsurface salinity. In the following dry season, ERT and EMI were measured in the extensive survey, with the measurement sites selected along four typical geological transects in the Tra Vinh province.

With a desire to use ERT alone to assess soil salinity, ERT data was then used to predict topsoil salinity along with EMI measurement. However, the results from ERT measurement seems to underestimated topsoil salinity due to the lack of measurement on the fields

compared to the EMI. The conductivity data collected from different land use types, showed that double rice crop fields are the most prone to salinity than other cropping patterns such as, triple rice, triple/double rice, and single rice. In general, however, topsoil salinity is not a critical issue in the study area compared to potential salinity from the near surface water table, which varies from a relatively shallow depths, from 2 m to 5 m depth, identified by ERT using a resistivity of less than 3 Ωm as the threshold for saline water. The saline water table is the Tra Vinh province increase with the proximity to the sea. As analyzing from resistivity maps, saltwater intrudes the subsurface groundwater from two directions: rivers along the province, and from the sea. Therefore, the double rice, single rice fields and small area of triple rice fields distributed along the two main rivers in the Tra Vinh province are highly affected by saline subsurface water. From the results we see that salinity affect land use in rice production system, and not another way round. Furthermore, we would like to prove for the first time the capability of ERT and EMI in evaluating soil salinity in the rice cultivation fields in the VMD. In addition, we suggested the powerful methods to capture and monitor saltwater intrusion into the rice fields from top to subsurface, which is necessary to improve and protect rice production.

Zusammenfassung

Im vietnamesischen Mekong-Delta (VMD) ist der Salzgehalt ein großes Problem für den Reisanbau, der aufgrund der Nähe zum Meer und der Gezeiteneinflüsse sehr anfällig für das Eindringen von Salzwasser ist. Der durch den Klimawandel bedingte Anstieg des Meeresspiegels, die Verringerung des Süßwasserzuflusses und die Landabsenkung verschärfen das Problem. Infolgedessen dringt Salzwasser in die Flüsse, Kanäle und Grundwasserleiter des VMD ein, wodurch die Verfügbarkeit von Süßwasser für die Bewässerung und die landwirtschaftliche Nutzung verringert wird. Als weltweit größter Reisexporteur sind die Auswirkungen der Salinität auf die Reisproduktion im VMD erheblich und stellen eine ernsthafte Bedrohung für die Ernährungssicherheit dar. Um die Auswirkungen von Salinität auf die Reisproduktion im VMD in den Griff zu bekommen, ist ein umfassender Ansatz zur Bewertung der Salzbelastung vom Oberboden bis zu den Unterbodenschichten erforderlich. Die vorliegende Studie wurde durchgeführt, um die Salzbelastung in Reisanbausystemen zu bewerten und den Zusammenhang zwischen Reisanbausystemen im VMD und Salinität mit Hilfe geophysikalischer Methoden herauszufinden. In dieser Studie wurden geophysikalische Methoden eingesetzt, darunter die elektromagnetische Induktion (EMI) und die elektrische Widerstandstomographie (ERT). EMI misst die elektrische Leitfähigkeit, während ERT den elektrischen Widerstand misst, der den Kehrwert der Leitfähigkeit darstellt und eng mit dem Salzgehalt des Bodens verbunden ist. ERT wurde eingesetzt, um den Salzgehalt des Untergrunds bis zu einer Tiefe von 40 m zu ermitteln, während EMI zur Feststellung der Salzbelastung des Oberbodens bis zu einer Tiefe von 1,5 m verwendet wurde. Als Fallstudie wurde die Provinz Tra Vinh im VMD für die Untersuchung des Salzgehalts im Boden ausgewählt. Die Messung des Bodensalzgehalts wurde während der Trockenzeit in verschiedenen Landnutzungsarten im Zusammenhang mit Reisanbausystemen in der VMD durchgeführt. Die Feldmessungen wurden in zwei aufeinanderfolgenden Trockenzeiten durchgeführt, in der Trockenzeit 2019-2020 und in der Trockenzeit 2020-2021. Die erste Messung wurde an fünf Fallstudienstandorten mit unterschiedlichen Anbaumustern durchgeführt, um die ERT-Daten zu validieren und die beiden Methoden zu vergleichen, um die beste Methode zur Untersuchung des Bodensalzgehalts zu ermitteln. Zur Validierung der ERT-Messung des unterirdischen Salzgehalts wurden fünf Bohrungen bis zu einer Tiefe von 40 m durchgeführt.

In der darauffolgenden Trockenzeit wurden ERT und EMI im Rahmen einer umfassenden Erhebung eingesetzt, wobei die Messstellen entlang von vier typischen geologischen Transekten in der Provinz Tra Vinh ausgewählt wurden.

In dem Bestreben, die Salzbelastung des Bodens allein mit dem ERT zu bewerten, wurden die ERT-Daten zusammen mit der EMI-Messung zur Vorhersage des Salzgehalts des Oberbodens verwendet. Die Ergebnisse der ERT-Messung scheinen jedoch den Salzgehalt des Oberbodens zu unterschätzen, da im Vergleich zum EMI keine Messungen auf den Feldern vorgenommen wurden. Die Leitfähigkeitsdaten, die von verschiedenen Bodennutzungsarten gesammelt wurden, zeigten, dass Felder mit Doppelreisanbau stärker zur Versalzung neigen als andere Anbaumuster wie Dreifachreis, Dreifach-/Doppelreis und Einfachreis. Im Allgemeinen ist die Versalzung des Oberbodens im Untersuchungsgebiet jedoch kein kritisches Problem, verglichen mit der potenziellen Versalzung durch den oberflächennahen Grundwasserspiegel, der in einer relativ geringen Tiefe von 2 bis 5 m liegt und vom ERT mit einem spezifischen Widerstand von weniger als 3 Ωm als Schwellenwert für salzhaltiges Wasser ermittelt wurde. Der Salzwasserspiegel in der Provinz Tra Vinh nimmt mit der Nähe zum Meer zu. Wie aus den Widerstandskarten hervorgeht, dringt Salzwasser aus zwei Richtungen in das unterirdische Grundwasser ein: aus den Flüssen der Provinz und aus dem Meer. Daher sind die Doppelreisfelder, die Einzelreisfelder und ein kleiner Bereich von Dreifachreisfeldern, die entlang der beiden Hauptflüsse in der Provinz Tra Vinh verteilt sind, stark vom salzhaltigen Grundwasser betroffen. Aus den Ergebnissen geht hervor, dass der Salzgehalt die Landnutzung im Reisanbausystem beeinflusst und nicht umgekehrt. Darüber hinaus konnten wir zum ersten Mal die Nutzbarkeit von ERT und EMI bei der Bewertung des Bodensalzgehalts in den Reisanbaugebieten im VMD nachweisen. Darüber hinaus haben wir leistungsfähige Methoden zur Erfassung und Überwachung des Eindringens von Salzwasser in die Reisfelder von oben bis zum Untergrund vorgeschlagen, die zur Verbesserung und zum Schutz der Reisproduktion notwendig sind.

Hydrogeology structure of Vietnam Mekong Delta

The following figure shows large scale of the hydrogeological structure of the Vietnam Mekong Delta. It supports the statements made in this thesis, which is mainly concerned with the shallow aquifers (Holocene).

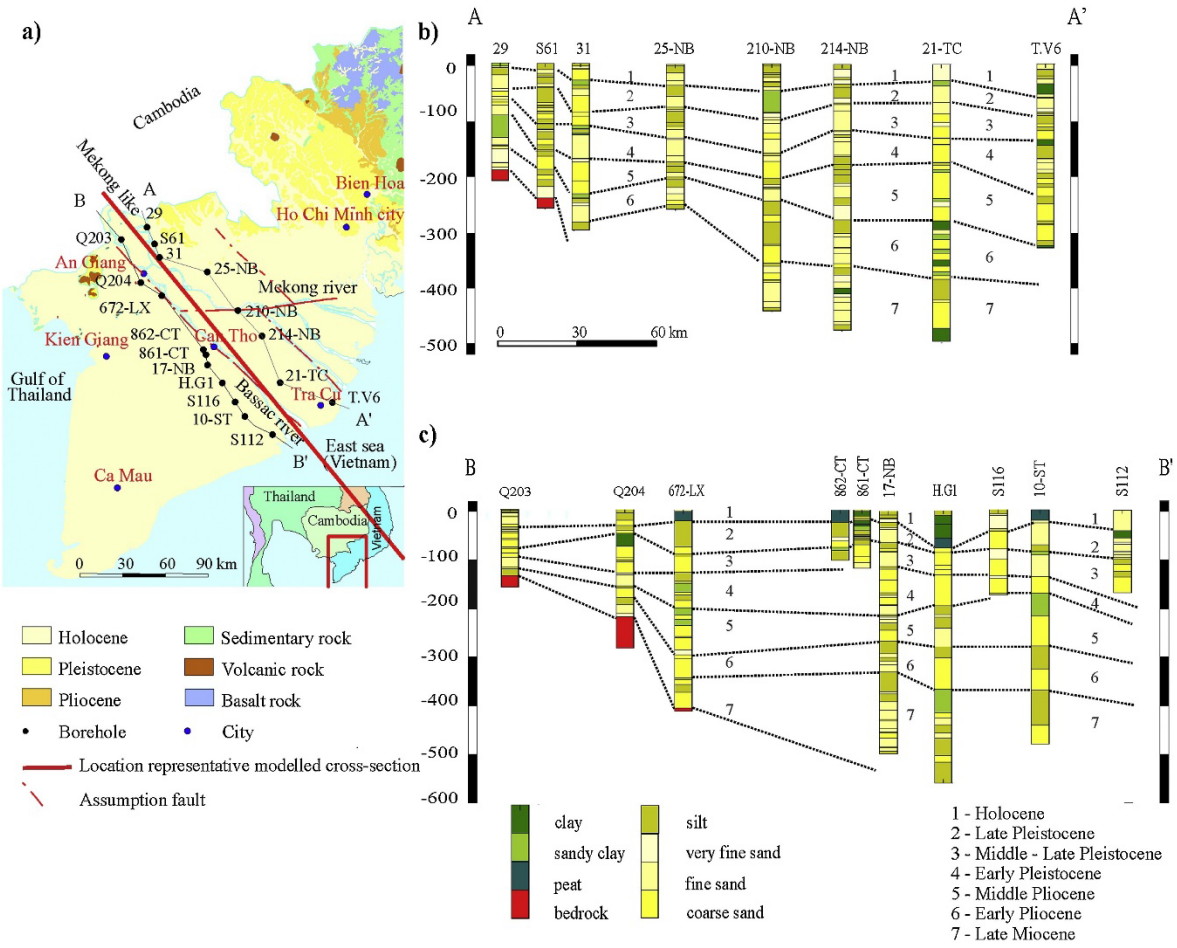

Source: Pham, H.V., Geer, F.C.V., Tran, V.B., Dubelaar, W., Essink, G.H.P.O. (2019). Paleo-hydrogeological reconstruction of the fresh-saline groundwater distribution in the Vietnamese Mekong Delta since the late Pleistocene. *Journal of Hydrology: Regional Studies* 23, 100594. https://doi.org/10.1016/j.ejrh.2019.100594

Geoelectrical values of sediments

The figure below gives an overview of electrical resistivity and conductivity for typical sediments and rocks to help understanding of the range of resistivity results presented in the thesis.

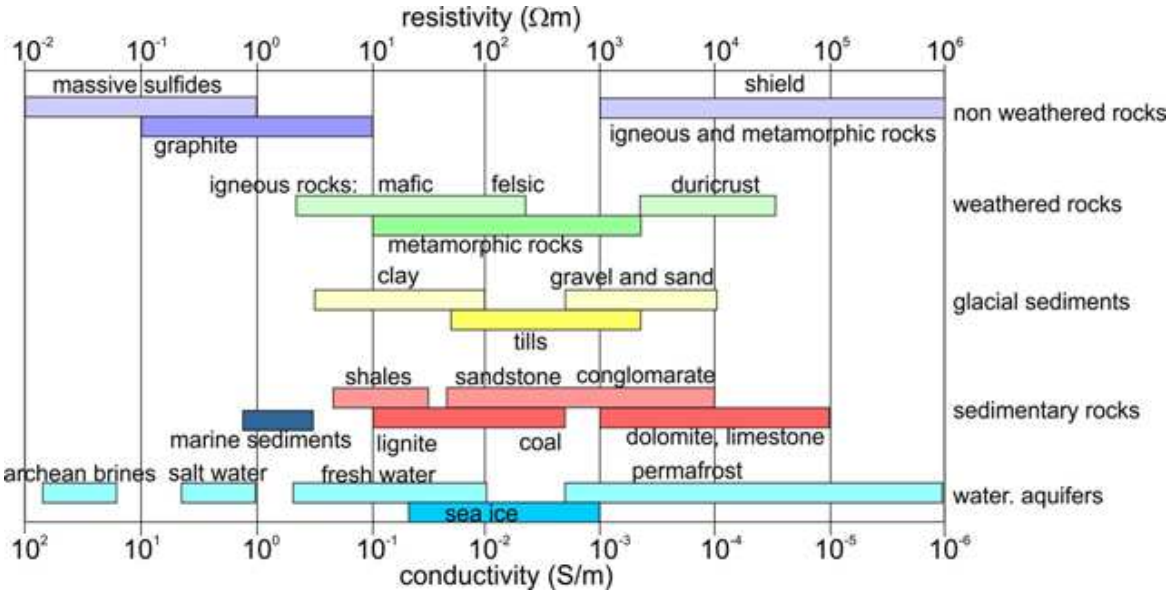

Source: www.bgr.bund.de

Chapter 1

General Introduction

1.1. The Vietnam Mekong Delta

The Mekong Delta comprises the lower reaches of the largest river in Southeast Asia, which flows through six countries, namely China, Myanmar, Laos, Thailand, Cambodia, and Vietnam (Le et al., 2007). Stretching from Cambodia to Vietnam, the Mekong Delta covers an area of about 60,000 km^2 (Anthony et al., 2015) including large portions contains of fertile alluvial soils (Cosslett and Cosslett, 2013).

The Vietnamese section of the Mekong Delta (VMD) accounts for about 78% of the entire delta corresponding to 12% of the total area of Vietnam. The VMD is one of the largest deltas in the world (Minderhoud et al., 2020), covering about 39,000 km^2, and is inhabited by about 18 million people (Tran et al., 2021).

The VMD comprises an interconnected system of rivers and canals, including nine estuaries and a dense network of canals which has been built over three centuries, starting from the 1980s – 1990s (Olson and Morton, 2018) with a main purpose was to irrigate rice paddy fields. As the result, over 10,000 km of canals (Van Kien et al., 2020), including 70% main and 30% interior canals, helps the VMD be a favorable place for agricultural development, particularly rice cultivation, where rice is grown on over 40% of the delta's total area (Vu et al., 2022). In addition to rice cultivation, with the extended canals systems, the VMD is also a major aquaculture and fruit growing area, contributing 65% and 70%, respectively, to Vietnam's total production (Schneider and Asch, 2020). The VMD therefore plays a crucial role in national food security and the economy, with agricultural exports alone accounting for up to 15% of the country's GDP (Park et al., 2022).

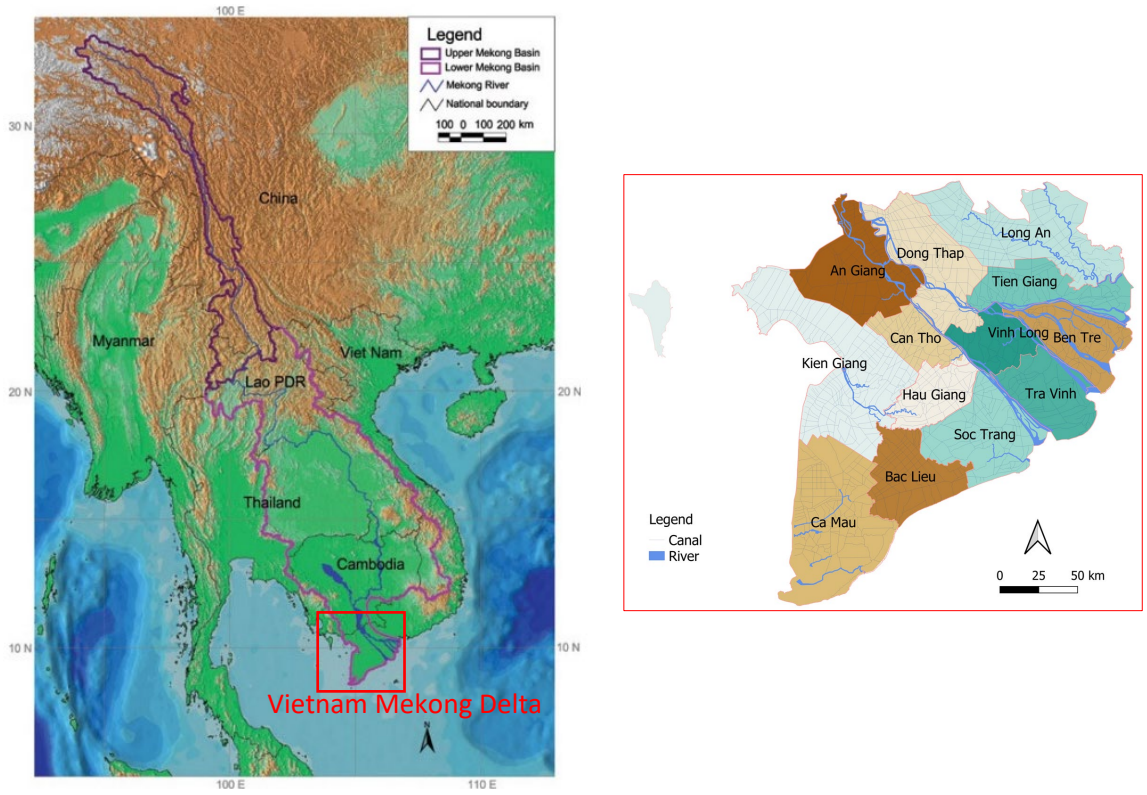

Figure 1 Position of the Vietnam Mekong Delta (VMD) in the Mekong basin (Hook et al., 2003) and the provincial map of the VMD.

1.2. Rice production and its distribution in the VMD

Rice is a staple food of half the world's population, and it is considered a vital part of the diet in countries in Asia, Latin America, and Africa (Muthayya et al., 2014). Between 1986 and 2005, global rice consumption increased about 100 million tons, from over 300 million tons to around 400 million tons (Abdullah et al., 2006). As the world's population continues to grow, rice will remain an important source of global nutrition, estimated to increase to 600 million tons by 2050 (Braun and Bos, 2005).

Around 90% of rice production originates from Asia (Kubo and Purevdorj, 2004), in which Vietnam contributed about 43 million tons per year, accounting for approximately 6% of the global rice production (FAOSTAT). Despite its relatively small share in rice production, Vietnam is the third largest rice exporter (FAOSTAT) of the world. Within Vietnam, the

VMD is a "rice basket" where rice cultivation covers approximate 1.7 million ha of the VMD area (Wassmann et al., 2019). Rice production in the VMD has increased last decades, which is related to the improvement and expansion of dike systems to protect rice fields from flood (Tri, 2012). This allows rice to be grown up to three times a year in some regions in the VMD.

With the huge planted area, rice production in the VMD exceeds the domestic need and can be exported in large quantities. Rice production in the VMD accounts for approximately 50% of national production and 90% of Vietnam's export rice (Schneider and Asch, 2020).

1.3. Major threats to rice production in the VMD

The development of agriculture in the VMD is exposed to various threats such as climate change, land subsidence, and freshwater shortage (Erban et al., 2014; Eslami et al., 2019). The increase in the number of upstream dams results in a decrease in the freshwater availability of the VMD (Dang et al., 2019). Especially in the dry season when water demand is high, the pressure of water resources for irrigation and the subsistence of the millions of people leads to overexploitation of groundwater which is a main reason caused land subsidence in the VMD (Erban et al., 2014; Minderhoud et al., 2020). In addition to freshwater shortages and land subsidence, mainly due to artefacts, the VMD is one of the third largest deltas in the world to be particularly threatened by sea-level rise due to climate change (Anthony et al., 2015).

Climate change, land subsidence and scarcity of freshwater put the VMD, a low-lying delta with an average elevation of less than 1 m above mean sea level (Minderhoud et al., 2019), at risk from saltwater intrusion, particularly during the dry season. In the dry season, droughts become more frequent (Phan et al., 2020), causing negative impacts on agriculture and livelihoods, and leading to salinization of the soil (Kaveney et al., 2023). It is estimated that approximate 1.8 million ha of land in the VMD is affected by saline water above 4 g l-1 during dry season every year (Wassmann et al., 2004). seawater usually intrudes into the major rivers of the VMD from the coast to the inland for about 40 to 60 km (Carew-Reid 2007). However, an increase in saltwater intrusion has been observed in the VMD over the

last two decades, with the distance of saltwater intrusion increasing to about 90 km in the drought year of 2006 and reaching 110 km in 2020 (Park et al., 2022).

1.4. Soil salinity measurements

Soil salinity can be determined through laboratory analysis, ground-based measurements and – as advanced methodology – remote sensing methods.

The traditional analysis of soil salinity in the laboratory is helpful in the case where specific knowledge of the saline solute is needed (Rhoades et al., 1999). However, it requires considerable time and effort in collecting samples and analyzing data. As this traditional analysis is performed as point values, it has limitation in providing a spatial distribution of soil salinity in a higher resolution (Romero et al., 2018).

Remote sensing, on the other hand, can give an impression of how soil salinity varies over large areas. For crop management purposes, remote sensing can be promising method in mapping soil salinity, but it can only investigate properties of the topsoil layers. In addition, soil salinity investigation using remote sensing can be confounded when there is the presence of vegetation or other features that cover the earth's surface (Metternicht and Zinck, 2003). In order to improve the validity of remote sensing data, ground-based measurements should be integrated for ground-truthing.

Ground-based soil salinity measurement refers to the process of determining the salt content or salinity levels in the soil using instruments and techniques on-site. Geo-physical methods are part of the ground-based methods. Geo-physical sensors play an important role in precision agriculture by providing valuable information about the properties of the soil, crop health, and water management. These methods use various geophysical techniques to collect data non-invasively and efficiently over large areas. In precision agriculture, the most commonly used geo-physical techniques are Electrical Resistivity Tomography (ERT), and Electromagnetic Induction (EMI) (Allred et al., 2008).

EMI is used to investigate topsoil salinity in agriculture (Heil and Schmidhalter, 2017). EMI measures the electrical conductivity of the soil, which is directly related to its salinity. It is

a useful tool for investigating the spatial variability of soil salinity at the agricultural field scale (Herrero et al., 2003; Jadoon et al., 2015) and for monitoring the temporal variation of topsoil salinity (Lesch et al., 1998; Zarai et al., 2022).

ERT is based on the measurement of the electrical resistivity of the soil, which is related to its salinity levels. An ERT survey can provide a detailed profile of the subsurface with greater depth than EMI. In ERT, an electric current is injected into the ground via two electrodes and the resulting electric potential is measured via two other electrodes (Brindt et al., 2019). The depth of the ERT profile is affected by the spacing between these electrodes. The greater the electrode spacing, the deeper the ERT profile investigated.

Figure 2 Soil salinity measurement in situ using geo-physics methods: a) ARES II, b) EM38-MK2.

1.5. Objectives of the study

The principal objective of the study is (1) to evaluate the application of geo-physics methods, using Electrical Resistivity Tomography (ERT) and Electro Magnetic Induction (EMI), in soil salinity in rice production systems, with emphasis on the salinization of the topsoil and

subsoil, and (2) to figure out if the rice production system affects the salinity of soil or vice versa. The specific objectives are:

1. to test the capability of the ERT method using ARES II to detect salinity of near surface water tables in order to evaluate potential risks of capillary rise of saline ground water to the rice production systems

2. to investigate topsoil salinity, and compare the versatility and accuracy of EMI and ERT to develop a new mapping technique for topsoil salinity, and

3. to map saline near surface groundwater under the rice fields at a provincial scale with the comprehensive ERT measurement.

The three specific objectives will be addressed in the next three chapters of this dissertation, which are as follows:

- Chapter 2: Soil resistivity measurements to evaluate subsoil salinity in rice production systems in the Vietnam Mekong Delta

- Chapter 3: Evaluating topsoil salinity by applying geophysical methods in rice production systems of the Vietnam Mekong Delta

- Chapter 4: Mapping saline groundwater under rice-paddy fields in Vietnam's Mekong Delta

REFERENCES

Abdullah, A.B, Shoichi, I., Kelali, A. (2006). Estimate of rice consumption in Asian countries and the world towards 2050. *Proceedings for Workshop and Conference on Rice in the World at Stake* (2).

Allred, B., Daniels, J.J., Ehsani, M.R. (Eds.). (2008). Handbook of Agricultural Geophysics (1st ed.). CRC Press. https://doi.org/10.1201/9781420019353

Anthony, E., Brunier, G., Besset, M. (2015). Linking rapid erosion of the Mekong River delta to human activities. *Scientific Reports* 5(1), 14745. https://doi.org/10.1038/srep14745

Braun, J.V, Bos, M.S. (2005). The changing economics and politics of rice: implications for food security, globalization, and environmental sustainability, in: Rice is Life: Scientific perspectives for the 21st Century. Proceedings of the World Rice Research Conference held in Tsukuba, Japan, 4-7 November 2004. International Rice Research Institute (IRRI), pp. 7–20.

Brindt, N., Rahav, M., Wallach, R. (2019). ERT and salinity – A method to determine whether ERT-detected preferential pathways in brackish water-irrigated soils are water-induced or an artifact of salinity. Journal of Hydrology 574, 35-45. https://doi.org/10.1016/j.jhydrol.2019.04.029

Carew-Reid, J. (2007). Rapid assessment of the extent and impact of sea-level rise in Viet Nam, 82. Brisbane: International Centre for Environment Management (ICEM).

CGIAR Research Program on Climate Change, Agriculture and Food Security - Southeast Asia (CCAFS SEA). (2016). Assessment Report: The drought and salinity intrusion in the Mekong River Delta of Vietnam. Hanoi, Vietnam: CGIAR Research Program on Climate Change, Agriculture and Food Security (CCAFS).

Cosslett, T.L., Cosslett, P.D. (2013). The Mekong Delta. In: Water Resources and Food Security in the Vietnam Mekong Delta. *Natural Resource Management and Policy*, vol 44. Springer, Cham. https://doi.org/10.1007/978-3-319-02198-0_1

Dang, V.H., Tran, D.D., Pham, T.B.T., Khoi, D.N., Tran, P.H., Nguyen, T.N. (2019). Exploring Freshwater Regimes and Impact Factors in the Coastal Estuaries of the Vietnamese Mekong Delta. *Water* 11(4). https://doi.org/10.3390/w11040782

Erban, L.E., Gorelick, S.M., Zebker, H.A. (2014). Groundwater extraction, land subsidence, and sea-level rise in the Mekong Delta, Vietnam. *Environmental Research Letters* 9, 084010. https://doi.org/10.1088/1748-9326/9/8/084010

Eslami, S., Hoekstra, P., Nguyen Trung, N., Kantoush, Doan, V.B., Do, D.D., Tran, Q.T., Vegt, M.V.D. (2019). Tidal amplification and salt intrusion in the Mekong Delta driven by anthropogenic sediment starvation. *Scientific Reports* 9, 18746. https://doi.org/10.1038/s41598-019-55018-9

FAO. (2016). "El NiÑo" event in Viet Nam - Agriculture, food security and livelihood needs assessment in response to drought and salt water intrusion. https://www.fao.org/3/i6020e/i6020e.pdf

FAOSTAT. (2020). http://www.fao.org/faostat/en/#data/QC (accessed 06.01.2023).

Heil, K., Schmidhalter, U. (2017). The application of EM38: Determination of soil parameters, selection of soil sampling points and use in agriculture and archaeology. *Sensors* 17(11), Article 2540. https://doi.org/10.3390/s17112540

Herrero, J., Ba, A.A., Aragüés, R. (2003). Soil salinity and its distribution determined by soil sampling and electromagnetic techniques. *Soil Use and Management* 19(2), 119-126. https://doi.org/10.1111/j.1475-2743.2003.tb00291.x

Hook, J., Novak, S., Johnston, R. (2003). Social Atlas of the Lower Mekong Basin. Mekong River Commission, Phnom Penh. 154 pages. ISSN: 1727-1800

Jadoon, K.Z., Moghadas, D., Jadoon A., Missimer, T.M., Al-Mashharawi S.K., McCabe, M. (2015). Estimation of soil salinity in a drip irrigation system by using joint inversion of multicoil electromagnetic induction measurements. *Water Resources Research* 51(5), 3490-3504. https://doi.org/10.1002/2014WR016245

Kaveney, B., Barrerr-Lennard, E., Minh, K.C., Duy, M.D., Thi, K.P.N., Kristiansen, P., Orgill, S., Stewart-Koster, B., Codon, J. (2023). Inland dry season saline intrusion in the Vietnamese Mekong River Delta is driving the identification and

implementation of alternative crops to rice. *Agricultural Systems* 207. https://doi.org/10.1016/j.agsy.2023.103632

Kubo, M., Purevdorj, M. (2004). The future of rice production and consumption. *Journal of Food Distribution Research* 35(1), 128–142. https://doi.org/10.22004/ag.econ.27145

Le, A.T., Chu, T.H., Miller, F., Sinh, B.T. (2007). Flood and salinity management in the Mekong Delta, Vietnam. In: Challenges to sustainable development in the Mekong Delta: Regional and National Policy Issues and Research Needs: Literature Analysis. Bangkok/Sustainable Mekong Research Network (Sumernet), Bangkok: Thailand, pp. 15-68.

Lesch, S.M., Herrero, J., Rhoades, J.D. (1998). Monitoring for temporal changes in soil salinity using electromagnetic induction techniques. *Soil Science Society of America Journal* 62(1), 232-242. https://doi.org/10.2136/sssaj1998.03615995006200010030x

Metternicht, G.I., Zinck, J.A. (2003). Remote sensing of soil salinity: potentials and constraints. Remote Sensing of Environment 85(1), 1-20. https://doi.org/10.1016/S0034-4257(02)00188-8

Minderhoud, P.S.J., Coumou, L., Erkens, G., Middelkoop, H., Stouthamer, E. (2019). Mekong delta much lower than previously assumed in sea-level rise impact assessments. Nature Communications 10, art. no. 3847. https://doi.org/10.1038/s41467-019-11602-1

Minderhoud, P.S.J., Middelkoop, H., Erkens, G., Stouthamer, E. (2020). Groundwater extraction may drown mega-delta: projections of extraction-induced subsidence and elevation of the Mekong delta for the 21st century. *Environmental research communications* 2(1). https://doi.org/10.1088/2515-7620/ab5e21

Muthayya, S., Sugimoto, J.D., Montgomery, S., Maberly, G.F. (2014). An overview of global rice production, supply, trade, and consumption. Ann. N. Y. Acad. Sci. 1324, 7–14. https://doi.org/10.1111/nyas.12540

Nguyen, L.D., Nguyen, T.V.K., Nguyen, D.V., Tran, A.T., Nguyen, H.T., Heidbüchel, I., Merz, B., Apel, H. (2021). Groundwater dynamics in the Vietnamese Mekong

Delta: Trends, memory effects, and response times. *Journal of Hydrology: Regional Studies* 33. https://doi.org/10.1016/j.ejrh.2020.100746

Nguyen, L.D., Nguyen, T.V.K., Nguyen, D.V., Tran, A.T., Nguyen, H.T., Ingo Heidbüchel, Bruno Merz, Heiko Apel. (2021). Groundwater dynamics in the Vietnamese Mekong Delta: Trends, memory effects, and response times. Journal of Hydrology: Regional Studies 33. https://doi.org/10.1016/j.ejrh.2020.100746

Olson, K.R., Morton, L.W. (2018). Polders, dikes, canals, rice, and aquaculture in the Mekong Delta. *Journal of Soil and Water Conservation* 73(4), 83A-89A. https://doi.org/10.2489/jswc.73.4.83A

Park, E., Ho, H.L., Doan, V.B., Kantoush, S. (2022). The worst 2020 saline water intrusion disaster of the past century in the Mekong Delta: Impacts, causes, and management implications. *Ambio* 51, 691–699. https://doi.org/10.1007/s13280-021-01577-z

Phan, V.H., Dinh, V.T., Su, Z. (2020). Trends in Long-Term Drought Changes in the Mekong River Delta of Vietnam. *Remote sensing* 12(18). https://doi.org/10.3390/rs12182974

Rao, V.V.S.G., Rao, G.T., Surinaidu, L., Rajesh, R., Mahesh, J. (2011). Geophysical and Geochemical Approach for Seawater Intrusion Assessment in the Godavari Delta Basin, A.P., India. *Water, Air, & Soil Pollution* 217, 503-514. https://doi.org/10.1007/s11270-010-0604-9

Rhoades, J.D., Chanduvi, F., Lesch, S. (1999). Soil salinity assessment: Methods and interpretation of electrical conductivity measurements. No. 57. Food & Agriculture Organization.

Romero-Ruiz, A., Linde, N., Keller, T., Or, D. (2018). A review of geophysical methods for soil structure characterization. *Reviews of Geophysics* 56(4), 672-697. https://doi.org/10.1029/2018RG000611

Schneider, P., Asch, F. (2020). Rice production and food security in Asian Mega deltas - A review on characteristics, vulnerabilities and agricultural adaptation options to cope with climate change. *Journal of Agronomy and Crop Science* 206, 491-503. https://doi.org/10.1111/jac.12415

Tran, D.A., Tsujimura, M., Pham, H.V., Nguyen, T.V., Ho, L.H., Le Vo, P., Ha, K.Q., Dang, T.D., Van Binh, D., Doan, Q.V. (2022). Intensified salinity intrusion in coastal aquifers due to groundwater over extraction: a case study in the Mekong Delta, Vietnam. Environmental Science and Pollution Research 29, 8996-9010. https://doi.org/10.1007/s11356-021-16282-3

Tran, D.D., Huu, L.H., Hoang, L.P., Pham, T.D., Nguyen, A.H. (2021). Sustainability of rice-based livelihoods in the upper floodplains of Vietnamese Mekong Delta: Prospects and challenges. *Agricultural Water Management* 243. https://doi.org/10.1016/j.agwat.2020.106495

Tri, V.K. (2012). Hydrology and Hydraulic Infrastructure Systems in the Mekong Delta, Vietnam. In: Renaud, F., Kuenzer, C. (eds) The Mekong Delta System. Springer Environmental Science and Engineering. Springer, Dordrecht. https://doi.org/10.1007/978-94-007-3962-8_3

Van Kien, N., Hoang Han N., Cramb R. (2020). Trends in Rice-Based Farming Systems in the Mekong Delta. In: Cramb R. (eds) White Gold: The Commercialisation of Rice Farming in the Lower Mekong Basin. Palgrave Macmillan, Singapore. https://doi.org/10.1007/978-981-15-0998-8_17

Vu, H.T.D., Tran, D.D, Schenk, A., Nguyen, C.P., Vu, H.L., Oberle, P., Trinh, V.C., Nestmann, F. (2022). Land use change in the Vietnamese Mekong delta: New evidence from remote sensing. *Science of the Total Environment* 813(151918). https://doi.org/10.1016/j.scitotenv.2021.151918

Wassmann, R., Ngo, D.P., Tran, Q.T., Chu, T.H., Nguyen, H.K., Nguyen, X.H., Vo, T.B.T., To, P.T. (2019). High-resolution mapping of flood and salinity risks for rice production in the Vietnamese Mekong Delta. *Field Crops Research* 236, 111-120. https://doi.org/10.1016/j.fcr.2019.03.007

Wassmann, R., Nguyen, X.H., Chu, T.H., Tuong, T.P. (2004). Sea level rise affecting the Vietnamese Mekong Delta: water elevation in the flood season and implications for rice production. *Climate Change* 66, 89-107. https://doi.org/10.1023/B:CLIM.0000043144.69736.b7

Yen, B.T., Son, N.H., Tung, L.T., Amjath-Babu, T.S., Sebastian, L. (2019). Development of a participatory approach for mapping climate risks and adaptive interventions (CS-MAP) in Vietnam's Mekong River Delta. Climate Risk Management 24, 59-70. https://doi.org/10.1016/j.crm.2019.04.004

Zarai, B., Walter, C., Michot, D., Montoroi, J.P., & Hachicha, M. (2022). Integrating multiple electromagnetic data to map spatiotemporal variability of soil salinity in Kairouan region, Central Tunisia. *Journal of Arid Land* 14, 186-202. https://doi.org/10.1007/s40333-022-0052-6

Zarroca, M., Bach, J., Linares, R., Pellicer, X.M. (2011). Electrical methods (VES and ERT) for identifying, mapping and monitoring different saline domains in a coastal plain region (Alt Empordà, Northern Spain). *Journal of Hydrology* 409(1-2), 407-422. https://doi.org/10.1016/j.jhydrol.2011.08.052

Chapter 2

Soil resistivity measurements to evaluate subsoil salinity in rice production systems in the Vietnam Mekong Delta *

Van Hong Nguyen[1], Jörn Germer[1], Van Nha Duong[2], Folkard Asch[1]

[1] University of Hohenheim, Institute of Agricultural Sciences in the Tropics (Hans-Ruthenberg Institute), Germany

[2] Kien Giang University, Agriculture and Rural Development Faculty, Vietnam

ACKNOWLEDGEMENTS

This work has been funded by the Federal Ministry of Education and Research (BMBF, Germany) in the project RiSaWa (project number 031B0724).

ABSTRACT

Rice is a staple crop in the Vietnam Mekong Delta (VMD) in which more than half of Vietnam's rice is produced. However, rice production in the VMD is threatened by increasing saltwater intrusion due to land subsidence and climate change induced sea level rise. Saltwater intrusion into lowland areas through the canal system or capillary rise of saline water from near surface saline water tables may result in salt accumulation in the topsoil. Therefore, it is important to disentangle the two effects and their relative importance to implement appropriate strategies for water and salinity management for adapting rice production systems of the VMD to climate change. Here, we report on the possibility of using geoelectrical methods to evaluate the potential threat of subsoil salinity to rice production. To evaluate the level of subsoil salinity, we measured soil electrical resistivity

* **This chapter is published as**: Nguyen, V.H., Germer, J., Duong, V.N., Asch, F. (2023). Soil resistivity measurements to evaluate subsoil salinity in rice production systems in the Vietnam Mekong Delta. *Near Surface Geophysics* 21(4), 288-299. http://doi.org/10.1002/nsg.12260

using an ARES II to a depth of 40 m in a case study comprising five locations in the VMD. Electrical resistivity measurements were calibrated to soil types, which were identified through evaluating 1 m core sections obtained by drilling down to 40 m depth. The relationship between drilling data and soil resistivity was determined by applying clustering and principal component analysis. Resistivity values smaller than 3 Ω m were clearly identified as indicative for a saline water table. The results show a direct link between the depth of the saline water table and the proximity to the sea, but not to the rice production system (single, double, or triple cropping). This study proved for the first time the applicability of the electrical resistivity tomography method for identifying groundwater tables and evaluating subsoil salinity on an agricultural field scale in the VMD.

Keywords: conductivity, electrical resistivity tomography, groundwater, site effect.

DATA AVAILABILITY STATEMENT

The data that support the findings of this study are available upon reasonable request from the corresponding author.

INTRODUCTION

The Vietnam Mekong Delta (VMD) is an alluvial delta that covers approximately 39,000 km2 comprising an irrigation canal system of about 10,000 km length (Van Kien et al., 2020). Rice production, aquaculture of shrimps and fish, as well as fruit production, are the main agricultural activities contributing 50%, 65% and 70% of Vietnam's total production, respectively. Depending on water quality and availability, rice is produced as single, double, or triple crop annually on the same area. Rice production in the VMD contributes 90% of Vietnam's rice exports (Schneider & Asch, 2020).

The fresh water supply for agricultural production in the low-lying delta with an average elevation of less than 1 m above mean sea level (Minderhoud et al., 2019) is threatened by saltwater intrusion caused by land subsidence and climate change induced sea level rise. Saltwater intrusion is aggravated by an increasing number of dams in the upstream of the Mekong River leading to reduced discharge flows (CGIAR, 2016). Triggered by an extreme

drought, the saltwater intrusion in 2016 caused a freshwater shortage that affected 339,000 ha of rice production (Yen et al., 2019) and caused severe yield losses during the winter/spring rice crop (FAO, 2016). Saltwater also intrudes into the near surface groundwater layers that are directly recharged from surface water (Nguyen et al., 2021; Tran et al., 2022).

Various approaches have been proposed for the VMD to cope with seasonally limited freshwater availability, such as changing cropping patterns or using water-efficient irrigation techniques. However, as irrigation practices, such as alternative wetting and drying irrigation, increase capillary rise from shallow water tables (Tan et al., 2014), salt may intrude into the top soil if the shallow groundwater is saline.

Geoelectric surveying is a non-invasive and cost-effective method for exploring the structure of the earth's subsurface and is used, for example, in groundwater exploration, monitoring landfills or agronomical management (Samouëlian et al., 2005). Common applications of geoelectric surveys are to detect and map groundwater (Mohamaden & Ehab, 2017; Riwayat et al., 2018), identify specific subsurface features, such as gypsum deposits (Gołębiowski & Jarosińska, 2019), and investigate saltwater intrusion into coastal areas and alluvial deltas (Cong-Thi et al., 2021; de Franco et al., 2009; Gemail et al., 2004; Galazoulas et al., 2015; Nowroozi et al., 1999).

In agricultural research, electrical resistivity tomography (ERT) is increasingly being used for monitoring soil moisture content (Rao et al., 2020), evaluating the effectiveness of irrigation systems on field scale through the spatio-temporal variation of soil moisture content (Araya et al., 2021), and, as recently reviewed by Cimpoiaşu et al. (2020), the relationship between resistivity and water uptake by plants under different irrigation conditions.

The aim of this study was to identify near surface water tables and assess their salinity at five case study sites contrasting in land use (single, double, and triple rice cropping) and proximity to the sea using ERT at agricultural field scale and to evaluate potential risks for capillary rise of saline ground water.

MATERIALS AND METHODS

Research area

Near surface water tables were identified at five sites with contrasting land-use in Tra Vinh province, a coastal province in the eastern VMD (Figure 1). The province lies between two main arms of the Mekong River and is pervaded by a system of irrigation and drainage canals. Under tidal influence, deposition of mud, silt, sand and gravel at the mouths of the Mekong's distributaries formed a floodplain of lowland swamps and sand dunes as typical topographic patterns. The elevation of the Tra Vinh province varies from 1 m to 3 m above mean sea level (Tran, 2020).

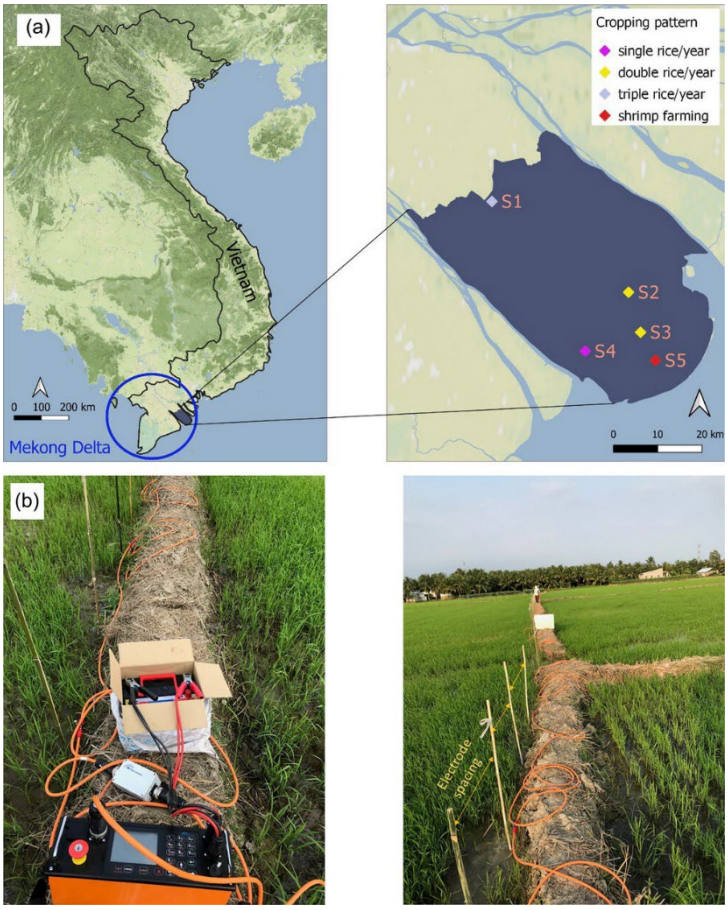

Figure 1 Location of the study area and in situ measurement of soil resistivity. (a) Map of the case study area in the Vietnam Mekong Delta including the five contrasting study sites. The sites represent different land-use types: S1 = triple rice cropping, S2, S3 = double rice cropping, S4 = single rice cropping – no shrimp production and S5 = shrimp production. (b) ARES II measurement in the field with electrode spacing marked with bamboo sticks.

Resistivity measurements

During a dry season in the case study in the VMD, soil electrical resistivity was measured using ARES II (GF Instruments s.r.o., Czech Republic). The ARES II/1 control unit was used with six 1-channel multi-electrode cables (eight electrodes per cable) connecting the stainless-steel electrodes and inserted into the ground. The electrodes were arranged following the Wenner–Schlumberger array configuration (Loke, 2021) along the bunds of the fields to allow measuring also when fields were flooded. Electrode spacings of 2, 3, 4 and 5 m allowed for effective measuring depths of 20–50 m. The roll-along technique was applied to extend the measurement line by moving the first cable to the end of the line to continue the measurement (Loke, 2021). At site S5, only one profile with 4 m electrode spacing was measured as the shrimp farm did not have parallel bunds of the same length. The number of electrodes used was a function of profile length and electrode spacing at the respective sites (Table 1). The 4 m electrode spacing was used in the analysis and for calibration with drilling data (see, section '2D ERT profiles').

Table 1. Site-specific profile lengths, number of electrodes (number in parentheses) used with different electrode spacings, water table level, maximum and minimum electrical conductivity of water and soil in the drill cores and soil resistivity extracted from the electrical resistivity tomography (ERT) profile at the borehole location corresponding to 2, 3, 4 and 5 m electrode spacing.

Site			**S1**	**S2**	**S3**	**S4**	**S5**
Profile length (m) and [number of electrodes]		2 m	318 [160]	190 [96]	190 [96]	190 [96]	-
		3 m	333 [112]	189 [64]	189 [64]	189 [64]	-
		4 m	348 [88]	188 [48]	188 [48]	188 [48]	252 [64]
		5 m	315 [64]	-	-	-	-
Water table (m)			8	5	4	4	3
EC_water (mS cm^{-1})		Max	6.1	5.7	6.0	7.9	49.6
		Min	2.0	3.0	3.7	4.8	31.6
EC_soil (mS cm^{-1})		Max	2.7	2.1	2.2	3.4	4.6
		Min	1.2	1.0	1.0	1.2	2.1
Resistivity (Ω m)	2 m	Max	16.2	386.1	160.4	27.5	-
		Min	1.5	0.7	0.6	0.6	-
	3 m	Max	19.5	74.8	83.0	18.9	-
		Min	1.2	1.1	0.6	0.6	-
	4 m	Max	12.3	61.9	147.2	11.2	3.2
		Min	1.1	1.2	0.4	0.6	0.3
	5m	Max	8.0	-	-	-	-
		Min	1.1	-	-	-	-

For three-dimensional (3D) mapping of resistivity, depending on site layout, five, three, six and eight parallel ERT profiles were measured at S1–S4, respectively.

ARES II measurements were processed with RES2DInv (version 4.10.8) to invert separate two-dimensional (2D) resistivity profiles and RES3DInv (version 3.18.4) to generate 3D resistivity maps from 2D parallel ERT profiles. The processing programmes use the smoothness-constrained Gauss–Newton least-squares method to produce a 2D or 3D model of the subsurface (Loke, 2021). The resistivity obtained from inversion procedure was visualized as contour graphs by using Surfer software (Golden Software, LLC).

Boreholes drilling

Boreholes were drilled by applying the rotary wash boring method using the drilling machine XY-1 (Zhengzhou Defy Mechanical & Electrical Equipment Co., Ltd.). During the drilling process, soil samples were collected from each 1 m down to 40 m depth of the boreholes. Soils from the cores were taken as undisturbed samples using a thin wall tube with Φ = 75 mm. Soil samples were separated in two parts: (1) stored in sealed and labelled plastic tubes (Φ = 75 mm, 20 cm in length) as undisturbed samples to analyse soil properties at the laboratory and (2) stored in labelled plastic bags to test electrical conductivity (EC) of the soil.

EC of the soil was measured using a Portable Multi-range Conductivity Meter (HI-8733, Hanna Instruments Ltd.), from 100 g soil suspended in water at a soil–water ratio of 1:5 at the end of each drilling day. From the undisturbed core samples moisture content, density, porosity, degree of saturation and soil structure was determined by the Laboratory of Soil Mechanics Construction Materials (Ho Chi Minh City, Vietnam).

In addition, during the drilling process, the drainage water from each sample core was collected for EC measurement with the mentioned conductivity meter.

Statistical analyses

Statistical analyses were performed with R (v4.1.14; R Core Team, 2021). The relationship between the resistivity of the soil sampled from the borehole cores, the soil properties and the presence of saltwater was analysed using heat map (pheatmap package (v1.0.12; Kolde,

2019)). Heat map clustering with hierarchical analysis was applied to detect patterns and similarities in the data set. A principal component analysis (PCA) was performed subsequently to confirm the clusters extracted from the heat map to find factors that influence soil resistivity. Eight variables were selected for cluster analysis, namely sand, clay, moisture content, bulk density, cropping types, EC of water and soil and resistivity.

RESULTS AND DISCUSSION

2D ERT profiles

Figure 2 shows the ERT profiles of site S1–S4 at the location of the boreholes measured with varying distances between the electrodes of the ARES II. Low resistivity (<2 Ω m) values indicate the presence of water. Measurements with a distance of 2 m between the electrodes allow a penetration depth of up to 20 m. At sites S1 and S4, the 2 m electrode spacing did not cover the depth necessary to assess the entire dimension of the low resistivity zone as the resistivity values stayed low up to 20 m depth. Similarly, a 3 m spacing indicated the end of the low resistivity zone at about 25 m depth at site S4, whereas no boundary was evident at site S1. At a 4 m spacing, the upper and lower limits of the low resistivity zone were evident at all sites. The maximum depth of the low resistivity zone at about 40 m at site S1 was confirmed by measuring a profile with 5 m spacing between the electrodes (data not shown). As the paddy fields in the Mekong delta are relatively small and the minimum length of bunds needed for 5 m spacing of electrodes is about 240 m, measuring at 5 m spacing was only possible at site S1. Therefore, we conclude that ERT using 4 m electrode spacing to be most suitable for assessing soil resistivity at sufficient depth in the paddy fields of the study area.

In general, the highest resistivity (>20 Ω m) was found at the surface of each site, whereas the lowest resistivity (<3 Ω m) was measured at medium depths (10–20 m) of all ERT profiles and all sites.

Based on the resistivity ranges from the ERT profiles and the location of the sites, three different resistivity zones were distinguished. S4, located near the sea and representing a single rice crop/year, was in the zone with the lowest resistivity (0.2–15.0 Ω m). Sites S3

and S2 were grouped into the high resistivity zone (0.8–184.2 Ω m) and S1, northern most site of the study area, in the medium resistivity zone (1.24–12.00 Ω m). The maximum and minimum resistivities of the ERT profiles at the five sites are summarized in Table 1.

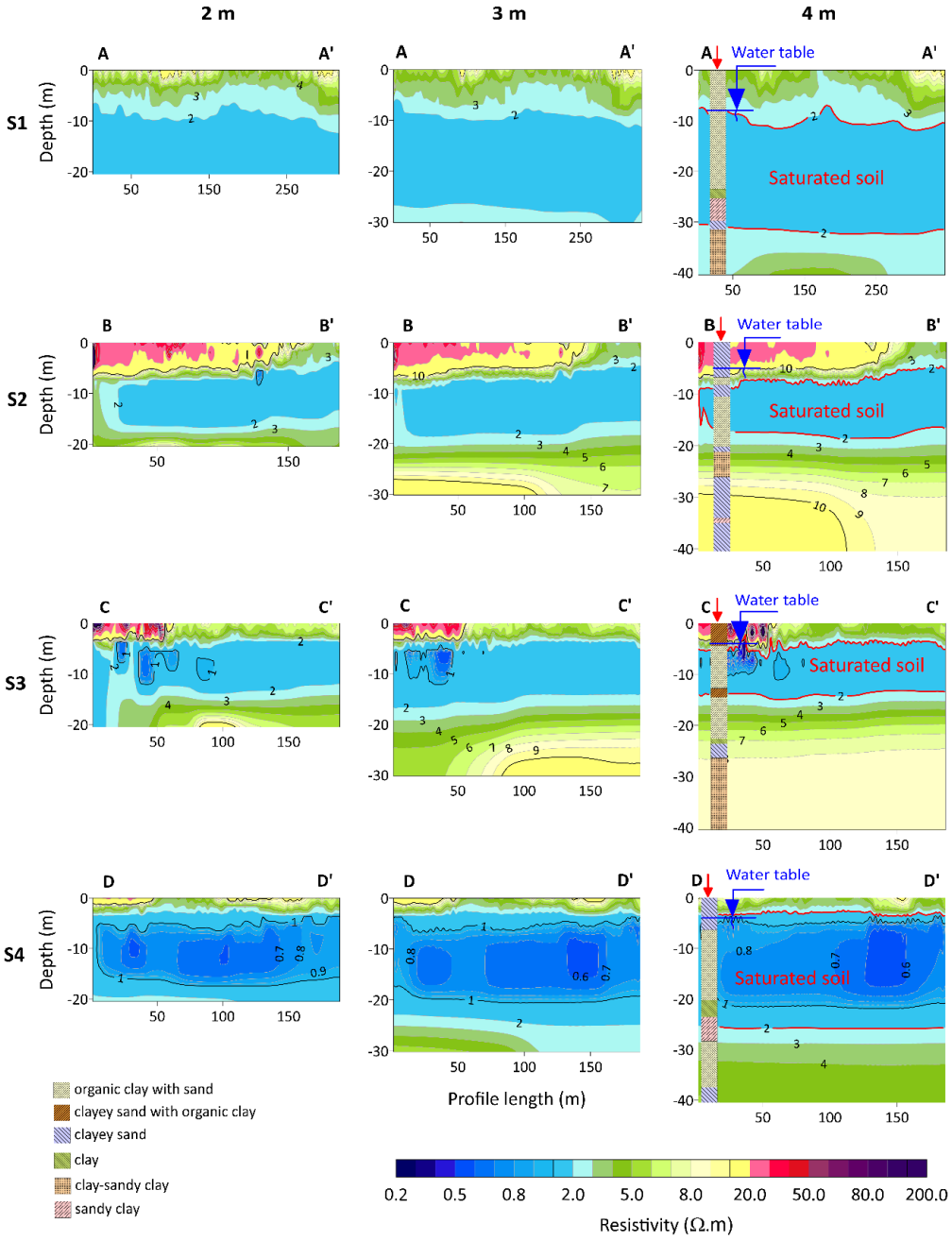

Figure 2 Two-dimensional (2D) electrical resistivity profiles with electrode spacing = 2 m, 3 m and 4 m at the four sites: S1 – triple rice/year, S2, S3 – double rice/year and S4 – single rice/year. The length of profiles depends on the size and bunds in each rice paddy, site S1 having the longest straight bunds. The contour interval is 1 Ω m. The colours of

electrical resistivity tomography (ERT) profiles are displayed in logarithmic scale. The letters A–A′, B–B′, C–C′ and D–D′ represent for sections marked in Figure 3. The arrows indicate the position of the boreholes. Soil properties of the boreholes are stacked in ERT profiles as borehole logs.

3D resistivity maps

Multiple profiles were used to generate 3D resistivity maps for the four case study sites shown in Figure 3, which were measured with an electrode spacing of 4 m. The 3D soil resistivity maps are similar to the 2D ERT profiles in terms of low resistivity at the medium depths. However, the resolution of the interpolated 3D maps in the upper and lower soil depths is lower than in the original 2D maps, and at these depths, the layers of higher electrical resistivity are located. Lowest resistivity was measured below 6 m depth at site S1 and from 8 to 20, 4 to 15 and 3 to 30 m at site S2, S3 and S4, respectively. The layer of low resistivity (<3 Ω m) approaches the surface as the distance to the sea decreases. As confirmed by the drilling data in Table 1, resistivity below 10 Ω m (yellow colour in Figure 3) indicates water saturated soil.

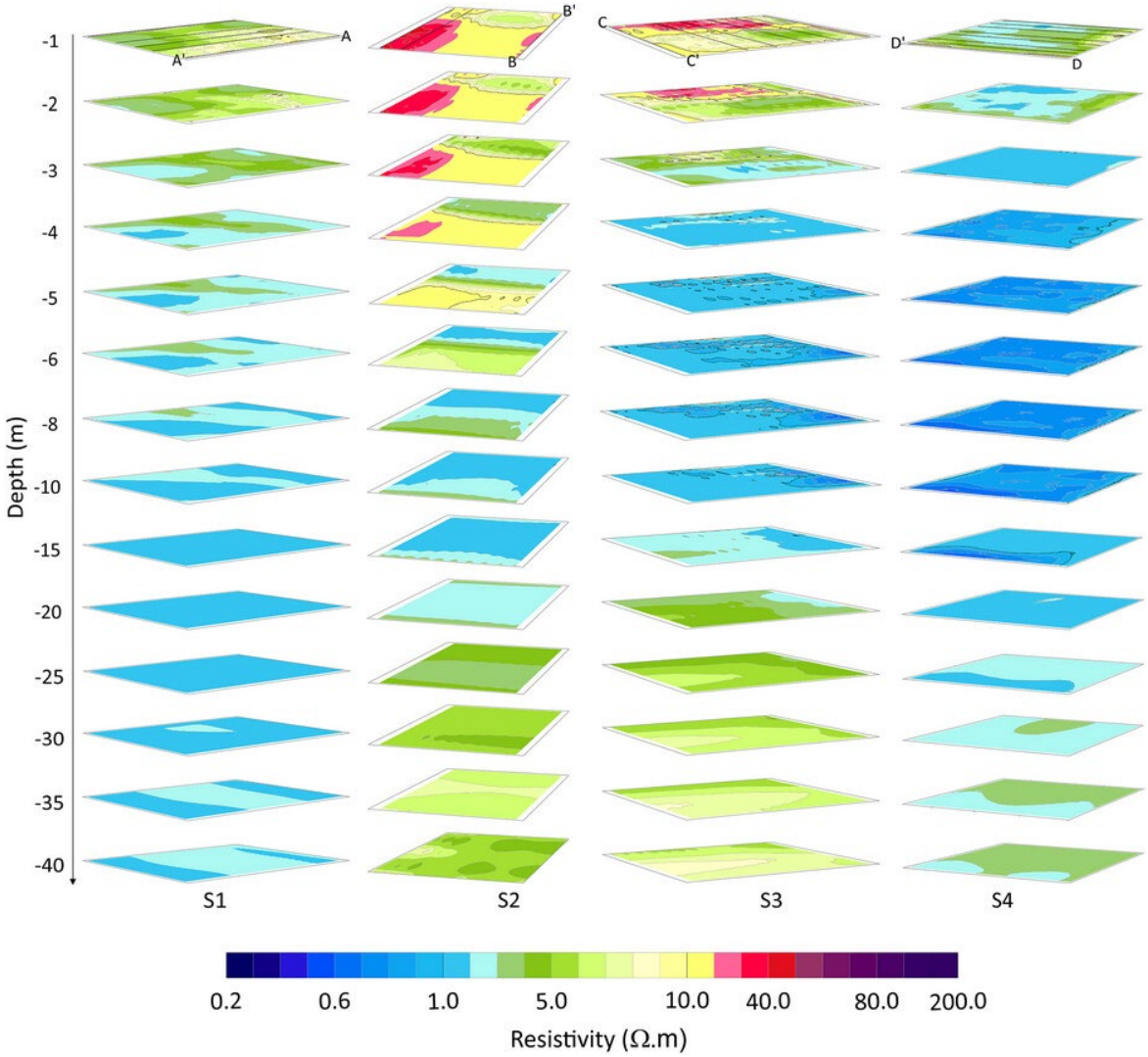

Figure 3 Three-dimensional (3D) resistivity maps obtained with 4 m electrode spacing for the four case study sites in true north orientation. From 1 to 6 m depth, the 3D planes are displayed at 1 m intervals due to high variation of resistivity in the upper soil layers. The intervals increase from 2 to 5 m for depths from 6 to 10 m and from 10 to 40 m depth, respectively, related to the homogeneity of soil properties and the decrease in electrical resistivity tomography (ERT) profile resolution. The colours represent resistivity on a logarithmic scale. Dotted lines on the surface layer at each site indicate the sections where two-dimensional (2D) ERTs were measured. The cross sections illustrated by A–A′, B–B′, C–C′ and D–D′ are the 2D ERT lines coinciding with borehole positions.

Calibrating electrical resistivity against soil properties

Site-specific electrical resistivity is known to be strongly influenced by soil properties, such as soil structure, moisture content, or porosity (Samouëlian et al., 2005). Therefore, to calibrate and interpret the resistivity data obtained with ARES II, boreholes were drilled to a depth of 40 m at each site, and the changes in soil and water properties were evaluated for each meter of depth. The data show that the depth of the shallow water table decreases towards the sea, from 8 m depth at site S1 to 3 m depth at site S5. In contrast to all other sites, site S5 shows a significantly higher water EC (>30 mS cm^{-1}, Table 1) combined with a low electrical resistivity of the soil (<3 Ω m, Table 1), which, with EC values above 4.5 mS cm^{-1}, indicates salinity, according to Brouwer et al. (1985).

Figure 4 illustrates the relationship between EC measurements from the core samples for soil and water and the ERT resistivity values extracted from the ARES II measurements. ERT resistivity of water saturated soil decreased towards the sea, from about 15 Ω m at site S2 to less than 2 Ω m at S5 (Figure 4). Soil layers with high EC water values (EC > 4.5 mS cm^{-1}) have ERT resistivity values smaller than 9 Ω m. Site S1 is an exception with low ERT resistivity values (<2 Ω m), where EC values of water do not allow to distinguish freshwater from saltwater, which may be due to differences in soil properties. With ERT resistivity values higher than 3 Ω m, it is clear that the EC of soil and water increases as ERT resistivity decreases, whereas this pattern cannot be seen with ERT resistivity lower than 3 Ω m.

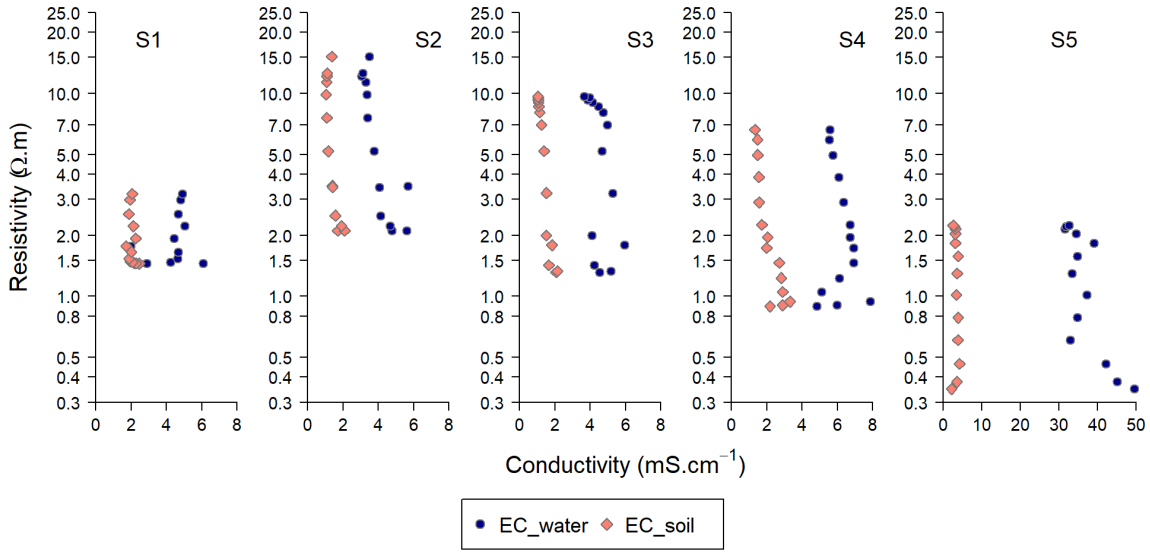

Figure 4 Relationship between electrical conductivity (EC) of soil and water for each 1 m depth interval in the soil core and electrical resistivity tomography (ERT) electrical resistivity values extracted from the ARES II measurement. The y-axis is logarithmically scaled.

Water tables may not easily be detected due to spatial changes in soil properties that may overlay soil–water boundaries (Palacky, 1987). Equally, high clay contents and, thus, lower resistivity values could be confused with soil salinity or soil moisture (Galazoulas et al., 2015; Giao et al., 2003; Samouëlian et al., 2005; Zohdy et al., 1993). Figure 5 illustrates the properties of the soil cores drilled at each study site and the respective soil and water EC values as well as electrical resistivity measured. At site S1, EC values of the drainage water from the cores clearly indicate saline water below 20 m depth. However, low resistivity (<2 Ω m) was measured from 10 m to 30 m depth. This shallow layer of low resistivity (10–20 m depth) at S1 was probably due to soil properties such as fine grain size, high porosity and high moisture content (Figure 5a, S1). Although some influence of soil properties on soil resistivity can also be seen at site S2–S4, the sharp decrease of resistivity values at 3–8 m in combination with high EC values clearly indicates the saline water table. The increase of resistivity in greater depths on the other hand may be related to changes in soil structure and moisture content.

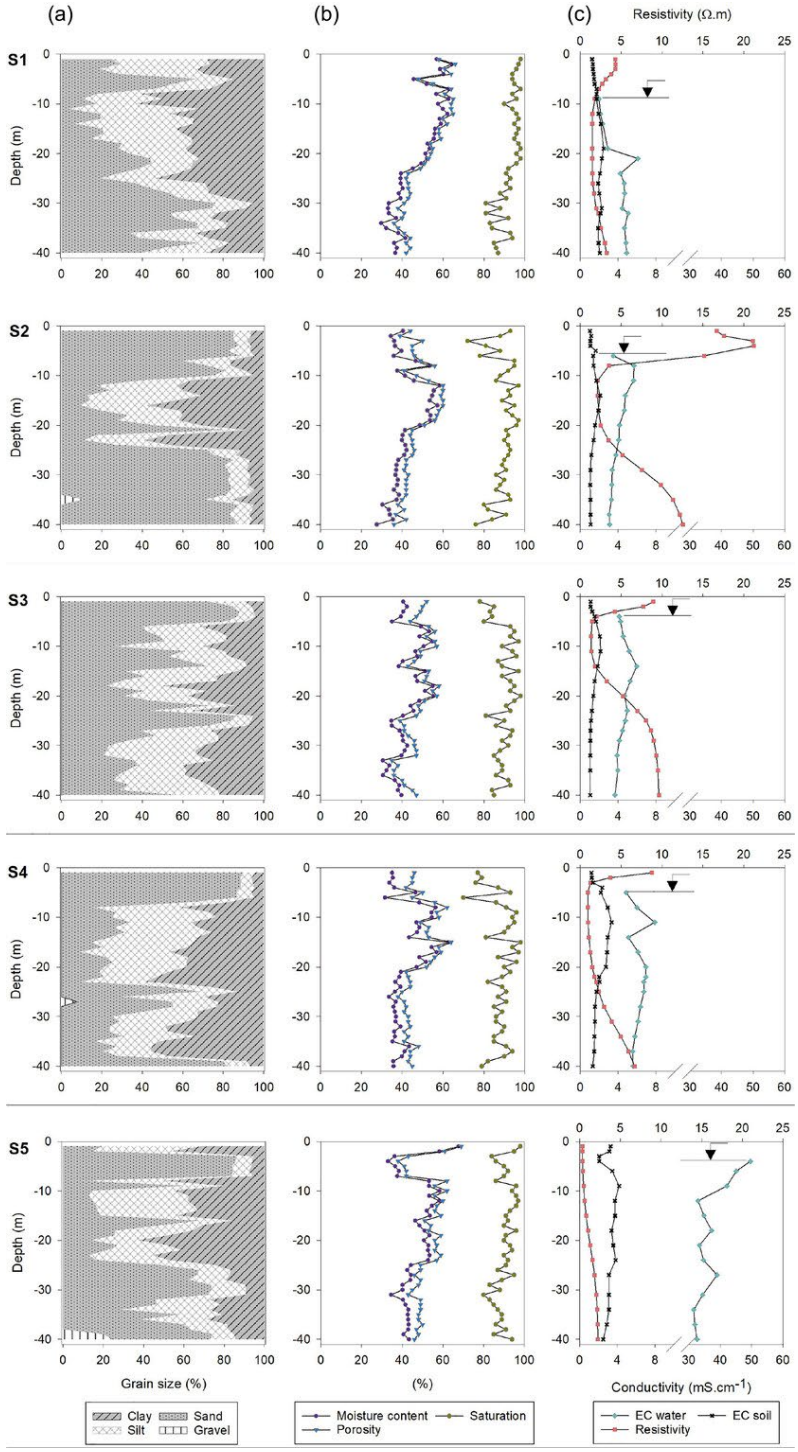

Figure 5 Soil properties obtained from cores at 1 m depth intervals at site S1–S4. Part (a) represents soil texture. (b) Moisture content, porosity and degree of saturation in the soil pores. (c) Electrical conductivity (EC) of soil and water and resistivity of soil extracted from electrical resistivity tomography (ERT) profiles at borehole positions. In (c) x-axes (conductivity axis) breaks were applied from EC 10 to 30 mS cm^{-1} due to the high EC of water at site S5. Arrows illustrate the water tables.

Characteristics of the shallow water table

Based on the range of resistivity of saline water (<4.5 Ω m) (Nowroozi et al., 1999), the low resistivity indicates saline water in the depth from 10 m to 20 m at all case studies sites. This confirms the presence of saltwater in the shallow aquifer in the Mekong delta as previously reported by Ha et al. (2022).

Relationship between resistivity and soil properties

Cluster analysis

In Figure 6, the properties of the 1 m borehole core samples are hierarchically analysed in an intensity heat map. The hierarchical analysis groups samples with similar characteristics of the five study sites using the Euclidean distance and complete linkage clustering method (El-Hamdouchi & Willett, 1989; Murtagh & Contreras, 2012). The height of the branches in the dendrogram represents the degree of dissimilarity between clusters; thus, the longer the branch, the greater the differences between clusters (Takahashi et al., 2019). Accordingly, the heat map distinguishes three major groups; A, B and C. Considering detail characteristics at a lower hierarchical level, group C is subdivided into C1 and C2.

Group A clusters samples characterized by high water conductivity larger than 31.6 mS cm^{-1}, that is very close to the EC of seawater (Tyler et al., 2017). All these samples belong to S5, which is characterized by its proximity to the sea and its distinct land use pattern (Figures 6 and 7).

Group B is dominated by soils with high proportions of fine grain (>54%) and high moisture content (>43%) (Figures 6 and 7). Resistivity values of the samples clustered in group B are in the narrow range from 0.9 Ω m to 5.9 Ω m, which is the typical range for clay soil (Giao et al., 2003; Shevnin et al., 2006).

Group C clusters samples having low EC values of soil and water (Figures 6 and 7) and predominantly high resistivity. The high resistivity values in this group are mainly due to low soil moisture (<40%). With the exception of S2, it has an exceptionally high resistivity (>5.8 Ω m) due to its high sand content (>75%, Figure 6) and thus forms sub-cluster C1.

Sub-cluster C2, on the other hand, represents a sample group with lower resistivity associated with high clay content and high EC of water and soil (Samouëlian et al., 2005).

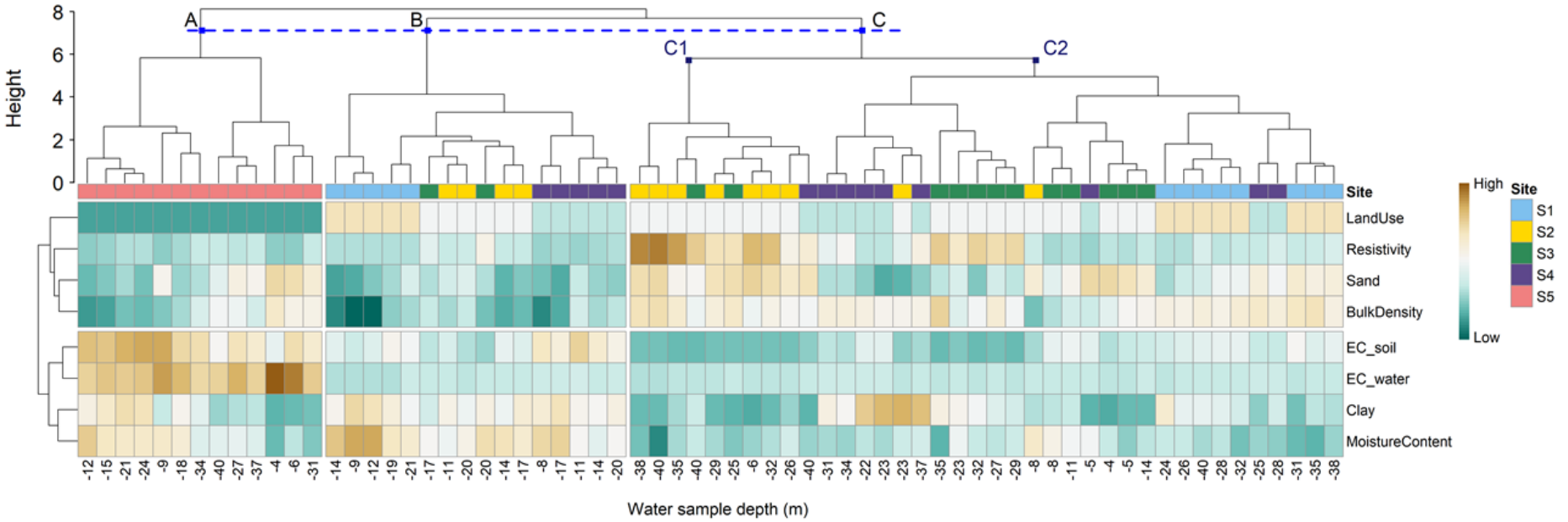

Figure 6 Heat map for soil properties and soil salinity at different sample depths at the five study sites. The heat map illustrates a hierarchical analysis with two dendrograms. The top dendrogram shows clusters based on sample depths, whereas the left dendrogram groups variables that have similar properties. Land-use is indicated as dark petrol for shrimp farming, light petrol for single rice cropping, white for double rice cropping and yellow for triple rice cropping. All other variables are shown on a standardized colour scale from low (dark petrol) to high (dark brown) by subtracting column means from columns and divide it by column standard deviations.

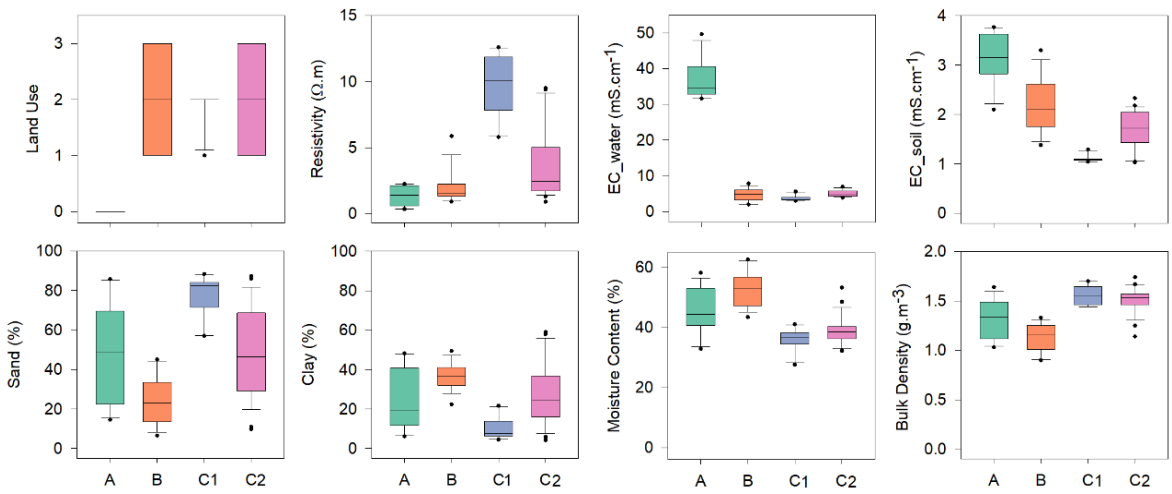

Figure 7 Representation of electrical resistivity and related variables in three main groups derived from the heat map in Figure 6 as boxplots. Group C is divided into two sub-groups: C1 and C2. For land-use, 0 = shrimp farming, 1 = single rice cropping, 2 = double rice cropping, 3 = triple rice cropping.

Principal component analysis

PCA was used to identify saline water tables and their depth based on the soil and water properties at case study sites S1–S4. Site S5 has not been included in the PCA due to its proximity to the sea and different land-use (Figure 6).

The PCA is a multivariate statistical method that reduces the dimensionality of large data sets. The number of principal components (PCs) corresponds to the number of variables used in the PCA analysis (Greenacre et al., 2022). In this section, seven variables were used for PCA analysis, including clay, sand, bulk density, moisture content, resistivity and EC of soil and water samples.

Two PCs (PC1 and PC2) explain 74.1% of the variance in the data set (Table 2). PC3 potentially explains additional 15%; however, PC3 was mainly linked to soil properties (data not shown), which are already sufficiently covered by the first two PC which clearly distinguish between clay and sandy soils.

Table 2. Contribution of seven principal components (PCs) to variance in the data set.

	PC1	PC2	PC3	PC4	PC5	PC6	PC7
Standard deviation	1.920	1.222	1.052	0.639	0.445	0.261	0.177
Proportion of Variance	0.527	0.214	0.158	0.058	0.028	0.010	0.005
Cumulative Proportion	0.527	0.741	0.899	0.957	0.986	0.996	1

In Figure 8, PC1 distinguishes groups B and C as clustered in Figure 6, whereas PC2 comprises two groups associated with water quality: saline water and non-saline water.

In the non-saline group, samples with high resistivity values combined with low EC values form a distinct cluster. This high resistivity cluster (>5.8 Ω m at S2 and >7.5 Ω m at S3) represents deeper soil layers in S2 (26–40 m) and in S3 (23–40 m). Samples in the top layer in S2 (6 m) and in S3 (4–5 m) also appear in this group. The elevated resistivity in this cluster is related to high sand content and low moisture content. In addition to the high resistivity cluster, samples from 9 m to 19 m of site S1 appear in the non-saline group with low resistivity (<1.6 Ω m) due to their high clay and moisture content.

Within the saline group, samples from shallow depths group in between the bi-plots of clay content and EC of soil, whereas samples of the medium depths cluster between the bi-plots of EC of soil and the bulk density. The cluster with medium depths comprises most samples of site S1 (26–40 m), S3 (11–14 m) and S4 (22–34 m). Resistivity values in this cluster vary from 1.6 Ω m to 3.3 Ω m, 1.4 Ω m to 2.1 Ω m and 1.8 Ω m to 5.3 Ω m for site S1, S3 and S4, respectively. Only the sample of site S4 at a shallow depth (5 m) appears in this cluster with a resistivity of 0.9 Ω m. However, most of the shallow samples at the remaining sites, including S1 (21 m), S2 (8 m) and S3 (8 m), are located between clay and EC of soil with resistivity of less than 2.5 Ω m. Low resistivity in the middle depths is mainly affected by salinity, whereas in the shallow depths, it is also influenced by soil properties, such as clay and moisture content.

The results from the PCA demonstrate that resistivity below 3 Ω m represents the threshold where the saline water table begins. The saline groundwater table decreases towards inland,

from 5 m at S4 to 20 m at S1, whereas the thickness of saline water table decreases from 23 m at S4 to 3 m at site S2.

With respect to the saline water level, the results from PCA are consistent with ERT profiles at most of case study sites, S2–S4 (Figure 2). At site S1, the interface between freshwater and saline water is unclear in the ERT profile due to the uniformity in resistivity (<2 Ω m) from around 10 m to 40 m depth.

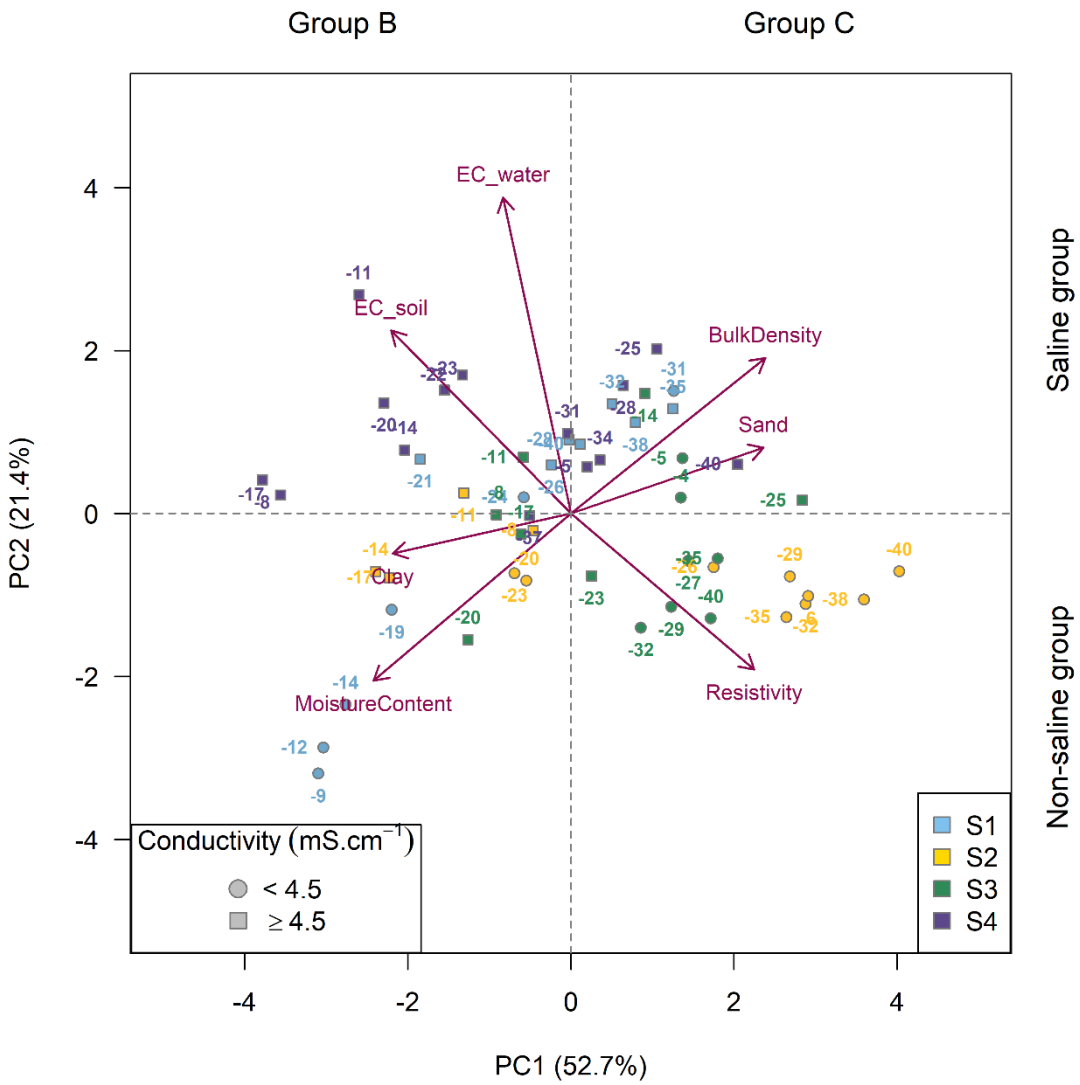

Figure 8 Principle component analysis for two principle components: PC1 and PC2 at four sites, S1–S4. The numbers indicate the depth in meters at which the water samples were taken.

CONCLUSIONS

The aim of this study was to evaluate the suitability of the ERT as a geophysical method for identifying saline groundwater tables that may pose a threat to rice production systems in the VMD due to capillary rise. The geophysical data from ARESII were supplemented with data from 40 m borehole cores to test the interpretability and thus the reliability of data from ERT. Combining the ARES II and the borehole data with the cluster and PCA analysis allowed identifying location and thickness of the shallow water table as well as the boundary between freshwater and saltwater layers at locations with highly variable resistivity. Resistivity values smaller than 3 Ω m were identified as indicative for saline water. Thus, we were able to show that the shallow groundwater below rice fields in the case study sites in Tra Vinh province consists of saline water, with the thickness of the saline water layer increasing towards the sea. Only at sites that yield nearly homogenous resistivity values, the interpretation of ARES II data may require additional drilling or geological reference data, such as soil type.

We found no clear link between the shallow saline water table and rice cropping patterns in Tra Vinh province, indicating no capillary rise between the shallow water table and the top soil; however, this may change with increasing sea level rise. Overall, ARES II showed great potential to detect and monitor eventual changes in extent and salinity of near surface water layers.

We have used ERT for the first time in the VMD, with the aim to detect and characterize salinity beneath rice fields. With the results, we have provided evidence that ERT is a powerful tool for characterizing and monitoring salt intrusion into the shallow water layer in the VMD and other rice-growing areas in river deltas around the world, which are prone to saltwater intrusion due to climate change induced sea level rise.

REFERENCES

Araya Vargas, J., Gil, P.M., Meza, F.J., Yáñez, G., Menanno, G., García-Gutiérrez, V., Luque, A.J., Poblete, F., Figueroa, R., Maringue, J., Pérez-Estay, N., Sanhueza, J., (2021) Soil electrical resistivity monitoring as a practical tool for evaluating irrigation systems efficiency at the orchard scale: a case study in a vineyard in Central Chile. *Irrigation Science* 39, 123-143. https:// doi.org/10.1007/s00271-020-00708-w

Brouwer, C., Goffeau, A., Heibloem, M., (1985) Irrigation Water Management: Training Manual No. 1 – Introduction to Irrigation. FAO, Rome, assessed 20 October 2022, https://www.fao.org/3/r4082e/r4082e08.htm#7.2%20salinity

CGIAR Research Program on Climate Change, Agriculture and Food Security - Southeast Asia (CCAFS SEA), (2016) Assessment Report: The drought and salinity intrusion in the Mekong River Delta of Vietnam. Hanoi, Vietnam: CGIAR Research Program on Climate Change, Agriculture and Food Security (CCAFS).

Cimpoiaşu, M.O., Kuras, O., Pridmore, T., Mooney, S.J., (2020) Potential of geoelectrical methods to monitor root zone processes and structure: A review. *Geoderma* 365, art. no. 114232. https://doi.org/10.1016/j.geoderma.2020.114232

Cong-Thi, D., Dieu, L.P., Thibaut, R., Paepen, M., Ho, H.H., Nguyen, F., Hermans, T., (2021) Imaging the structure and the saltwater intrusion extent of the luy river coastal aquifer (Binh Thuan, Vietnam) using electrical resistivity tomography. *Water (Switzerland)* 13, art. no. 1743. https://doi.org/10.3390/w13131743

de Franco, R., Biella, G., Tosi, L., Teatini, P., Lozej, A., Chiozzotto, B., Giada, M., Rizzetto, F., Claude, C., Mayer, A., Bassan, V., Gasparetto-Stori, G., (2009) Monitoring the saltwater intrusion by time lapse electrical resistivity tomography: The Chioggia test site (Venice Lagoon, Italy). *Journal of Applied Geophysics* 69, 117-130. https://doi.org/10.1016/j.jappgeo.2009.08.004

El-Hamdouchi A., Willett P., (1989) Comparison of hierarchic agglomerative clustering methods for document retrieval. *The Computer Journal* 32, 220-227. https://doi.org/10.1093/comjnl/32.3.220

FAO, (2016) “El NiÑo” event in Viet Nam - Agriculture, food security and livelihood needs assessment in response to drought and salt water intrusion. https://www.fao.org/3/i6020e/i6020e.pdf

Galazoulas, E.C., Mertzanides, Y.C., Petalas, C.P., Kargiotis, E.K., (2015) Large Scale Electrical Resistivity Tomography Survey Correlated to Hydrogeological Data for Mapping Groundwater Salinization: A Case Study from a Multilayered Coastal Aquifer in Rhodope, Northeastern Greece. *Environmental Processes* 2, 19-35. https://doi.org/10.1007/s40710-015-0061-y

Gemail K., Samir, A., Oelsner, C., Mousa, S.E., Ibrahim, S., (2004) Study of saltwater intrusion using 1D, 2D and 3D resistivity surveys in the coastal depressions at the eastern part of Matruh area, Egypt. *Near Surface Geophysics* 2, 103-109. https://doi.org/10.3997/1873-0604.2004007

Giao, P.H., Chung, S.G., Kim, D.Y., Tanaka, H., (2003) Electric imaging and laboratory resistivity testing for geotechnical investigation of Pusan clay deposits. *Journal of Applied Geophysics* 52, 157-175. https://doi.org/10.1016/S0926-9851(03)00002-8

Gołębiowski, T., Jarosińska, E., (2019) Application of GPR and ERT methods for recognizing of gypsum deposits in urban areas. *Acta Geophysica* 67, 2015–2030.

Greenacre, M., Groenen, P.J.F., Hastie, T., D’Enza, A.I., Markos, A., Tuzhilina, E., (2022) Principal component analysis. *Nature Reviews Methods Primers* 2, 100. https://doi.org/10.1038/s43586-022-00184-w

Ha, Q.K., Tran Ngoc, T.D., Le Vo, P., Nguyen, H.Q., Dang, D.H., (2022) Groundwater in Southern Vietnam: Understanding geochemical processes to better preserve the critical water resource. *Science of the Total Environment* 807, part 2. https://doi.org/10.1016/j.scitotenv.2021.151345

Kolde, R., (2019) pheatmap: Pretty Heatmaps. R package version 1.0.12. https://CRAN.R-project.org/package=pheatmap

Loke, M.H., (2021) Tutorial: 2-D and 3-D Electrical Imaging Surveys, accessed 17 August 2022, https://www.researchgate.net/publication/264739285_Tutorial_2-D_and_3-D_Electrical_Imaging_Surveys

Minderhoud, P.S.J., Coumou, L., Erkens, G., Middelkoop, H., Stouthamer, E., (2019) Mekong delta much lower than previously assumed in sea-level rise impact assessments. *Nature Communications* 10, art. no. 3847. https://doi.org/10.1038/s41467-019-11602-1

Mohamaden, M., Ehab, D., (2017) Application of electrical resistivity for groundwater exploration in Wadi Rahaba, Shalateen, Egypt. *NRIAG Journal of Astronomy and Geophysics* 6, 201-209. https://doi.org/10.1016/j.nrjag.2017.01.001

Murtagh, F., Contreras, P., (2012) Algorithms for hierarchical clustering: an overview. *Wiley Interdisciplinary Reviews: Data Mining and Knowledge Discovery* 2, 86-97. https://doi.org/10.1002/widm.53

Nguyen, L.D., Nguyen, T.V.K., Nguyen, D.V., Tran, A.T., Nguyen, H.T., Ingo Heidbüchel, Bruno Merz, Heiko Apel, (2021) Groundwater dynamics in the Vietnamese Mekong Delta: Trends, memory effects, and response times. *Journal of Hydrology: Regional Studies* 33. https://doi.org/10.1016/j.ejrh.2020.100746

Nowroozi, A.A., Horrocks, S.B., Henderson, P., (1999) Saltwater intrusion into the freshwater aquifer in the eastern shore of Virginia: a reconnaissance electrical resistivity survey. *Journal of Applied Geophysics* 42, 1-22. https://doi.org/10.1016/S0926-9851(99)00004-X

Palacky, G.J., (1987) Resistivity characteristics of geologic targets. *Electromagnetic Methods in Applied Geophysics* 1, 53-129. https://doi.org/10.1190/1.9781560802631.ch3

R Core Team, (2021) R: A language and environment for statistical computing. R Foundation for Statistical Computing, Vienna, Austria. https://www.R-project.org/

Rao, S., Lesparre, N., Flores-Orozco, A., Wagner, F., Kemna, A., Javaux, M., (2020) Imaging plant responses to water deficit using electrical resistivity tomography. *Plant and Soil* 454, 261-281. https://doi.org/10.1007/s11104-020-04653-7

Riwayat, A.I., Ahmad Nazri, M.A., Zainal Abidin, M.H., (2018) Application of Electrical Resistivity Method (ERM) in Groundwater Exploration. *Journal of Physics: Conference Series* 995, art. no. 012094. https://doi.org/10.1088/1742-6596/995/1/012094

Samouëlian, A., Cousin, I., Tabbagh, A., Bruand, A., Richard, G., (2005) Electrical resistivity survey in soil science: A review. *Soil and Tillage Research* 83, 173-193. https://doi.org/10.1016/j.still.2004.10.004

Schneider, P., Asch, F., (2020) Rice production and food security in Asian Mega deltas - A review on characteristics, vulnerabilities and agricultural adaptation options to cope with climate change. *Journal of Agronomy and Crop Science* 206, 491-503. https://doi.org/10.1111/jac.12415

Shevnin, V., Delgado Rodríguez, O., Mousatov, A., Flores Hernández, D., Zegarra Martínez, H., Ryjov, A., (2006) Estimation of soil petrophysical parameters from resistivity data: Application to oil-contaminated site characterization. *International Geophysics* 45, 179-193.

Takahashi, A., Hashimoto, M., Hu, J., Takeuschi, K., Tsai, M., (2019) Hierarchical cluster analysis of dense GPS data and examination of the nature of the clusters associated with regional tectonics in Taiwan. *Geophysical Research Letters: Solid Earth* 124, 5174-5191. https://doi.org/10.1029/2018JB016995

Tan X., Shao D., Liu H., (2014) Simulating soil water regime in lowland paddy fields under different water managements using HYDRUS-1D. *Agricultural Water Management* 132*,* 69-78. https://doi.org/10.1016/j.agwat.2013.10.009

Tran, D.A., Tsujimura, M., Pham, H.V., Nguyen, T.V., Ho, L.H., Le Vo, P., Ha, K.Q., Dang, T.D., Van Binh, D., Doan, Q.-V., (2022) Intensified salinity intrusion in coastal aquifers due to groundwater over extraction: a case study in the Mekong Delta, Vietnam. *Environmental Science and Pollution Research* 29, 8996-9010. https:// doi.org/10.1007/s11356-021-16282-3

Tran, P.H., (2020) Assessment of changes in the structure land use in Tra Vinh Province under the scenarios of climate change and sea level rise. *Vietnam Journal of Science and Technology* 58, 70-83. https://doi.org/10.15625/2525-2518/58/1/13982

Tyler, R. H., Boyer, T. P., Minami, T., Zweng, M. M., Reagan, J. R., (2017) Electrical conductivity of the global ocean. *Earth, Planets and Space* 69, 1-10. https://doi.org/10.1186/s40623-017-0739-7

Van Kien, N., Hoang Han N., Cramb R., (2020) Trends in Rice-Based Farming Systems in the Mekong Delta. In: Cramb R. (eds) White Gold: The Commercialisation of Rice Farming in the Lower Mekong Basin. Palgrave Macmillan, Singapore. https://doi.org/10.1007/978-981-15-0998-8_17

Yen, B.T., Son, N.H., Tung, L.T., Amjath-Babu, T.S., Sebastian, L., (2019) Development of a participatory approach for mapping climate risks and adaptive interventions (CS-MAP) in Vietnam's Mekong River Delta. *Climate Risk Management* 24, 59-70. https://doi.org/10.1016/j.crm.2019.04.004

Zohdy, A.A.R., Martin, P.M., Bisdorf, R. J., (1993) A study of seawater intrusion using direct-current soundings in the southeastern part of the Oxnard Plain, California. Vol. 93. *US Geological Survey*. https://doi.org/10.3133/ofr93524

Chapter 3

Evaluating topsoil salinity via geophysical methods in rice production systems in the Vietnam Mekong Delta*

Van Hong Nguyen[1], Jörn Germer[1], Folkard Asch[1]

[1] University of Hohenheim, Institute of Agricultural Sciences in the Tropics (Hans-Ruthenberg Institute), Germany

ACKNOWLEDGEMENTS

This work has been funded by the Federal Ministry of Education and Research (BMBF, Germany) in the project RiSaWa (project number 031B0724).

Abstract

The Vietnam Mekong Delta (VMD) is threatened by increasing saltwater intrusion due to diminishing freshwater availability, land subsidence, and climate change induced sea level rise. Through irrigation, saltwater can accumulate in the rice fields and decrease rice production. The study aims at evaluating topsoil salinity and examining a potential link between topsoil salinity and rice production systems in a case study in the Tra Vinh province of the VMD. For this, we applied two geophysical methods, namely, 3D electrical resistivity tomography (ARES II) and electromagnetic induction (EM38-MK2). 3D ARES II measurements with different electrode spacings were compared with EM38-MK2 topsoil measurements to evaluate their respective potential for monitoring topsoil salinity on an agricultural scale and the relationship between land-use types and topsoil salinity. Results show that EM38-MK2 is a rapid and powerful tool for obtaining high-resolution topsoil

* **This chapter is published as**: Nguyen, V.H., Germer, J., Asch, F. (2023). Evaluating topsoil salinity via geophysical methods in rice production systems in the Vietnam Mekong Delta. *Journal of Agronomy and Crop Science* 210(1), e12676. https://doi.org/10.1111/jac.12676

salinity maps for rice fields. With ARES II data, 3D maps up to 40 m depth can be created, but compared with EM38-MK2 topsoil maps, topsoil salinity was underestimated due to limitations in resolution. Salt contamination of above 300 mS m−1 was found in some double-cropped rice fields, whereas in triple-cropped rice fields salinity was below 200 mS m−1. Results clearly show a relation between topsoil salinity and proximity to the saline water sources; however, a clear link between rice production and topsoil salinity could not be established. The study proved that geophysical methods are useful tools for assessing and monitoring topsoil salinity at agricultural fields scale in the VMD.

Keywords: electrical conductivity, electrical resistivity, EMI, ERT, salinity stress.

Key Points

- Rice production systems are threatened by saltwater intrusion.
- Inadequate water management can cause topsoil salinization.
- Comparing geophysical methods, EM38-MK2 and ARES II, to evaluate and monitor topsoil salinity.
- EM38-MK2 is an effective tool for assessing topsoil salinity on an agricultural scale.
- No acute salt contamination was found in the topsoil of the rice fields.

INTRODUCTION

Saltwater intrusion is a threat in the Vietnam's Mekong Delta (VMD), where rice is grown on nearly 4 million ha, representing over 40% of the delta's total area (Vu et al., 2022). The expansion of triple cropping in the VMD increased the area irrigated in the dry season. However, the irrigation water resources in the VMD are increasingly threatened by saltwater intrusion due to sea level rise caused by climate change and land subsidence (Vu et al., 2022) as well as by reduced freshwater availability (CGIAR, 2016). The saltwater not only intrudes to the irrigation canal systems, but may also penetrate shallow aquifers in the delta (Nguyen, Nguyen, et al., 2021; Tran et al., 2022).

Saline water in canals and shallow saline aquifer lead to topsoil salinization through irrigation practices (Rhoades et al., 1999) or capillary rise from saline water tables (Tan et al., 2014), which in turn affects crop growth and yields (Zörb et al., 2018). In the VMD, the salinity of the soil is commonly assessed by taking soil samples to analyse the total dissolved salts (TDS) to determine the EC of the soil (Hens et al., 2009; Lam et al., 2020; Nguyen et al., 2008). However, this method is both time- and labour-intensive, and thus not practical when it is necessary to collect a large number of soil samples in order to assess the salinity of soil over a large area. Recently, some attempts have been made to map soil salinity via remote sensing (Nguyen et al., 2020) or remote sensing combined with machine learning (Nguyen, Tran, et al., 2021; Pham et al., 2019). Although remote sensing-based methods are capable of monitoring soil salinity over large areas, its effectiveness when applied in the VMD is controversial due to the distribution of floodplains causing errors during interpolation (Silvestri et al., 2022).

Geophysical methods exploit the relationship between resistivity and soil properties (Samouëlian et al., 2005). In agricultural sciences, the three commonly used geophysical methods are radar penetration, electrical resistivity tomography (ERT), and electromagnetic induction (EMI) (Allred et al., 2008). EMI is often applied to examine soil salinity and soil properties in agriculture or archaeology (Heil & Schmidhalter, 2017), being a useful tool for mapping the spatial distribution (Herrero et al., 2003; Jadoon et al., 2015), and monitoring the temporal variation of topsoil salinity (Lesch et al., 1998; Zarai et al., 2022). Probably due to the intense presence of ponded water layers, EMI has not often been employed to characterize or monitor paddy fields (Adam et al., 2012; Herrero & Hudnall, 2014).

In contrast, ERT has not been frequently used at agricultural scales; however, more recently, ERT has increasingly been applied to monitor the dynamics of soil salinity (Walter et al., 2018), soil moisture content (Rao et al., 2020), or water uptake by plants to improve water management (Araya Vargas et al., 2021), and as recently reviewed by Cimpoiaşu et al. (2020), the structure of the root zone.

The aim of the present study is to investigate topsoil salinity at a case study area in the VMD, comparing the versatility and accuracy of EMI and ERT as a new approach for mapping of topsoil salinity in rice production systems in the VMD. The specific objectives were to (i) assess the topsoil salinity in rice production systems, (ii) identify the most adequate

geophysical method to map topsoil salinity and (iii) investigate a potential link between land-use and topsoil salinity in the case study area in the VMD.

MATERIALS AND METHODS

Research area

The study was conducted at six sites with contrasting land-use patterns in Tra Vinh province in the east, near the coast of the VMD (Figure 1). These included triple-rice, double-rice and single-rice cropping per year. The province is located between two arms of the Mekong River and is crisscrossed by a system of canals for irrigation and drainage. The interaction of the Mekong River and the sea created lowlands, swamps and sand dunes which form a typical topographic pattern in this province, with elevations varying between 1 and 3 m above mean sea level (Tran et al., 2020).

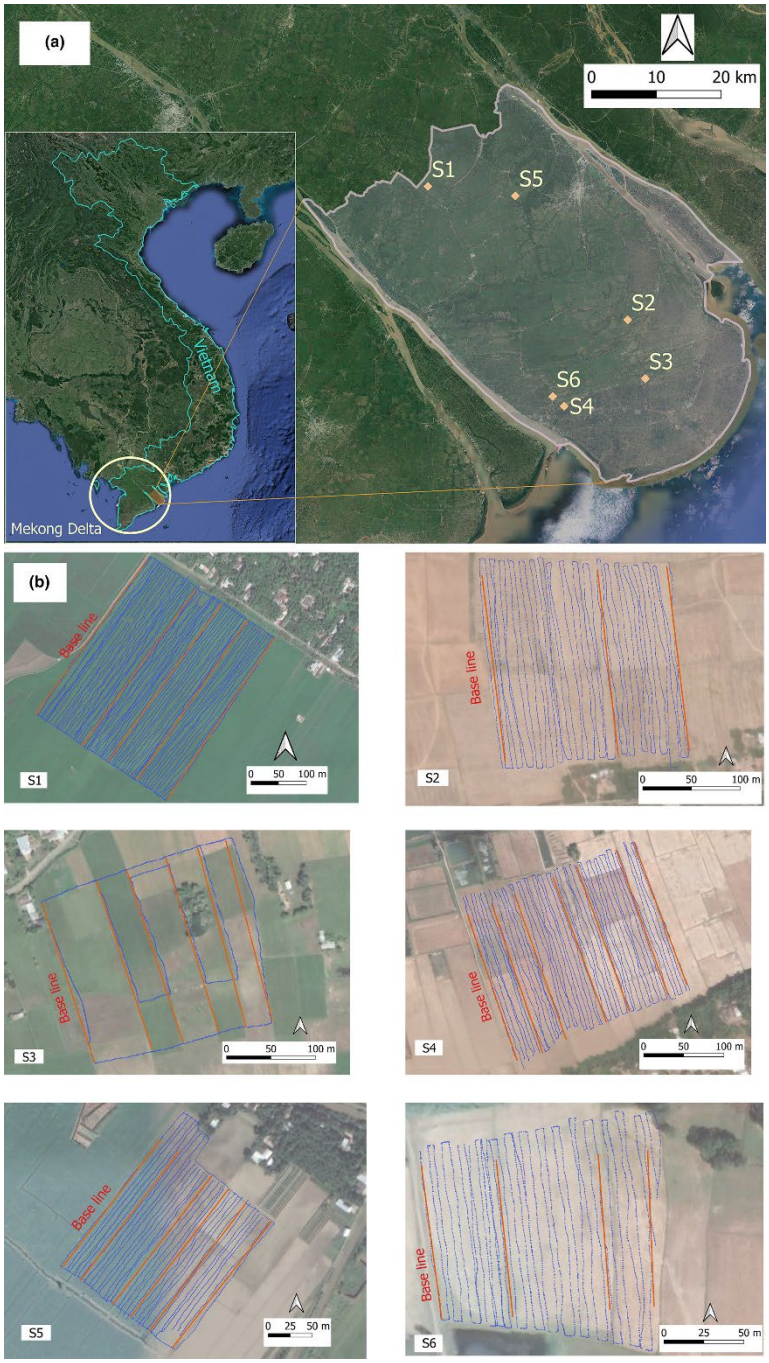

Figure 1 Map of the case study area in the Vietnam's Mekong Delta showing the six contrasting study sites. The locations represent different land-use types: S1, S5 = triple-rice cultivation; S2, S3, S6 = double-rice cultivation; S4 = single-rice cultivation. The orange lines are ERT measurement sections (using ARES II), the blue dots are EMI measurements (using EM38-MK2). ARES II electrode spacing of 2–4 m was measured at site S1–S4, whereas electrode spacing of 1 and 2 m was conducted at smaller field sizes at S5 and S6.

Electrical resistivity tomography

Soil electrical resistivity of the rice paddy fields was measured during the dry season and after rice harvest. The measurement was conducted using ARES II (GF Instruments s.r.o., Czech Republic) and interpreted and visualized as described in Nguyen et al. (2023). The ARES II measurements were carried out with different electrode spacings from 1 to 4 m, allowing an effective depth of up to 10, 20, 30 and 40 m of resistivity measurements, respectively. However, as this study focuses on topsoil salinity, only soil layer information from 1.5 m to above was extracted from the datasets for analysis. Topsoil resistivity was obtained from three-dimensional maps from a depth of 1.5 m to the surface. ERT was measured along the bunds of the fields as landmarks. Therefore, for three-dimensional mapping resistivity of the fields, depending on site layout, five, three, six, seven, six, and four ERT profiles were measured at S1, S2, S3, S4, S5 and S6, respectively.

Electrical conductivity via electromagnetic induction

The salinity of the upper soil was measured in the form of parallel lines at a distance of 5 m between the lines with the portable EM38-MK2 (Geonics Limited, Canada) in vertical dipole mode. The EM38-MK2 has two receiver coils separated by 1.0 and 0.5 m from the transmitting coil. The two receiver coils allow electrical conductivity values to be determined in two different depth ranges, in the vertical dipole mode from 1.50 to 0.75 m and in the horizontal dipole mode from 0.750 to 0.375 m (Heil & Schmidhalter, 2015). The EM38-MK2 was connected to the data logger (Mesa2) via Bluetooth, and tracking was done via a GPS connection. The EC values obtained with the EM38-MK2 were integrated into contour maps using the Surfer software (Golden Software, LLC) with the Kriging method for interpolation. The EM38-MK2 measurement was carried out after completion of the resistivity measurement with ARES II.

Statistical analyses

SigmaPlot version 14.0 (Systat Software, San Jose, CA) was used to perform statistical analyses. One-way ANOVA and Holm-Sidak test were applied to determine the relationship between topsoil salinity with different land-use types, including triple rice, triple/double rice, double rice, single rice cultivation, and shrimp farming. For each land-use type, data from

three fields were used for this analysis, with the exception of the double/triple rice crop, only two fields were included in the survey.

RESULTS AND DISCUSSION

Distribution of soil salinity in rice fields using EM38-MK2

The results of the EM38-MK2 measurement are shown as EC maps in Figure 2. The distribution of soil salinity in the rice fields is similar for both coil distances. In general, the variation in measured soil salinity is higher with a coil spacing of 1.0 m than with a spacing of 0.5 m, as indicated by a low coefficient of variation (see Table 1). The EC maps show higher soil salinity at 1.0 m coil spacing than at 0.5 m, except at site S1. There, the maximum EC at 0.5 m coil spacing was 286.2 mS m^{-1}, but at 1.0 m coil spacing, it was only 236.6 mS m^{-1}.

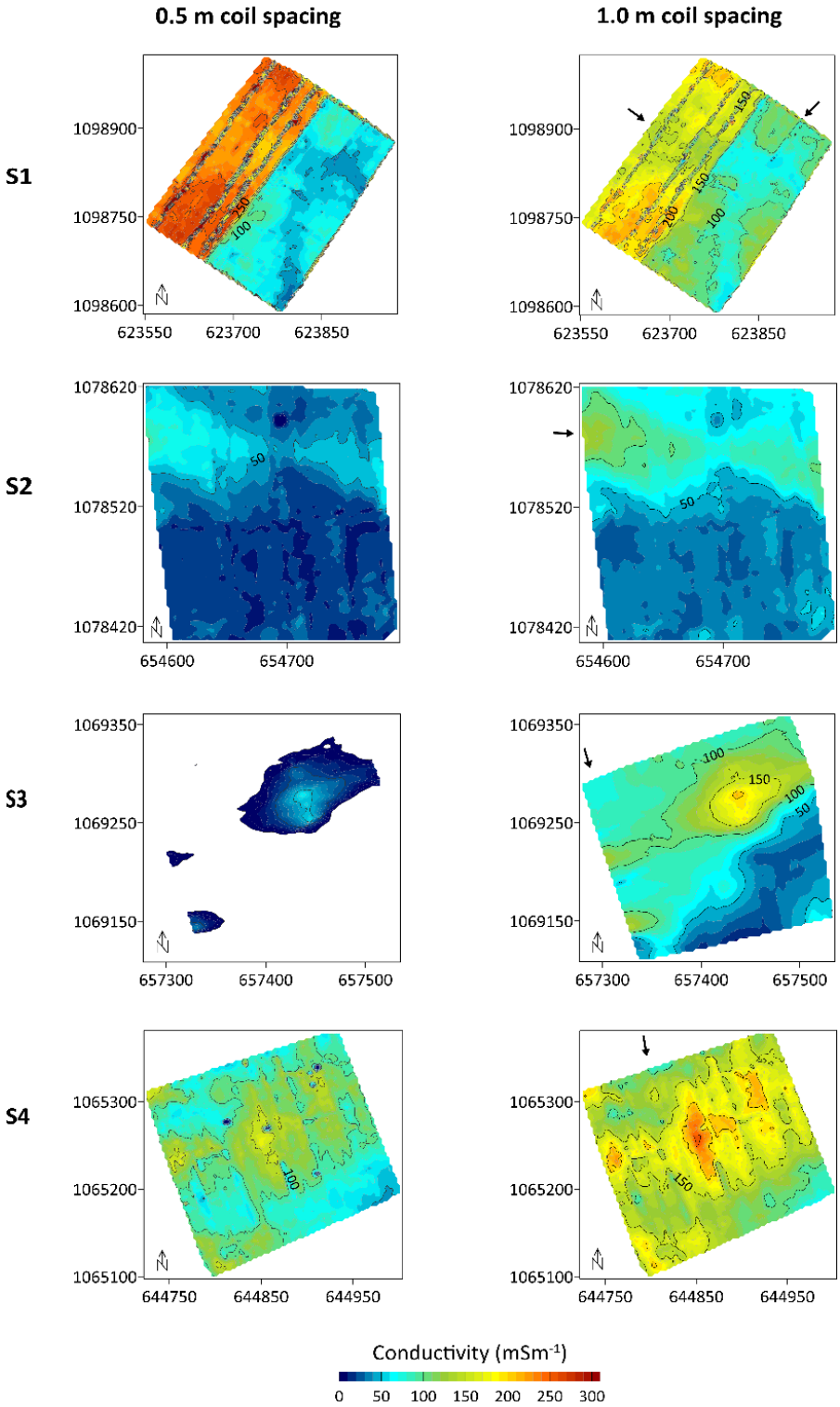

Figure 2 Maps of EC values determined with EM38-MK2 coil spacings of 0.5 and 1.0 m at the case study sites S1–S4. The axes are displayed in the Universal Transverse Mercator (UTM) coordinate system with coordinates given in metres. The arrows indicate the position of the irrigation and drainage sluices to the nearby channels that run parallel to the fields. The distance between the contour line is 10 mS m^{-1}.

Table 1. Summary of EM38-MK2 and ARES II results at six case study sites.

		S1	S2	S3	S4	S5	S6
Soil properties	Clay (%)	28.0	6.1	9.7	3.9	-	-
	Silt (%)	47.2	8.2	17.6	5.9	-	-
	Sand (%)	24.8	85.6	72.8	90.1	-	-
EC_0.5 m ($mS\ m^{-1}$)	Min	11.8	1.1	0.0	0.5	13.4	8.7
	Max	286.2	111.7	76.1	238.3	159.7	60.4
	Mean	167.2	36.0	20.4	102.7	91.7	37.1
	Std Dev	87.0	15.8	17.2	24.2	17.7	7.7
EC_1 m ($mS\ m^{-1}$)	Min	2.7	1.6	5.0	54.7	59.5	23.4
	Max	236.6	148.8	218.5	261.3	187.1	87.0
	Mean	134.5	53.5	78.5	150.8	126.9	53.3
	Std Dev	43.5	24.5	38.2	31.9	17.6	8.7
Resistivity 1 m (Ωm)	Min	-	-	-	-	1.1	8.8
	Max	-	-	-	-	65.1	248.4
	Mean	-	-	-	-	6.4	23.8
	Std Dev	-	-	-	-	8.0	19.6
Resistivity 2 m (Ωm)	Min	4.5	6.5	5.1	3.3	8.1	8.8
	Max	154.2	127.7	218.6	41.4	26.0	85.0
	Mean	14.4	28.2	35.5	9.7	14.7	20.3
	Std Dev	6.4	17.8	29.4	4.6	2.7	12.6
Resistivity 3 m (Ωm)	Min	4.2	6.9	74.5	2.4	-	-
	Max	33.1	79.3	116.1	24.8	-	-
	Mean	10.0	28.4	22.6	6.6	-	-
	Std Dev	3.2	14.9	15.5	3.3	-	-
Resistivity 4 m (Ωm)	Min	3.1	6.0	3.7	1.8	-	-
	Max	25.9	53.0	90.1	13.7	-	-
	Mean	8.0	20.9	15.6	3.7	-	-
	Std Dev	2.8	10.1	8.8	1.8	-	-

Note: EM38-MK2 measurements were recorded at 0.5 and 1.0 m coil spacing. ARES II data were recorded with four different electrode spacings (1, 2, 3 and 4 m) at six sites. Soil properties adapted from Nguyen et al. (2023).

At a coil spacing of 1.0 m, the variation in topsoil salinity was higher at sites S1 and S3, where EC values range from 2.7 to 236.6 mS m^{-1} and 5.0 to 218.5 mS m^{-1}, respectively. The results of EM38-MK2 also show the movement of water within the paddy fields with lower EC values following irrigation flow, which is evident at site S1 and S2.

At a coil spacing of 0.5 m, the highest EC values were found in site S1, which is further, and where the triple-rice crop is grown. The high soil conductivity at S1 could be due to the high clay content in the top soil (Table 1) (Gebbers et al., 2009; Rhoades et al., 1999). The EC values of S1 can be divided into two areas on the map, one with high EC (>200 mS m^{-1}) and one with low EC (<200 mS m^{-1}). The results obtained on S1 with a coil spacing of 0.5 m indicate a higher conductivity than with a coil spacing of 1.0 m.

Negative EC values were recorded at 0.5 m coil distance (these values are not shown in the maps, Figure 2). This is probably due to the fact that the EM38-MK2 was at a height of about 0.25–0.40 m above the ground during the measurement, while the effective depth when measuring with 0.5 and 1.0 m coil spacing is 0.75 and 1.50 m. Due to the distance between the device and the ground, a significant portion of the transmitted signal measured with 0.5 m coil spacing cannot reach the ground (Heil & Schmidhalter, 2017). Therefore, EC values determined with 0.5 m coil spacing are unreliable and were not used to analyse the salinity of the topsoil.

The maximum EC values in the paddy fields of the case studies sites (S1–S6) were below 300 mS m^{-1} for both coil distances (Table 1). According to the FAO (2022) classification of saline soils, site S2, S5 and S6 are non-saline (0–200 mS m^{-1}) when measured at 1 m coil spacing and other sites are slightly saline (200–400 mS m^{-1}). The highest soil salinity (EC = 261.3 mS m^{-1}) occurs near the coast in the centre of site S4.

Soil electrical resistivity mapping with ARES II

Mean electrical resistivity was calculated from 3D resistivity data to generate topsoil resistivity maps. The topsoil resistivity was assessed with ARES II to verify EC results obtained with the EM38-MK2 and to evaluate topsoil salinity on a field scale.

The topsoil resistivity maps (Figure 3) show a similar distribution of soil salinity in the rice fields as the EC maps, with the similarity being strongest in two double-cropped rice fields,

S2 and S3, whereas resistivity at S1 and S4 does not show the clear patterns seen in the EC maps (Figure 2). Here, the maps indicate near uniform resistivity across the fields, particularly at 4 m electrode spacing which results from reduced resolution caused by increased distance between electrodes. Wider electrode distances cause a decrease in the number of measurements (Loke, 2021), so that a larger soil volume is integrated into the calculated topsoil resistivity (Gebbers et al., 2009). This leads to reduced variation of topsoil resistivity as seen at the four study sites.

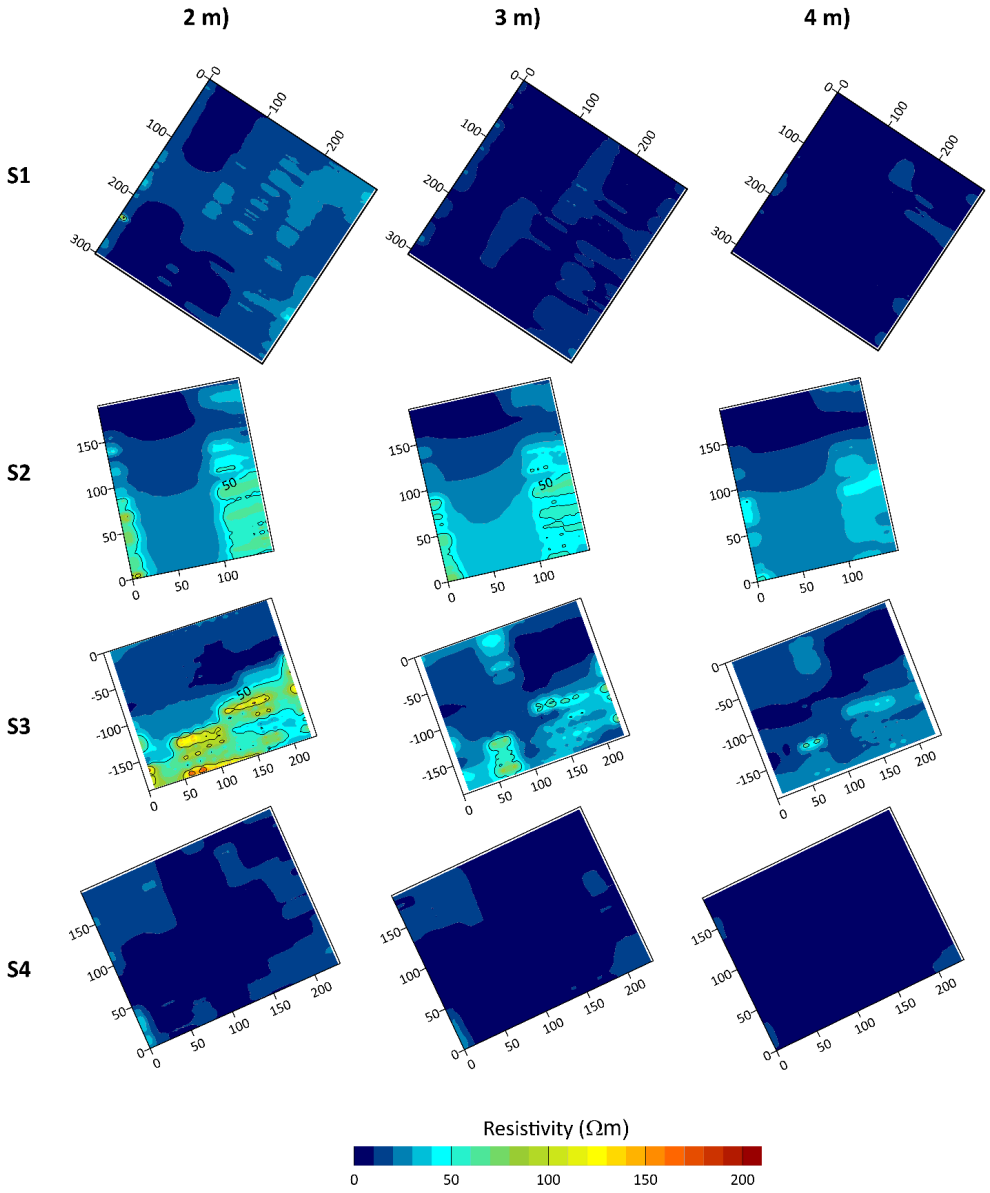

Figure 3 Topsoil resistivity contour maps from ARES II at 2, 3 and 4 m electrode spacings on four rice paddy fields from the case-study sites. The maps are oriented to true North. The axes are in metres and the contour interval is 10 Ωm.

Topsoil resistivity at S1 and S4 was relatively low with mean resistivities varying from 3.7 to 14.4 Ωm (Table 1). Increased resistivity was found at S2, S3 and S6, with mean resistivity ranging from 15.6 to 35.5 Ωm. The highest resistivity, 248.4 Ωm, was recorded at site S6 with 1 m electrode spacing (Table 1).

According to Samouëlian et al. (2005), resistivity lower than 3 Ωm indicates soil salinity. The most saline topsoil among case study sites was found at S4, where minimum resistivity ranged from 3.3 to 1.8 Ωm at all electrode spacings. This is consistent with EC maps of site S4, where highest EC values were measured.

Comparison of EM38-MK2 and ARES II data sets

We compare topsoil EC measured with EM38-MK2 at a coil distance of 1.0 m and topsoil resistivity measured with the ARES II at different electrode spacings firstly by comparing a single profile section and secondly on field scale.

The arrangement of the ERT profile sections and EM38-MK2 measurement on the fields was different. The distance between ERT profiles varied from 20 to 120 m depending on the layout of the fields, whereas the distance between EM38-MK2 measurement lines was 5 m. Therefore, to reduce errors caused by the interpolation into soil salinity maps, we compare values from a single section where both, topsoil resistivity with ARES II and topsoil EC with EM38-MK2, were measured. For this, resistivity of the first profile section (Base line, Figure 1b) of the six study sites was selected. Baseline data were extracted at 20 m intervals to correlate the resistivity of ARES II and EC of EM38-MK2 measurement.

Resistivity data obtained from triple-cropped rice fields, S1 and S5, were weakly correlated with topsoil EC at all electrode spacings (Table 2) and predictability was low ($R^2 < 0.48$). For these fields, resistivity was nearly homogenous along the base lines as indicated by the relatively steep slopes of the regressions. Predictability for EM38-MK2 readings through ARES II readings was better for sites S2, S3, S4 and S6 ($R^2 > 0.55$), which show a greater variation of topsoil resistivity (Figure 4; Table 2).

Table 2. Correlation between EC from EM38-MK2 and resistivity from ARES II measurement of the base line profile and soil salinity maps at different electrode spacings at six sites in the case study areas.

Location	S1			S2			S3			S4			S5		S6	
Electrode spacing	2 m	3 m	4 m	2 m	3 m	4 m	2 m	3 m	4 m	2 m	3 m	4 m	1 m	2 m	1 m	2 m
Correlation between EC and resistivity data of the base line																
R^2	0.48	0.17	0.36	0.74	0.74	0.79	0.55	0.55	0.58	0.74	0.76	0.56	0.25	0.24	0.80	0.77
Slope	-5.89	-1.69	-4.05	-3.21	-2.42	-2.63	-0.51	-1.55	-4.21	-1.43	-1.57	-1.93	-1.91	-2.37	-1.28	-1.12
Intercept	217.75	188.95	198.78	120.92	107.52	114.00	102.12	118.24	136.69	166.44	166.69	168.81	105.88	111.05	83.14	84.37
Correlation between EC and resistivity data from the maps																
R^2	0.01	0.13	0.12	0.51	0.76	0.84	0.26	0.01	0.03	0.11	0.25	0.45	0.04	0.02	0.11	0.19
Slope	-0.93	-4.63	-4.43	-0.86	-1.38	-2.30	-0.50	-0.21	-1.06	-3.28	-7.48	-20.24	-0.46	-0.38	-0.13	-0.17
Intercept	154.31	188.39	186.13	71.21	86.51	95.54	108.33	98.64	108.77	184.19	198.58	224.87	133.20	131.14	62.23	63.09

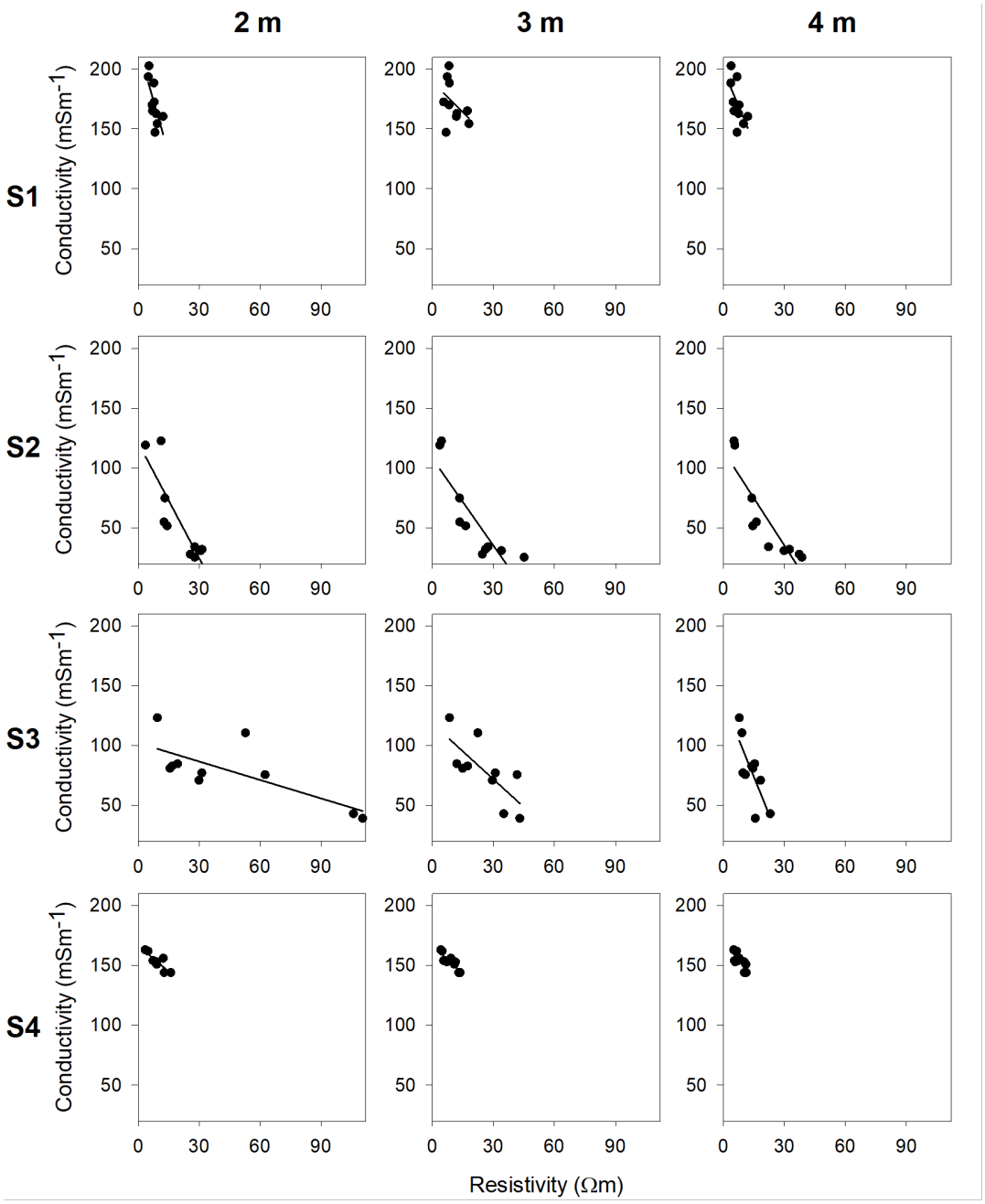

Figure 4 Predictability of EM38-MK2 readings (topsoil EC) via ARESII data (topsoil resistivity) of the base line (Figure 1) at electrode spacings of 2, 3 and 4 m at sites S1–S4.

ARES II data from the base lines have a higher degree of predictability for EM38-MK2 readings when they originate from double-cropped and single-cropped rice fields (S2, S3, S4 and S6), where sand content was relatively high (>70%) (Table 1). Whereas, predictability is compromised with data obtained from triple-cropped rice fields with low sand content (24.5% at S1).

For ARES II data to be used to replace EM38-MK2 measurements for topsoil salinity determination, the two data sets need to correlate at field scale. Therefore, data from EC and resistivity maps were extracted at the same grid size (50 × 50 m) for six case study sites at different ARES II electrode spacings and regressed against each other. Predictability was generally low with an R2 of less than 0.45 (Table 2) with the exception of S2, where R2 ranged from 0.51 to 0.84. Compared with the base line data, the data sets extracted from the maps correlated only weakly, probably owing to the fact that depending on the layout and size of the fields, only 3–7 ARES II profiles were produced at each site ranging in distance from about 20 to 120 m, whereas the EM38-MK2 distance between measurement lines was about 5 m. Therefore, ARES II renders a much smaller topsoil salinity data density than EM38. Thus, the accuracy of the ARES II data for topsoil EC is limited and cannot replace the EM38-MK2 in assessing the horizontal variation of topsoil salinity at large scales.

Relationship between topsoil salinity and land-use types

To investigate a potential link between land-use patterns and topsoil salinity, topsoil EC was measured with the EM38-MK2 at 14 fields differing in land-use, including triple-cropped rice, triple-cropped/double-cropped rice, double-cropped rice, single-cropped rice, and shrimp farming (Figure 5a). The double/triple-cropped rice fields were fields where the number of rice crops per year depends on the availability of irrigation water in a given year.

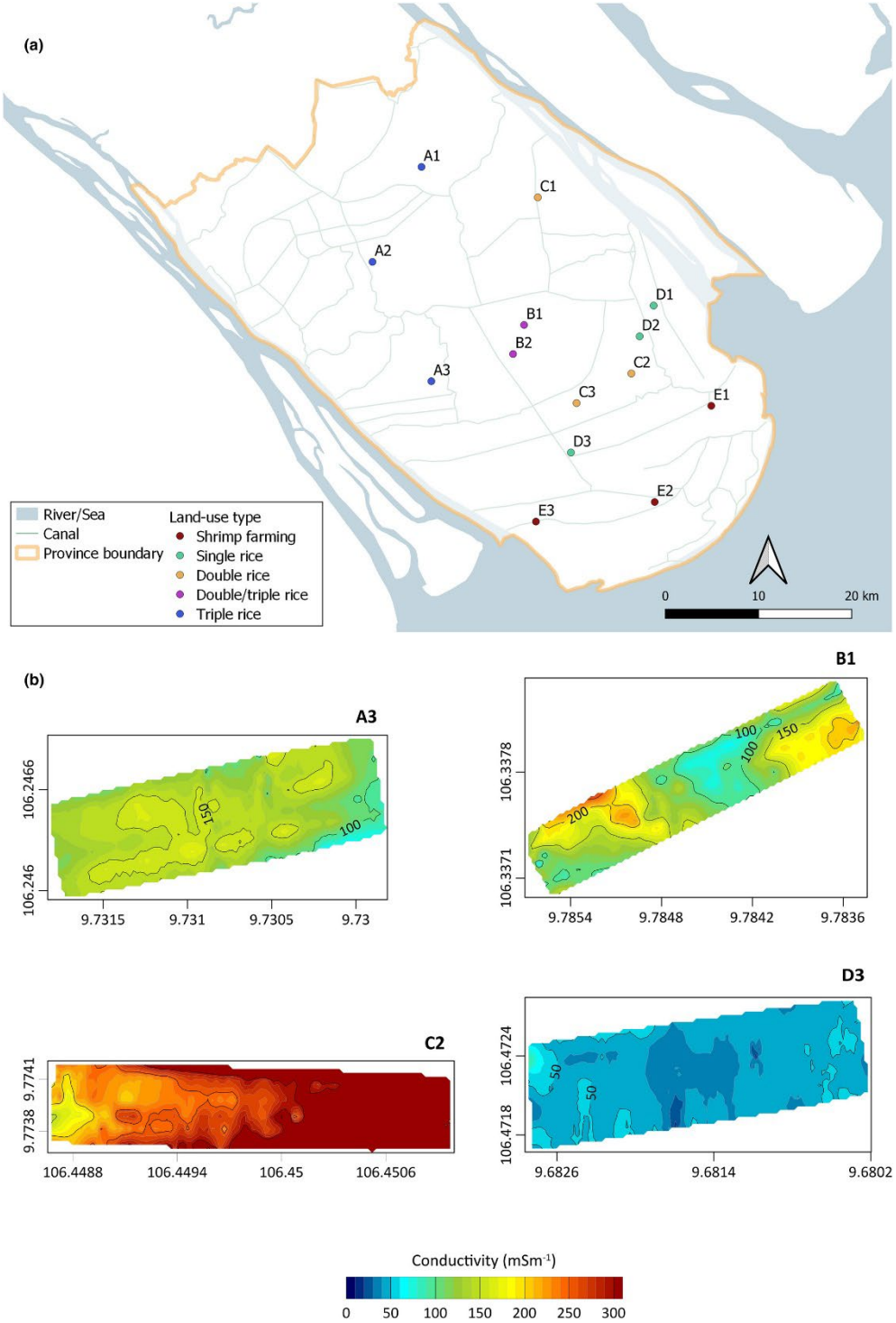

Figure 5 Soil electrical conductivity of different land-use types. (a) measurement locations, (b) topsoil EC at locations representing triple-rice cropping (A3), double/triple-rice cropping (B1), double-rice cropping (C2) and single- rice/year (D3). The axes are displayed in the UTM coordinate system with coordinates given in metres.

Figure 5b shows the topsoil EC maps of four typical rice production types in the study area. The highest EC values (>300 mS m^{-1}), indicating slightly saline soil, were found in C2 under double-rice cropping. In contrast, EC values of <100 mS m^{-1} in D3 under single-rice cropping indicate that the topsoil is not saline. Soil salinity level in the triple-cropped and double-cropped/triple-cropped rice fields were similar, with EC values below 200 mS m^{-1}.

The EC values of the topsoil under five land-use types in the case study area are shown in Figure 6 to assess the relationship between land-use types and topsoil salinity. As expected, the topsoil of shrimp farms was significantly more saline than the rice fields, except for fields that were double-cropped with rice which showed a mean soil salinity above 300 mS m^{-1}, which represents slightly saline soil (FAO, 2022). Except for single-cropped rice fields that are only cultivated in the rainy season (Chen et al., 2011; Sakamoto et al., 2006) and thus not prone to be affected by salinity, the type of rice production seems not to be a determinant of topsoil salinity. Double-cropped rice fields face a higher risk to be contaminated with saline water through irrigation than other rice farming systems because of their proximity to canals carrying saline water (see Figure 5a).

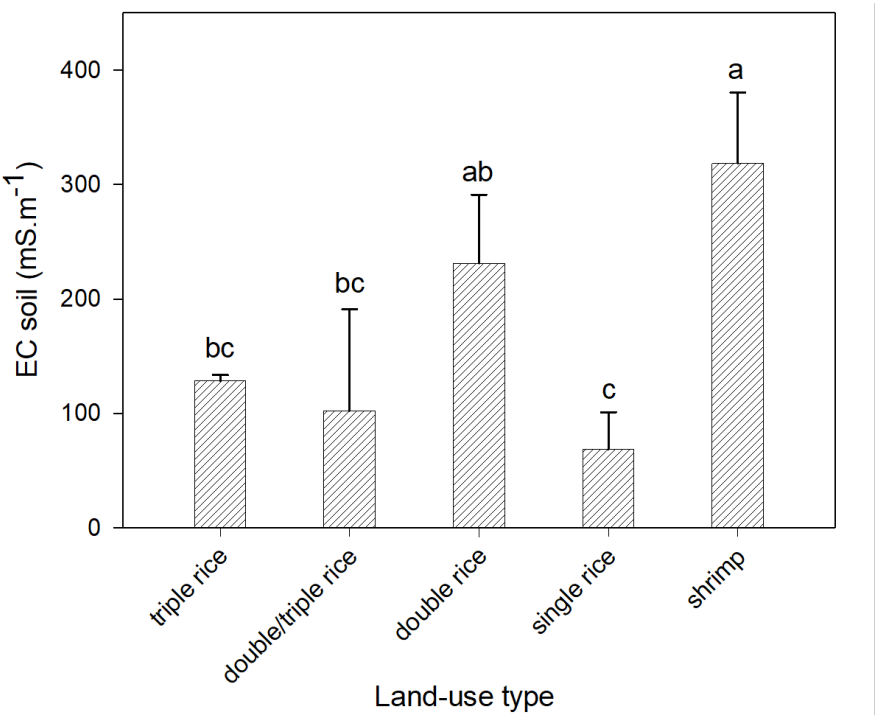

Figure 6 Electrical conductivity of topsoil under five different land-use types in the study area of Tra Vinh province. The error bars indicate the standard deviation and the letters above error bars indicate significant differences.

CONCLUSIONS

Topsoil salinity was investigated for the first time in the Tra Vinh province of the VMD using geophysical methods with the aim of finding promising methods for monitoring topsoil salinity. Compared with ARES II, the EM38-MK2 offers better resolution for mapping topsoil salinity in large scale areas such as agricultural fields. It is a robust instrument that allows rapid horizontal measurement of EC and is accurate enough to detect spatial changes in EC in agricultural fields. Thus, it allows surface water fluxes and microrelief to be detected by high EC values on conductivity maps. However, EM38-MK2 does not provide information about deeper soil layers and the detail of soil salinity in different depth layers. ARES II, on the other hand, proved to be a powerful tool for investigating the vertical distribution of salt in the soil.

While the large number of electrical resistivity measurements in the field was challenging and time-consuming, EM38-MK2 proved to be a more manageable method for the detailed detection of salinity in the topsoil of agricultural fields.

Moreover, the data from both methods showed that there was no acute salt contamination in the topsoil of the rice fields in the case study. The only distinction between land-use systems based on topsoil salinity could be made between shrimp farms and rice farming systems. In rice farming systems, double-cropped rice fields require more efficient irrigation practices to prevent an increase in topsoil salinity.

REFERENCES

Adam, I., Michot, D., Guero, Y., Soubega, B., Moussa, I., Dutin, G., & Walter, C. (2012). Detecting soil salinity changes in irrigated Vertisols by electrical resistivity prospection during a desalinisation experiment. *Agricultural Water Management*, 109, 1–10. https://doi.org/10.1016/j.agwat.2012.01.017

B. Allred, J. J. Daniels, & M. R. Ehsani (Eds.). (2008). Handbook of agricultural geophysics (1st ed.). *CRC Press*. https://doi.org/10.1201/9781420019353

Araya Vargas, J., Gil, P. M., Meza, F. J., Yáñez, G., Menanno, G., García-Gutiérrez, V., Luque, A. J., Poblete, F., Figueroa, R., Maringue, J., Pérez-Estay, N., & Sanhueza, J. (2021). Soil electrical resistivity monitoring as a practical tool for evaluating irrigation systems efficiency at the orchard scale: A case study in a vineyard in Central Chile. *Irrigation Science*, 39, 123–143. https://doi.org/10.1007/s00271-020-00708-w

CGIAR Research Program on Climate Change, Agriculture and Food Security—Southeast Asia (CCAFS SEA). (2016). Assessment report: The drought and salinity intrusion in the Mekong River Delta of Vietnam. CGIAR Research Program on Climate Change, Agriculture and Food Security (CCAFS). https://ccafs.cgiar.org/resources/publications/drought-and-salinity-intrusion-mekong-river-delta-vietnam-assessment

Chen, C., Nguyen, T. S., Chang, L., & Chen, C. (2011). Monitoring of soil moisture variability in relation to rice cropping systems in the Vietnamese Mekong Delta using MODIS data. *Applied Geography*, 31(2), 463–475. https://doi.org/10.1016/j.apgeog.2010.10.002

Cimpoiaşu, M. O., Kuras, O., Pridmore, T., & Mooney, S. J. (2020). Potential of geoelectrical methods to monitor root zone processes and structure: A review. *Geoderma*, 365, 114232. https://doi.org/10.1016/j.geoderma.2020.114232

Food and Agriculture Organization of the United Nations. (2022). Saline soils and their management. Accessed November 24, 2022. https://www.fao.org/3/x5871e/x5871e04.htm

Gebbers, R., Lück, E., Dabas, M., & Domsch, H. (2009). Comparison of instruments for geoelectrical soil mapping at the field scale. *Near Surface Geophysics*, 7(3), 179–190. https://doi.org/10.3997/1873-0604.2009011

Heil, K., & Schmidhalter, U. (2015). Comparison of the EM38 and EM38-MK2 electromagnetic induction-based sensors for spatial soil analysis at field scale. *Computers and Electronics in Agriculture*, 110, 267–280. https://doi.org/10.1016/j.compag.2014.11.014

Heil, K., & Schmidhalter, U. (2017). The application of EM38: Determination of soil parameters, selection of soil sampling points and use in agriculture and archaeology. *Sensors*, 17(11), 2540. https://doi.org/10.3390/s17112540

Hens, L., Vromant, N., Nguyen, T., & Nguyen, T. H. (2009). Salination of surface water, groundwater, and soils in the shrimp farming areas of the coastal Cai Nuoc district, South Vietnam. *International Journal of Environmental Studies*, 66(1), 69–81. https://doi.org/10.1080/00207230902760192

Herrero, J., Ba, A. A., & Aragüés, R. (2003). Soil salinity and its distribution determined by soil sampling and electromagnetic techniques. *Soil Use and Management*, 19(2), 119–126. https://doi.org/10.1111/j.1475-2743.2003.tb00291.x

Herrero, J., & Hudnall, W. H. (2014). Measurement of soil salinity using electromagnetic induction in a paddy with a densic pan and shallow water table. *Paddy and Water Environment*, 12, 263–274. https://doi.org/10.1007/s10333-013-0371-5

Jadoon, K. Z., Moghadas, D., Jadoon, A., Missimer, T. M., Al-Mashharawi, S. K., & McCabe, M. (2015). Estimation of soil salinity in a drip irrigation system by using joint inversion of multicoil electromagnetic induction measurements. *Water Resources Research*, 51(5), 3490–3504. https://doi.org/10.1002/2014WR016245

Lam, V. T., Tran, T., & Ho, H. L. (2020). Soil and water quality indicators of diversified farming systems in a saline region of the Mekong Delta, Vietnam. *Agriculture*, 10(2), 38. https://doi.org/10.3390/agriculture10020038

Lesch, S. M., Herrero, J., & Rhoades, J. D. (1998). Monitoring for temporal changes in soil salinity using electromagnetic induction techniques. *Soil Science Society of*

America Journal, 62(1), 232–242. https://doi.org/10.2136/sssaj1998.03615995006200010030x

Loke, M. H. (2021). Tutorial: 2-D and 3-D electrical imaging surveys. Accessed August 17, 2022. https://www.researchgate.net/publication/264739285_Tutorial_2-D_and_3-D_Electrical_Imaging_Surveys

Nguyen, K. A., Liou, Y. A., Tran, H. P., Hoang, P. P., & Nguyen, T. H. (2020). Soil salinity assessment by using near-infrared channel and vegetation soil salinity index derived from Landsat 8 OLI data: A case study in the Tra Vinh province, Mekong Delta, Vietnam. *Progress in Earth and Planetary Science*, 7, 1. https://doi.org/10.1186/s40645-019-0311-0

Nguyen, L. D., Nguyen, T. V. K., Nguyen, D. V., Tran, A. T., Nguyen, H. T., Heidbüchel, I., Merz, B., & Apel, H. (2021). Groundwater dynamics in the Vietnamese Mekong Delta: Trends, memory effects, and response times. *Journal of Hydrology: Regional Studies*, 33, 100746. https://doi.org/10.1016/j.ejrh.2020.100746

Nguyen, T., Vromant, N., Nguyen, T. H., & Hens, L. (2008). Soil salinity and sodicity in a shrimp farming coastal area of the Mekong Delta, Vietnam. *Environmental Geology*, 54, 1739–1746. https://doi.org/10.1007/s00254-007-0951-z

Nguyen, T. G., Tran, N. A., Vu, P. L., Nguyen, Q. H., Nguyen, H. D., & Bui, Q. T. (2021). Salinity intrusion prediction using remote sensing and machine learning in data-limited regions: A case study in Vietnam's Mekong Delta. *Geoderma Regional*, 27, e00424. https://doi.org/10.1016/j.geodrs.2021.e00424

Nguyen, V. H., Germer, J., Duong, V. N., & Asch, F. (2023). Soil resistivity measurements to evaluate subsoil salinity in rice production systems in the Vietnam Mekong Delta. *Near Surface Geophysics*, 21(4), 288–299. http://doi.org/10.1002/nsg.12260

Pham, V. H., Nguyen, V. G., Nguyen, A. B., Le, V. H. H., Pham, T. D., Hasanlou, M., & Bui, D. T. (2019). Soil salinity mapping using SAR Sentinel-1 data and advanced machine learning algorithms: A case study at Ben Tre province of the Mekong

River Delta (Vietnam). *Remote Sensing*, 11(2), 128. https://doi.org/10.3390/rs11020128

Rao, S., Lesparre, N., Flores-Orozco, A., Wagner, F., Kemna, A., & Javaux, M. (2020). Imaging plant responses to water deficit using electrical resistivity tomography. *Plant and Soil*, 454, 261–281. https://doi.org/10.1007/s11104-020-04653-7

Rhoades, J. D., Corwin, D. L., & Lesch, S. M. (1999). Geospatial measurements of soil electrical conductivity to assess soil salinity and diffuse salt loading from irrigation. *Geophysical Monograph Series*, 108, 197–215. https://doi.org/10.1029/GM108p0197

Sakamoto, T., Nguyen, N. V., Ohno, H., Ishitsuka, N., & Yokozawa, M. (2006). Spatio-temporal distribution of rice phenology and cropping systems in the Mekong Delta with special reference to the seasonal water flow of the Mekong and Bassac rivers. *Remote Sensing and Environment*, 100(1), 1–16. https://doi.org/10.1016/j.rse.2005.09.007

Samouëlian, A., Cousin, I., Tabbagh, A., Bruand, A., & Richard, G. (2005). Electrical resistivity survey in soil science: A review. *Soil and Tillage Research*, 83(2), 173–193. https://doi.org/10.1016/j.still.2004.10.004

Silvestri, S., Nguyen, D. N., & Chiapponi, E. (2022). Comment on "Soil salinity assessment by using near-infrared channel and vegetation soil salinity index derived from Landsat 8 OLI data: A case study in the Tra Vinh province, Mekong Delta, Vietnam" by Kim-Anh Nguyen, Yuei-an Liou, Ha-Phuong Tran, phi-Phung Hoang and Thanh-hung Nguyen. *Progress in Earth and Planetary Science*, 9, 45. https://doi.org/10.1186/s40645-022-00490-7

Tan, X., Shao, D., & Liu, H. (2014). Simulating soil water regime in lowland paddy fields under different water managements using HYDRUS-1D. *Agricultural Water Management*, 132, 69–78. https://doi.org/10.1016/j.agwat.2013.10.009

Tran, D. A., Tsujimura, M., Pham, H. V., Nguyen, T. V., Ho, L. H., Le Vo, P., Ha, K. Q., Dang, T. D., van Binh, D., & Doan, Q. V. (2022). Intensified salinity intrusion in coastal aquifers due to groundwater over extraction: A case study in

the Mekong Delta, Vietnam. *Environmental Science and Pollution Research*, 29, 8996–9010. https://doi.org/10.1007/s11356-021-16282-3

Tran, P. H., Hoang, P. H., Nguyen, T. H., Duong, B. M., Danh, M., Dang, H. V., Phan, T. B. T., Tran, V. T., Nguyen, T. N., Tran, A. P., & Ngo, H. D. L. (2020). Assessment of changes in the structure land use in Tra Vinh Province under the scenarios of climate change and sea level rise. *Vietnam Journal of Science and Technology*, 58(1), 70–83. https://doi.org/10.15625/2525-2518/58/1/13982

Vu, H. T. D., Tran, D. D., Schenk, A., Nguyen, C. P., Vu, H. L., Oberle, P., Trinh, V. C., & Nestmann, F. (2022). Land use change in the Vietnamese Mekong Delta: New evidence from remote sensing. *Science of the Total Environment*, 813, 151918. https://doi.org/10.1016/j.scitotenv.2021.151918

Walter, J., Lück, E., Bauriegel, A., Facklam, M., & Zeitz, J. (2018). Seasonal dynamics of soil salinity in peatlands: A geophysical approach. *Geoderma*, 310, 1–11. https://doi.org/10.1016/j.geoderma.2017.08.022

Zarai, B., Walter, C., Michot, D., Montoroi, J. P., & Hachicha, M. (2022). Integrating multiple electromagnetic data to map spatiotemporal variability of soil salinity in Kairouan region, Central Tunisia. *Journal of Arid Land*, 14, 186–202. https://doi.org/10.1007/s40333-022-0052-6

Zörb, C., Geilfus, C. M., & Dietz, K. J. (2018). Salinity and crop yield. *Plant Biology*, 21(1), 31–38. https://doi.org/10.1111/plb.12884

Chapter 4

Mapping saline groundwater under rice-paddy fields in Vietnam's Mekong Delta*

Van Hong Nguyen[1], Jörn Germer[1], Tien Pham Duy[2,3], Folkard Asch[1]

[1] University of Hohenheim, Institute. of Agricultural Sciences in the Tropics (Hans-Ruthenberg Institute), Germany

[2] Faculty of Agriculture and Natural Resources, An Giang University, Vietnam

[3] Vietnam National University, Ho Chi Minh city, Vietnam

ACKNOWLEDGEMENTS

This work has been funded by the Federal Ministry of Education and Research (BMBF, Germany) in the project RiSaWa (project number 031B0724).

Abstract

Climate change, decreased river flow, and land subsidence lead to saltwater intrusion posing a significant threat to rice production in Vietnam's Mekong Delta (VMD), one of the world's largest rice exporting regions. Soil salinity in the VMD can be caused by saltwater intrusion into lowland areas through the canal system, or by capillary rise of water from near surface saline water table, both resulting in salt accumulation in the top soil. Developing appropriate management strategies for adapting rice production systems of the VMD to climate change both in terms of water and salinity management, requires characterizing and subsequently monitoring of the spatial distribution and temporal dynamics of salinity in the near-surface aquifers underneath the rice producing area. The distribution of subsurface salinity was investigated using Electrical Resistivity Tomography in the VMD's province, Tra Vinh, as case study area. Soil salinity was measured for profiles of approximately 300 m length at 44

* The content of this chapter has been submitted to the Journal of Near Surface Geophysics and is currently under review.

locations along geological transects in a case study area. Results show that saline water appears in a shallow depth, particularly along the coast and the lower reaches of rivers. Double-cropped rice fields seem to be more susceptible to salinization via the near-surface aquifer than other rice cropping systems. The study suggests that temporal fluctuations of the near-surface aquifer and the dynamics of the exchange between the river and the shallow aquifer need to be investigated in future research.

Keywords: electrical conductivity, electrical resistivity tomography, ERT, salt water intrusion, soil salinity, shallow groundwater.

INTRODUCTION

Groundwater salinization in the coastal areas of Vietnam's Mekong Delta (VMD) is increasing due to intensive use of Mekong River water in the upper reaches, land subsidence due to unsustainable groundwater extraction, and sea level rise driven by climate change (Sharan et al., 2023; Abd-Elaty, et al., 2022; Pauw, De Louw and Oude Essink, 2012). Groundwater near the surface can rise capillary into the topsoil and reach the root zone, which then impairs agricultural production (Wassmann et al., 2019) and thus endangers the livelihood of rice farmers (Ceuppens et al., 1997, Setiawan et al., 2022). This potential risk to agricultural production and population is underestimated compared to risks associated with deep aquifers (Hoover et al., 2017; Setiawan et al., 2022).

Especially in areas where coastal agriculture is an important sector of the economy and contributes significantly to the global food supply, salinization of near-surface groundwater becomes a geopolitical concern. About 90% of Vietnam’s rice exports originate in the VMD (Schneider and Asch, 2020), making Vietnam one of the largest rice exporters (Hui et al., 2022). Currently, a total area of over 1.7 million ha, accounting for 44% of rice cultivation is threatened by salinization in the VMD (Wassmann et al., 2019).

Thus, it is necessary to have methods and instruments allowing determining and accurately monitoring of the spatial distribution and temporal dynamics of near-surface groundwater salinity. While salinity of near-surface groundwater is not clearly related to land-use types with respect to rice cultivations (Nguyen et al., 2023a), double-cropped rice has been shown

to be prone to topsoil salinity (Nguyen et al., 2023b) at several case study sites in the VMD. However, a small number of case study sites may bias the potential link between land-use types of rice cultivation and salinity, and therefore the number of study sites needs to be increased for a higher coefficient of determination.

Electrical resistivity tomography (ERT) is a well-known geophysical method that has recently been employed e.g. to assess soil moisture in precision agriculture (Rao et al., 2020), plant water uptake (Araya et al., 2021), root zone structure (Cimpoiaşu et al. (2020) and near-surface aquifer salinity below rice paddy fields to help improving water management (Nguyen et al., 2023a). ERT has been proved to be a robust and time-saving method for monitoring spatial and temporal distribution of subsurface salinity (Bauer et al., 2006; de Franco et al., 2009; Grünenbaum et al., 2023).

In this study, the ERT method has been applied for the assessment of near-surface salinity at provincial level in the VMD. The main objective of this study is (1) to assess the distribution of saline water below rice fields, (2) mapping saline water tables, and (3) to analyze if there is a link between saline water tables and land-use types.

MATERIALS AND METHODS

Research area

The survey was carried out along latitude and longitude transects in the coastal province Tra Vinh in the VMD. The province is characterized by a flat topography with elevations of less than 1 m above mean sea level (amsl), similar to most of the VMD (Minderhoud et al., 2019), except for some sand dunes with average elevations varying from 1 to 3 m amsl (Tran, 2020), and in exceptional cases varying from 5 m to 10 m.

As a peninsula, Tra Vinh Province is not only affected by saltwater intrusion from the sea in the southeast-northwest, but also from the two main tributaries in the northeast-southwest direction. These two main intrusion path ways, are taken into account by the latitude and longitude transects. In addition, the longitudinal transect was used also to analyze whether a single transect could be sufficient to map near-surface salinity.

The latitude transects followed the topographic contours formed by the tide-river interactions (Nguyen et al., 2023a), while the longitude transect was chosen centrally in the province between the two arms of the Mekong river (Figure 1). Due to the complexity of the geology in the study area, particularly in the lower part where sand dunes and swamps are present (Nguyen et al., 2020), the longitude transect includes data from four latitude transects in addition to the main data points, S1 to S4 (Figure 1).

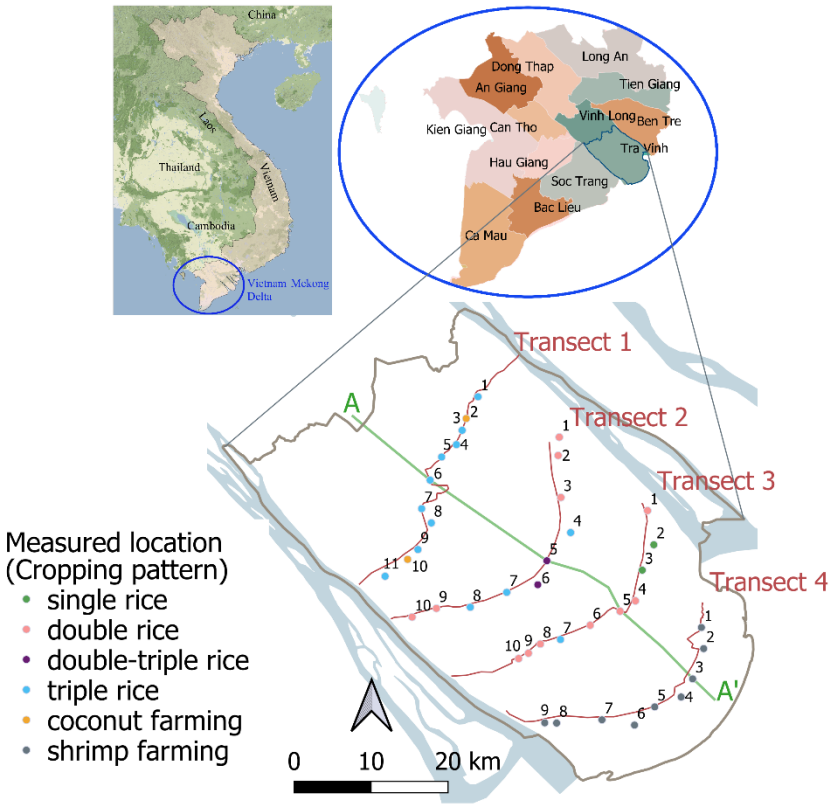

Figure 1 Positions of the survey transects in the Tra Vinh province, Vietnam Mekong Delta. Measurement locations following latitude transects, transect 1 to 4, and longitude transect A-A'.

Subsoil resistivity measurement

Soil resistivity was assessed using data from the ARES II measurement (GF Instruments s.r.o., Czech Republic). Most of the ARES II data was obtained during the dry season of 2020-2021, while the data from S1 and S3 (refer to Figure 1) were collected during the measurement of the dry season of 2019-2020. Measurements were carried out to cover approximately 300 m in length at 4 m electrode spacing with total of 64 electrodes using the

Wenner-Schlumberger configuration, giving an effective measuring depth up to 40 m (Nguyen et al., 2023a).

Resistivity data was interpreted using the inversion software RES2DInv (v.4.10.8, Aarhus GeoSoftware, Denmark), which uses the smoothness-constrained least-squares and finite-element method to produce the "true" resistivity of the subsurface from the apparent resistivity of the measured data. The number of iterations was set at 5 to obtain the best fit between the measured and calculated apparent resistivity data (Loke, 2021). In the RES2DInv program, the final image of the subsurface resistivity is referred to as the "Inverse Model Resistivity Section", which is the main target of the inversion and is used for further geological interpretation (Loke, 2021).

The resistivity obtained from inversion procedure was visualized as contour maps using the Kriging method in the Surfer software v.18.1.186 (Golden Software, LLC).

The subsoil resistivity was investigated following four latitude transects in northeast – southwest direction and a longitude transect in northwest – southeast direction (Figure 1). Along each latitude transect, resistivity was measured at 10 locations with 5 to 8 km distance between them. The resistivity profiles were taken perpendicularly to the latitude transects, whereas this arrangement was not applied for the longitude transect where ERT profiles were measured without predefined orientation. The soil resistivity measurements covered different land-use types, such as rice production systems (including triple rice, double/triple rice, double rice, and single rice cultivation), as well as coconut or shrimp farms (Figure 1).

For spatially explicit 3-D soil resistivity maps across all ERT profiles, resistivity data were extracted at 1-m intervals from the surface to a depth of 40 m. This extraction was done at a distance of 130 m from the beginning of each ERT profile, where the density of measurements is highest and the penetration depth of the signal is deeper compared to the edges of the profiles (Loke, 2021).

Land-use map

A land-use map of rice production systems in Tra Vinh province was obtained using Sentinel-1A synthetic-aperture radar satellite images for the period from November 2020 to December 2021. A set of 14 dual polarization images with 10 m spatial resolution were

collected, recording an annual rice crop cycle and different growth stages. Rice cropping patterns were identified via temporal backscatter coefficient analysis (Mansaray et al., 2017). Images in the Ground Range Detected (GRD) format were processed using the SNAP toolbox (SNAP - ESA Sentinel Application Platform), a standard software for Sentinel imagery and remote sensing image processing (Mansaray et al., 2017). The generated land-use map for the year 2021 was validated using ground-truthed data with a total of 811 points by applying coefficients for overall classification accuracy and the Kappa coefficient.

RESULTS

The assessment of subsurface salinity in the study area was carried out using a series of 44 ERT profiles at sites of different land-use, to map subsurface salinity and identify the land-use resulting in or exposed to the most severe salinity.

ERT profiles at different cropping patterns

The ERT profiles showed resistivity values of 2 Ωm up to 64 Ωm within the first few meters of profile depth, indicating agriculturally used soils with different levels of clay content and different levels of compaction (Samouëlian et al., 2005; Seladji et al., 2010). Highest resistivity (> 28 Ωm) was found in the topsoil layers of double rice and single rice fields located in lower part of the Tra Vinh province (refer to Figure 1). Starting at varying depths, the subsoil of all land-use types showed low resistivity values indicating the presence of near-surface aquifers. Resistivity of less than 3 Ωm indicate saline water (Nguyen et al., 2023a). Resistivity values of less than 1 Ωm were detected in the subsoil of the shrimp and coconut farms (Figure 2). Similar low resistivity values but less widely distributed were also found in the subsoil of double/triple-cropped rice, double and single-cropped rice fields. Resistivity of less than 1 Ωm occurred below 10 m depth at the coconut farm, whereas at the shrimp farm it appears from 4 m depth. In the triple rice-cropped fields, resistivity varied between 1 Ωm to 5 Ωm from 4 m to 40 m depth.

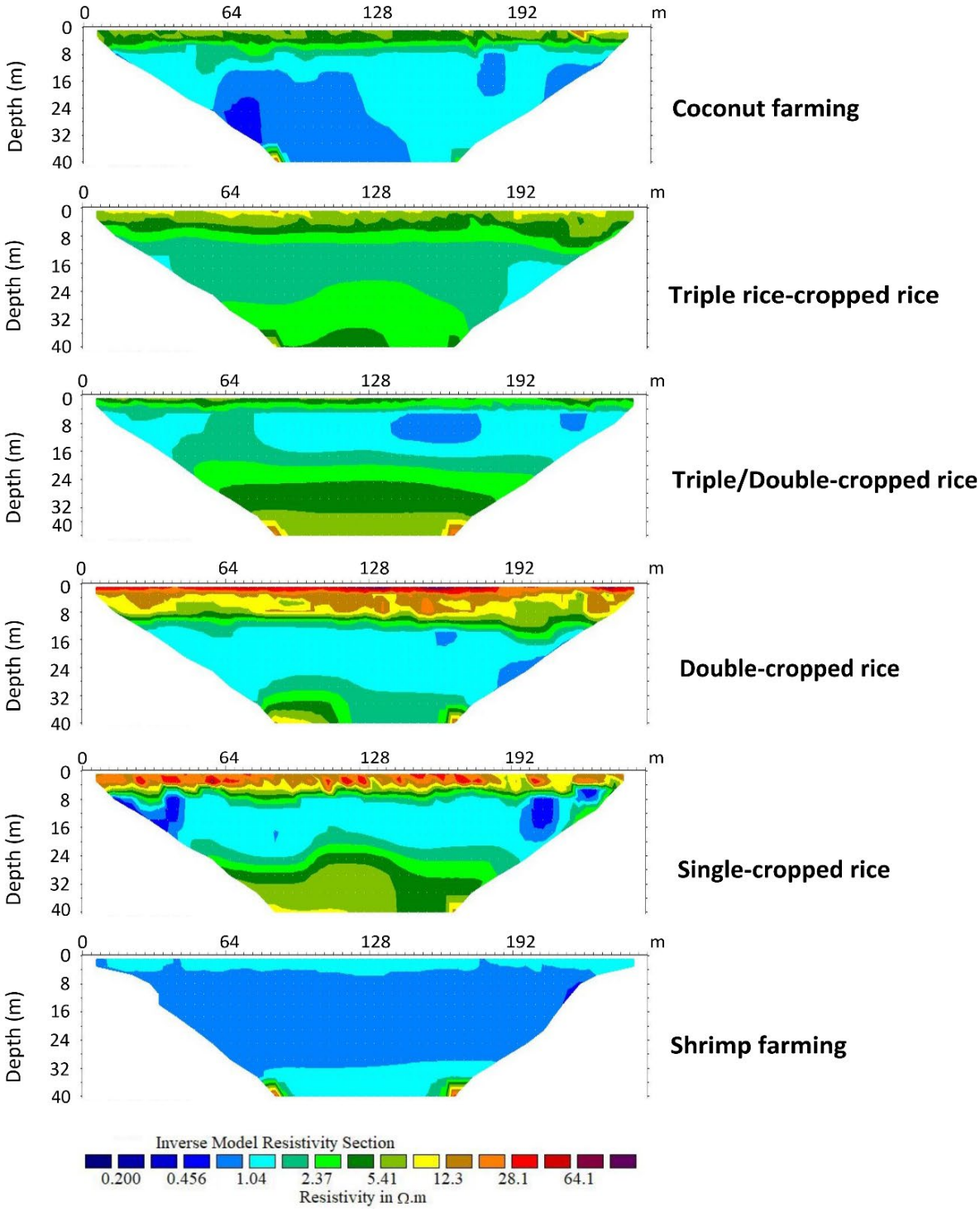

Figure 2 Soil resistivity profiles for typical cropping systems in the Tra Vinh province of the Vietnam's Mekong Delta. From the top, ERT profiles are displayed for sites: 2-Transect 1, 4-Transect 1, 6-Transect 2, 5-Transect 3, 3-Transect 3, and 2-Transect 4.

Mapping saline groundwater along latitude transects

Soil resistivity values less than 3 Ωm have been shown to indicate saline groundwater in the study area of the Tra Vinh province (Nguyen et al., 2023a). Based on this threshold, a saline aquifer was identified that runs through the entire province at a depth of 5 to 20 m as indicated by the isoline of resistivity between 1 and 3 Ωm in Figure 3. Only at transect 4, which is closest to the sea, the saline groundwater (with resistivity values of less than 1 Ωm) was found close to the soil surface and extended to 40m depth. In transect 3 to 1, resistivity values of 1 Ωm were found between 10 m and 20 m depth with no clear position for the saline water table in transect 3 as the isoline for resistivity values of 1 Ωm is scattered across the aquifer (Figure 3). In contrast, in transect 1 and 2 isolines for resistivity values of 1 Ωm and below penetrates the aquifer from the sides forming saline water wedges on the edges of the province. These wedges are most prominent in transect 2, particularly on the east side of the province.

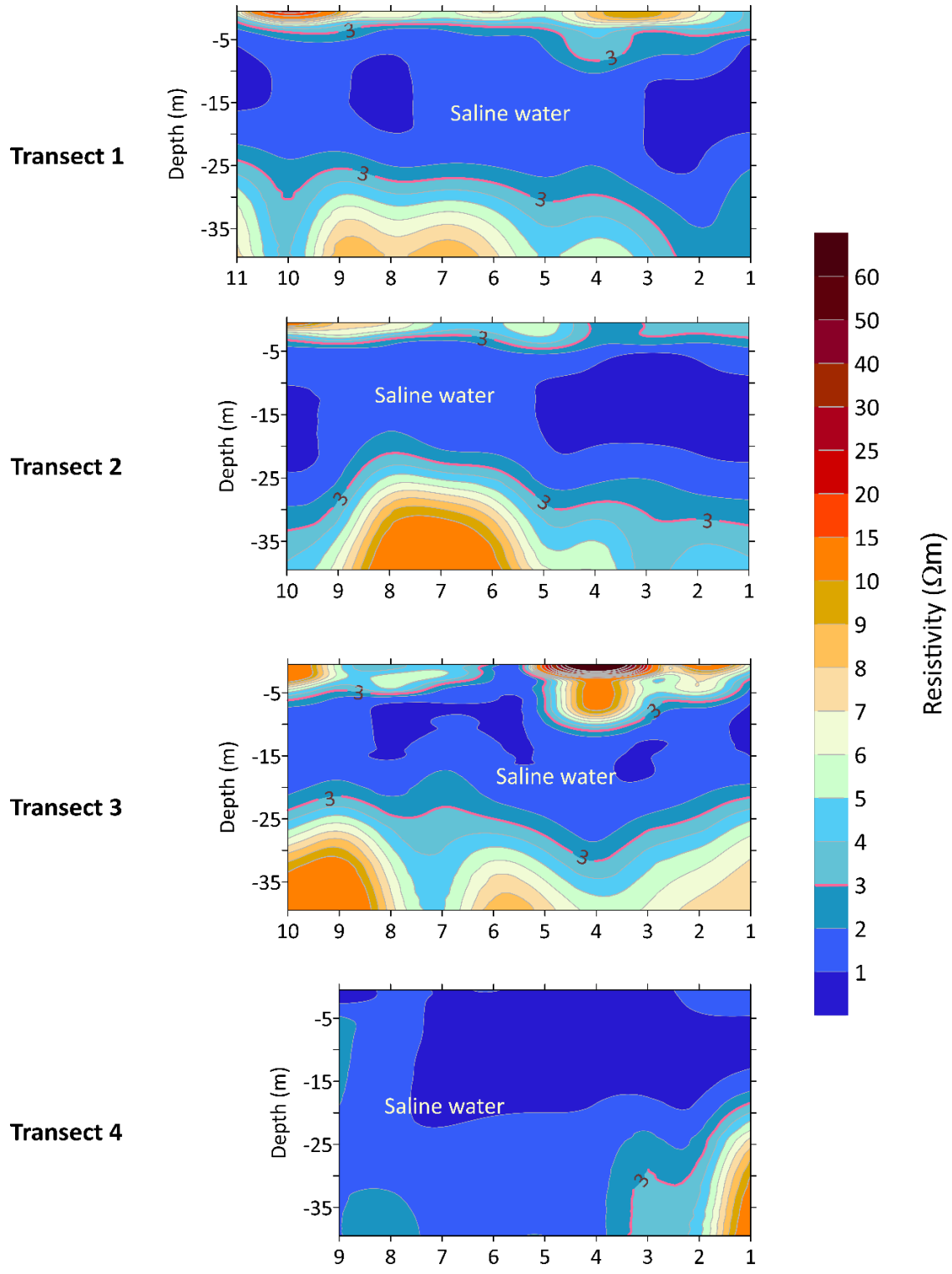

Figure 3 Vertical resistivity profiles along the four latitude transects in the Tra Vinh province of the Vietnamese Mekong Delta. The numbers on the x-axes represent the locations of the ERT profiles along latitude transects referred to in Figure 1. The resistivity of less than 3 Ωm indicates saline aquifers.

Table 1. Statistical summary of soil resistivity (Ωm) along the A-A' transect, including data from S1 to S4 and four sites 6, 5, 5, 3 of Transect 1, 2, 3 and 4 respectively (see Figure 1). Data of S1 and S3 were included from Nguyen et al. (2023a).

Location	Mean	Std Dev	Max	Min	Median
S1	2.44	1.53	8.85	1.44	2.08
6_Transect 1	3.17	2.33	8.27	1.17	1.98
5_Transect 2	2.43	1.76	6.61	0.91	1.55
S2	1.92	1.44	4.90	0.72	1.23
S3	6.14	4.33	12.84	1.31	5.61
5_Transect 3	2.68	2.12	7.49	1.03	1.50
S4	3.57	2.64	8.29	0.92	2.62
3_Transect 4	2.06	1.50	4.24	0.50	1.65

Saline groundwater table along longitude transect

Resistivity measurements were conducted along a longitude transect to evaluate the distribution of salinity of near surface aquifers from the sea landward.

The saline groundwater table along the A-A' transect varies from the surface near the coast to a depth of about 5 m inland (Figure 4). The thickness of the saline aquifer tends to increase towards the north of the province, from 25 m near the coast to 35 m inland. Along transect A-A', the thickness of the saline aquifer displays the shape of a bottleneck at the position of S3, where the thickness of the saline aquifer decreases sharply to less than 15 m. This bottle neck shape seems to represent the separation of the saline aquifer into two parts: from S3 to the upstream and from S3 to the sea.

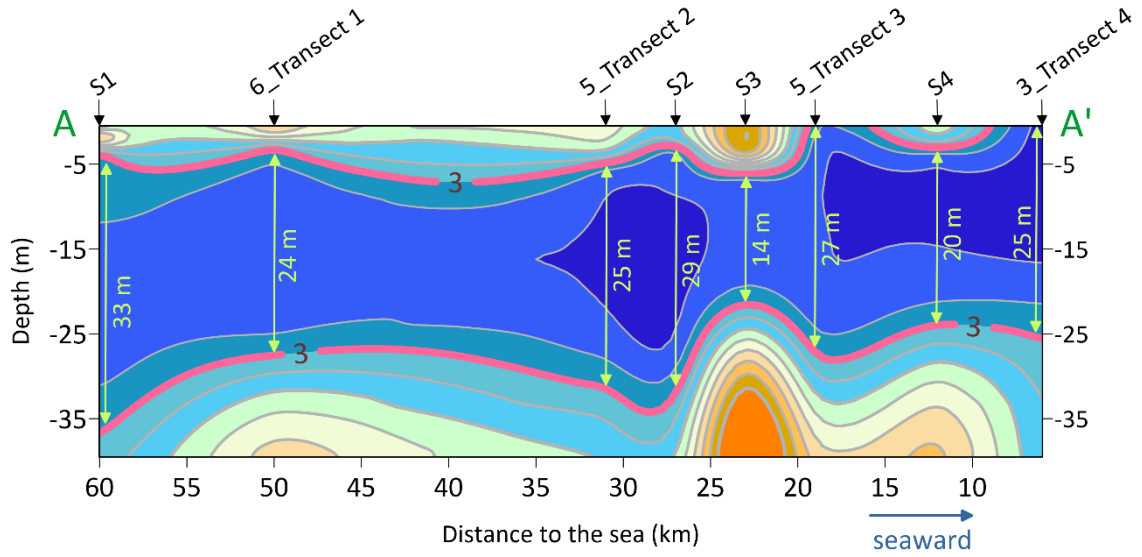

Figure 4 Thickness of the saline near-surface aquifer along A-A' transect (refer to Figure 1). The upper and lower boundaries of saline near-surface aquifer are determined using resistivity of less than 3 Ωm. Green numbers indicate the thickness of the saline aquifers along A-A' transect.

Similar pattern can be seen in Figure 5, representing resistivity values of saline water (resistivity < 3 Ωm) along the A-A' transect. The saline aquifer can be divided between S2 and S3 into two distinct parts. The upper part reaches from around 27 km distance to the sea to upper boundary of the province, while the lower part covers the area from 23 km to the sea. The resistivity in both parts increases towards the North of the province. On the other hand, the resistivity of ground water identified as saline increases from site 3 of transect 4 from lowest resistivity at 0.50 Ωm to 1.31 Ωm at S3, whereas at the upper part resistivity starts at 0.72 Ωm at S2 and increases to 1.44 Ωm at S1 (Table 1).

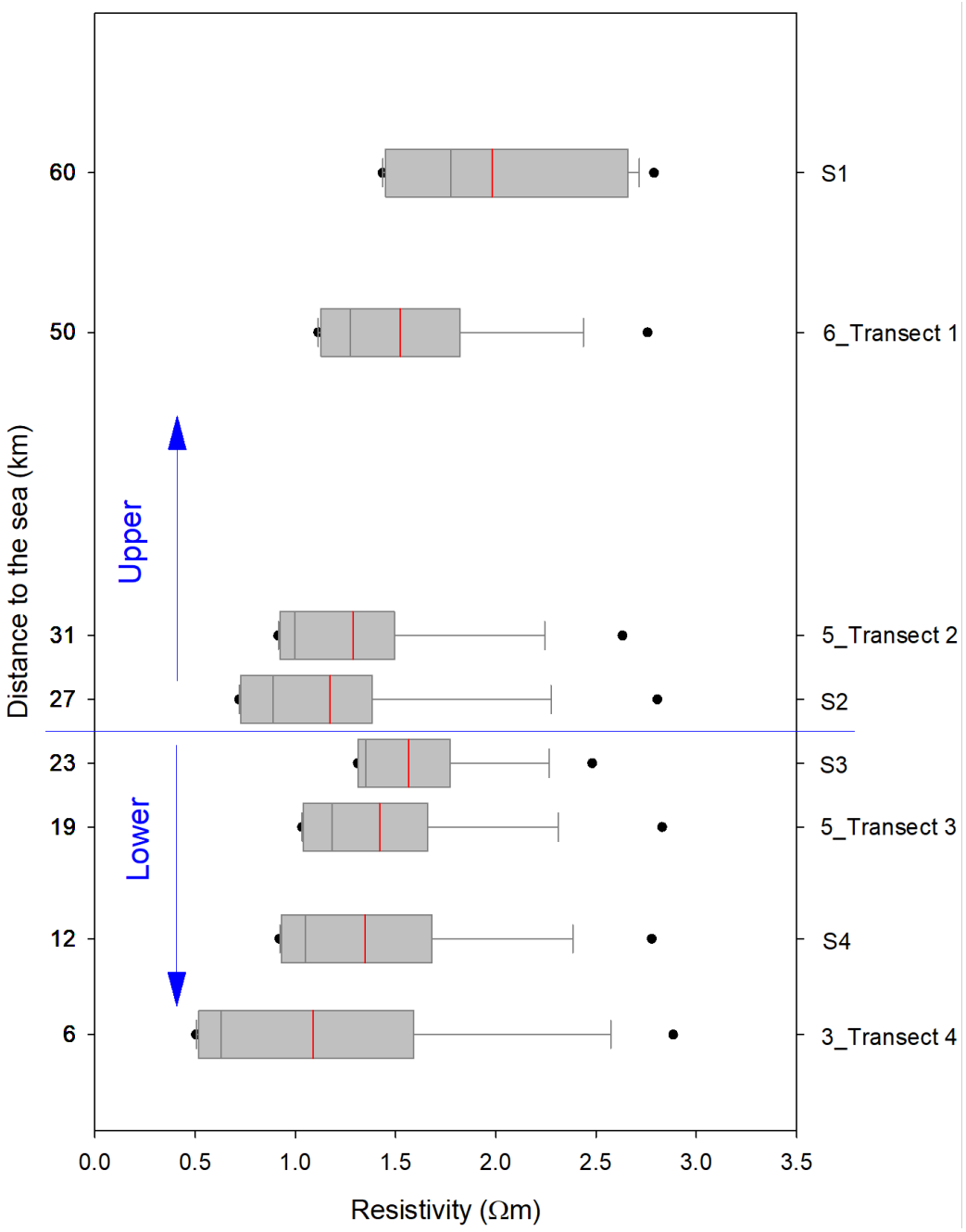

Figure 5 Resistivity distribution of saline groundwater (resistivity < 3 Ωm) of locations along A-A' transect (refer to Figure 1). The gray line of the boxplot indicates median, red line is mean resistivity of saline water. Resistivity of saline water separated the A-A' transect as lower and upper parts.

Spatial distribution of saline groundwater

The spatial distribution of saline groundwater in the case study area is illustrated by resistivity contour maps at depths from 1 m to 40 m in Figure 6. At 2 m depth, the resistivity of less than 3 Ωm already appears and distributed along transect 4 and along the rivers of both sides of the peninsula. Whereas, high resistivity was observed in the center section of transect 3 with resistivity values larger than 10 Ωm.

Throughout the province, resistivity less than 3 Ωm could be measured at depths ranging from 5 m to 25 m. Furthermore, it can be seen from the contour map that low resistivity at 1 m depth indicates high salinity under double rainfed rice and a small part of triple rice fields in the northeast of the province. This low resistivity still exists but is smaller at 2 m depth compared to 1 m depth.

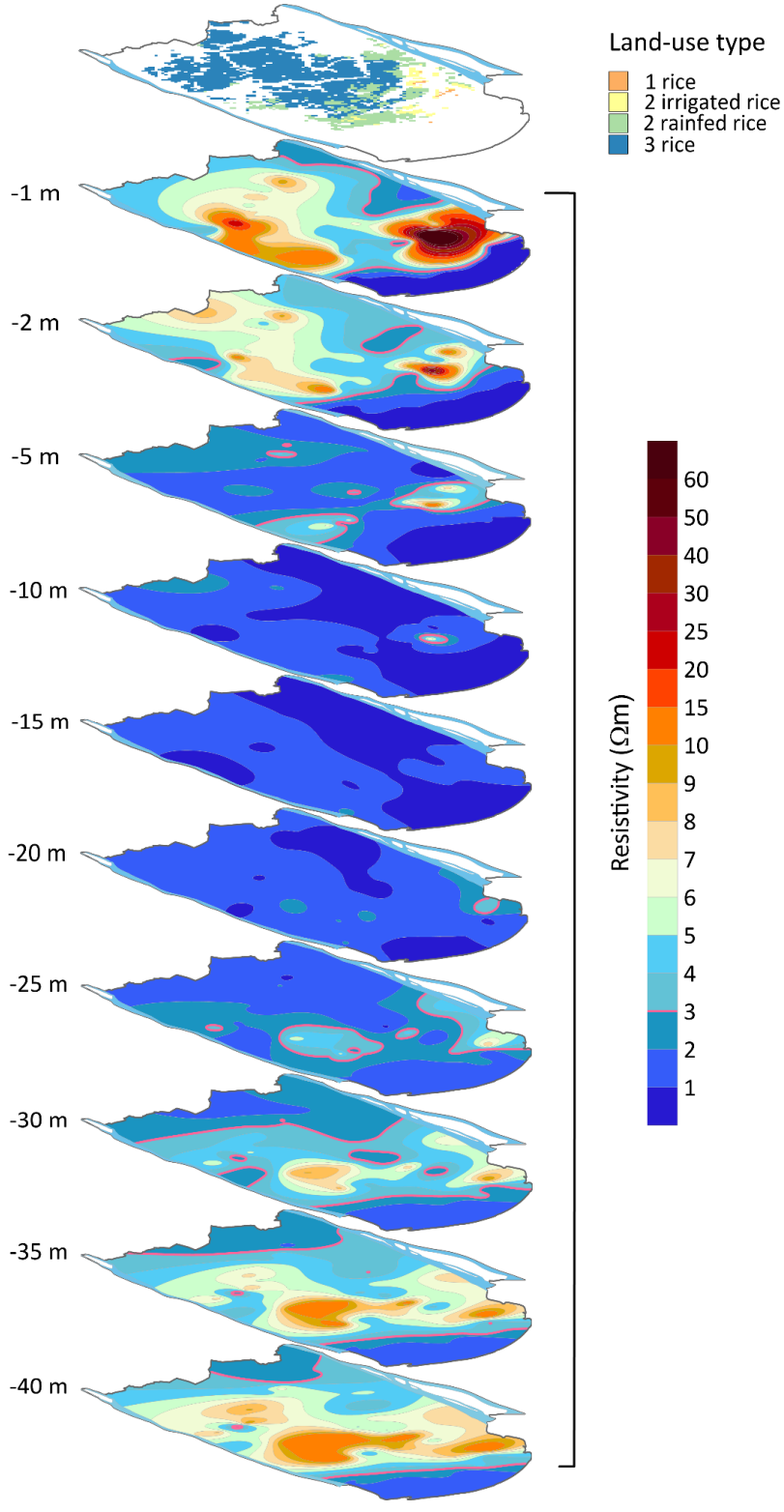

Figure 6 Maps of land-use types and the horizontal distribution of soil electrical resistivity in Tra Vinh province from 1 m to 40 m depths. Contour interval is 1 for resistivity less than 10 Ωm, and 5 for resistivity greater than 10 Ωm. Blue contours less than 3 Ωm represent saline aquifers.

Evaluating the quality of vertical and spatial maps

The performance of the Kriging method in subsurface resistivity mapping for four vertical maps along latitudinal transects and spatial map at different depths was evaluated by cross-validation (see Figure 7 and Table 2). Cross-validation errors were calculated using a subset of 100 data points for each latitude map and 40 data points for each horizontal map.

Figure 7 shows the relation between estimated and measured values using Kriging method. Estimation using Kriging gets better as the best fitted line gets closer to the reference line (ESRI, 2023).

Table 2 summarizes the cross-validation parameters typically used to assess the Kriging mapping quality. The root mean square of the predicted errors shows how close the observed and predicted values are. The rank coefficient, ranging from -1 to 1, expresses the relationship between observed and predicted values. A positive rank coefficient indicates that both observed and predicted values follow the same, whereas a negative coefficient suggests a contrasting trend. Rank coefficient closer to 1 and -1 indicate a strong correlation (Surfer® (Golden Software, LLC)).

According to the cross-validation results (Table 2), the performance of kriging is better for vertical maps than for spatial maps. The spatial maps have low rank coefficients (< 0.21), while the root mean square error and standard deviation values are generally higher than for the vertical maps.

The vertical maps, on the other hand, with dense data points spaced about 5 to 8 km apart, have high rank coefficients (> 0.90) while other parameters are lower than 1, indicating good prediction. An exception was found in transect 3, which shows high values of root mean square error and standard deviation (> 2.20 Ωm) (Figure 7 and Table 2), representing the high values of resistivity (see transect 3 - Figure 3), which tend to be underpredicted by Kriging (ESRI, 2023).

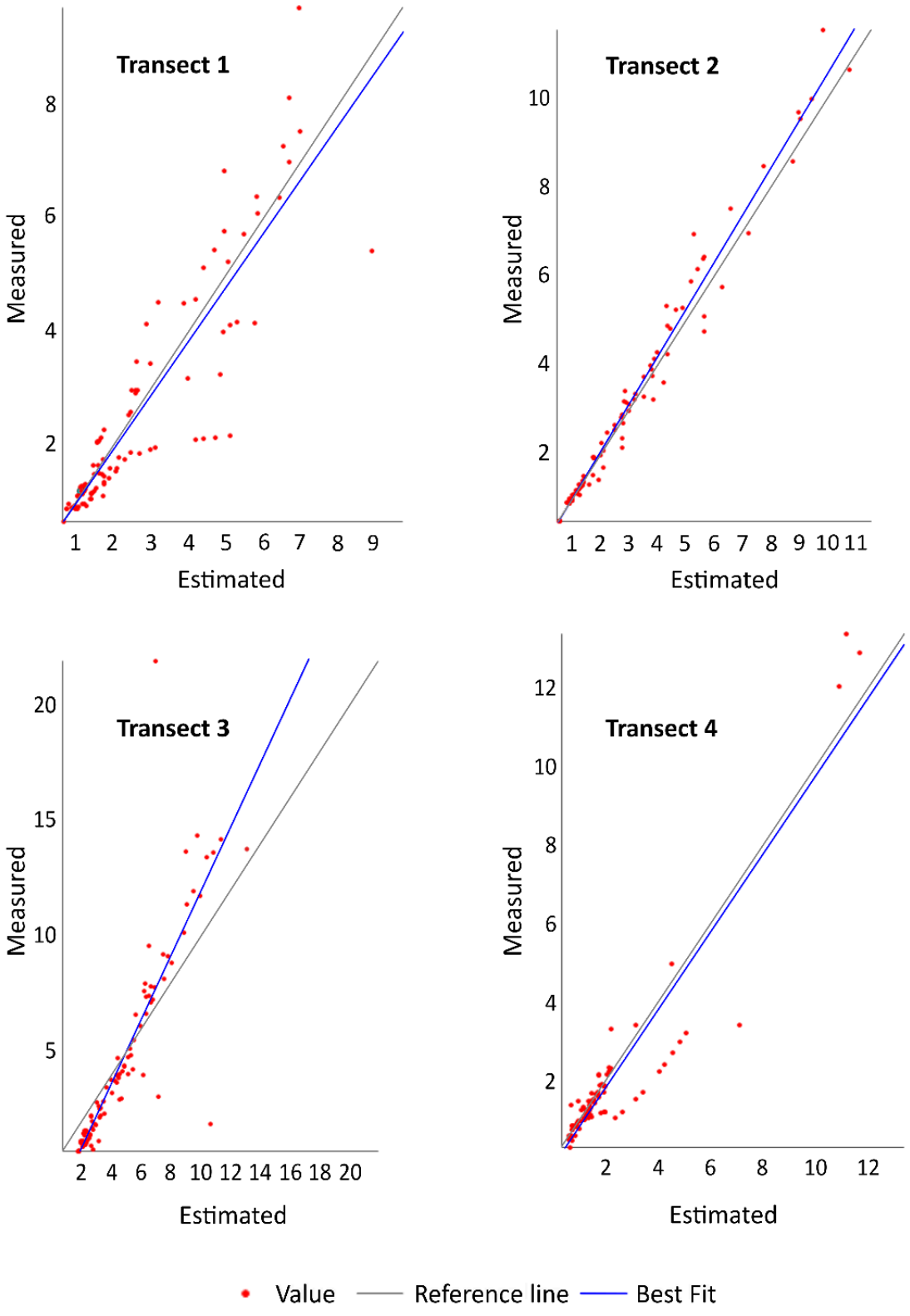

Figure 7 Relationship between measured and estimated values for vertical maps of the four latitude transects. The best fit line is regression of the data used in cross-validation. The reference line shows how close estimated values to measured values.

Table 2. Cross-validation parameters of the maps using Kriging method. Root mean square error, median absolute deviation and standard deviation are parameters of predicted error. Rank coefficient represents rank correlation between observed and predicted values.

	Root mean square error (Ωm)	Median absolute deviation (Ωm)	Standard deviation (Ωm)	Rank coefficient
Vertical maps				
Transect 1	0.88	0.34	0.88	0.94
Transect 2	0.41	0.12	0.40	0.99
Transect 3	2.23	0.49	2.24	0.93
Transect 4	0.73	0.12	0.72	0.90
Spatial maps at different depths				
1 m	20.35	2.85	17.98	0.24
2 m	15.30	2.34	15.47	0.32
5 m	3.12	0.76	3.15	0.23
10 m	1.32	0.38	1.34	0.21
15 m	0.47	0.27	0.47	0.09
20 m	0.90	0.43	0.91	-0.01
25 m	1.86	0.75	1.88	0.15
30 m	2.68	1.18	2.71	0.37
35 m	3.09	1.89	3.13	0.45

DISCUSSION

For the first time, a comprehensive ERT measurement campaign was conducted to map saline groundwater beneath agricultural land during the dry season at the landscape scale in the VMD. The ERT served as an independent method for analyzing and evaluating the salt content in the soil profile down to a depth of 40 m. Thus, ERT covers deeper soil layers than typical geophysical methods used in agriculture, which usually penetrate soil profiles of less than 2 m depth (Banton et al., 1997; Allred et al., 2010).

The results of the exploration of near-surface aquifers using ERT in this study have shown saline water layers close to the surface of agriculturally used land (< 2 m of depth) indicating a potential threat to various agricultural cultivation systems in the VMD from saline water layers, which may rise to a few meters below the ground surface. With progressive land subsidence and expected sea level rise (Erban et al., 2014; Schmitt et al., 2017; Wassmann et al., 2019), saline groundwater shoaling is unavoidable (Corwin, 2021), which increases the risk of salinization of the top soil and, thus, the root zone.

Resistivity maps: Interpretation and reliability

The measured resistivity values near the surface of the 2D ERT profiles are highly variable, while the values at intermediate profile depth, where the saline groundwater is located, are almost uniform. Thus, in order to develop maps of the horizontal distribution of salinity of the subsurface with the purpose of studying the saline water tables from each 2D ERT profile, a set of data was extracted from each profile representing the most homogenous data density at a specific location in the profile.

When reading the resistivity map, it should be noted that low soil resistivity can also be due to fine soil texture, especially as the clay content increases, which can cause the resistivity to decrease by up to 1 Ωm (Giao et al., 2003). According to Nguyen et al. (2023a), resistivity of 5 Ωm in the shallow depths of Tra Vinh province suggest the presence of the saline water. However, the author also noted that low resistivity in this province also can be distorted by high clay content in some areas. Thus, to ensure accurate identification of saline water tables, the resistivity threshold of 3 Ωm was employed as an indicator for saline water in this study.

The significantly increased resistivity at some locations, such as around site S3 and transect 3, was most likely related to high sand content (Galazoulas et al., 2015; Nguyen et al., 2023a), which according to Nguyen et al. (2020) is due to the presence of sand dunes, resulting in remarkable resistivity variation around this area as shown in Table 1 and Figure 5. Therefore, drilling data and geological information should be obtained to gain a better understanding when using resistivity maps.

Furthermore, through the cross-validation, the spatial density of the measurement should also be considered to improve the performance of Kriging interpolation in mapping, particularly in spatial maps for the whole province (Figure 6). Specifically, for future research it is recommended to increase the number of measured data points between latitude transects, while reducing the number of data points along each latitude transect to have a better grid size, thus improving the accuracy of Kriging.

The present study provides detailed maps of the near-surface saline aquifers in Tra Vinh province in the VMD; however, the ERT measurements were mostly conducted during one dry season, from December to April, 2020-2021. According to Nguyen et al. (2021) and Tran et al. (2022), near-surface aquifers interact with the nearby rivers in the VMD and thus salinity in the near surface aquifers is likely to oscillate with seasons and tidal movements. The connection between shallow aquifers and the rivers or the sea is likely to be a source for forming the saline water wedges seen along the latitude and longitude transects in Figure 3 and 4. To assess the reliability of these wedges, it is necessary to validate it by water sampling along the transect combined with observation of wedge fluctuation used ERT for long-term period.

Long term persistent changes in salinity are likely to be most accurately reflected during the dry seasons when the freshwater availability is most limited and thus the actual extend of salinization becomes more apparent. This allows employing the monitoring proposed here mainly annually towards the end of the dry season to be able to judge the potential threat of salinity to agricultural productivity.

The link between land-use and salinity

Elaboration of subsurface resistivity maps by extracting data from 2D ERT profiles has allowed the identifying areas at high risk of salinization under rice fields. In our case study, these are delineated as double-cropped rice fields where the saline water table is likely to start at a depth of 1 m. This cropping pattern is mainly distributed along rivers or near the coast, where salinity of the shallow aquifers is directly recharged by the rivers or by tidal fluctuations from the sea (Tran et al., 2022; Nguyen et al., 2021). In addition, the double-cropped rice fields are also known to be exposed to topsoil salinity due to inappropriate irrigation (Nguyen et al., 2023b).

In general, the link between land use types and saline groundwater is unclear. The only link found was between shrimp farming and saline groundwater, which occurs at a depth of about 1 m. Rice production systems were not found to be associated with saline groundwater. Low resistivity (< 3 Ωm) is observed at 1 m depth along rivers and the coast where triple rice, double rice and also single rice fields are cultivated. Whereas, similar cropping patterns but distributed in the middle of the province have high resistivity (see Figure 6). The variation of the saline water level of the shallow aquifers is strongly influenced by the distance to the saline water sources, such as the proximity to the sea or rivers, rather than by the agricultural activities on the surface.

CONCLUSIONS

This study provides detailed information on the near-surface saline aquifers established through a sequence of 44 ERT profiles along longitude and latitude transects in Tra Vinh province in the VMD. Through the mapping exercise, we have demonstrated that the ERT approach is robust, time and cost effective for understanding patterns of subsurface salinity at the landscape scale and for delineating critical salt prone areas of the agricultural production in the VMD. The study showed that salinity from shallow aquifers is a potential risk to agricultural activities in the VMD, although no causal link between land-use types and salinity was found.

ERT has been shown to be a promising method for monitoring saltwater intrusion into shallow aquifers induced by climate change and land subsidence. However, it needs to be validated at a higher temporal resolution, since only data from two consecutive dry seasons were considered in this study. For this reason, we recommend that future studies in this direction should take into account the temporal variation of salinity in the near surface aquifers in the longer term.

In conclusion, the study has shown that ERT is a suitable method to monitor near-surface aquifers for salt intrusion on a regular and long-term basis with little effort.

REFERENCES

Abd-Elaty, I., Kushwaha, N.L., Grismer, M.E., Elbeltagi, A., Kuriqi, A. (2022). Cost-effective management measures for coastal aquifers affected by saltwater intrusion and climate change. Science of the Total Environment 836, Article number 155656. https://doi.org/10.1016/j.scitotenv.2022.155656

Allred, B., Daniels, J.J., Ehsani, M.R. (Eds.). (2008). Handbook of Agricultural Geophysics (1st ed.). CRC Press. https://doi.org/10.1201/9781420019353

Allred, B.J., Freeland, R.S., Farahani, H.J., Collins, M.E. (2010). Agricultural Geophysics: Past, Present, and Future. Proceedings of the Symposium on the Application of Geophysics to Engineering and Environmental Problems, SAGEEP 1, 190-202. https://doi.org/10.4133/1.3445432

Araya Vargas, J., Gil, P.M., Meza, F.J., Yáñez, G., Menanno, G., García-Gutiérrez, V., Luque, A.J., Poblete, F., Figueroa, R., Maringue, J., Pérez-Estay, N., Sanhueza, J. (2021). Soil electrical resistivity monitoring as a practical tool for evaluating irrigation systems efficiency at the orchard scale: a case study in a vineyard in Central Chile. Irrigation Science 39, 123-143. https://doi.org/10.1007/s00271-020-00708-w

Banton, O., Cimon., M.A., Seguin, M.K. (1997). Mapping field-scale physical properties of soil with electrical resistivity. Soil Science Society of America Journal 61(4), 1010-1017. https://doi.org/10.2136/sssaj1997.03615995006100040003x

Bauer, P., Supper, R., Zimmermann, S., Kinzelbach, W. (2006). Geoelectrical imaging of groundwater salinization in the Okavango Delta, Botswana. Journal of Applied Geophysics 60 (2), 126-141. https://doi.org/10.1016/j.jappgeo.2006.01.003

Ceuppens, J., Wopereis, M. C. S., Miézan, K. M. (1997). Soil salinization processes in rice irrigation schemes in the Senegal River Delta. Soil Science Society of America Journal 61(4), 1122-1130. https://doi.org/10.2136/sssaj1997.03615995006100040019x

Cimpoiaşu, M.O., Kuras, O., Pridmore, T., Mooney, S.J. (2020). Potential of geoelectrical methods to monitor root zone processes and structure: A review. Geoderma 365, 114232. https://doi.org/10.1016/j.geoderma.2020.114232

Corwin, D.L. (2021). Climate change impacts on soil salinity in agricultural areas. European Journal of Soil Science 72(2), 842-862. https://doi.org/10.1111/ejss.13010

de Franco, R., Biella, G., Tosi, L., Teatini, P., Lozej, A., Chiozzotto, B., Giada, M., Rizzetto, F., Claude, C., Mayer, A., Bassan, V., Gasparetto-Stori, G. (2009). Monitoring the saltwater intrusion by time lapse electrical resistivity tomography: The Chioggia test site (Venice Lagoon, Italy). Journal of Applied Geophysics 69, 117-130. https://doi.org/10.1016/j.jappgeo.2009.08.004

Erban, L.E., Gorelick, S.M., Zebker, H.A. (2014). Groundwater extraction, land subsidence, and sea-level rise in the Mekong Delta, Vietnam. Environmental Research Letters 9(8), Article number 084010. https://doi.org/10.1088/1748-9326/9/8/084010

ESRI. Performing cross-validation and validation. https://desktop.arcgis.com/en/arcmap/latest/extensions/geostatistical-analyst/performing-cross-validation-and-validation.htm. Assessed June 01, 2023.

FAO. https://www.fao.org/sustainability/news/detail/es/c/1275817/

Galazoulas, E.C., Mertzanides, Y.C., Petalas, C.P., Kargiotis, E.K. (2015). Large Scale Electrical Resistivity Tomography Survey Correlated to Hydrogeological Data for Mapping Groundwater Salinization: A Case Study from a Multilayered Coastal Aquifer in Rhodope, Northeastern Greece. Environmental Processes 2, 19-35. https://doi.org/10.1007/s40710-015-0061-y

Giao, P.H., Chung, S.G., Kim, D.Y., Tanaka, H. (2003). Electric imaging and laboratory resistivity testing for geotechnical investigation of Pusan clay deposits. Journal of Applied Geophysics 52, 157-175. https://doi.org/10.1016/S0926-9851(03)00002-8

Golden Software, LLC. PO Box 281. Golden, CO 80402-0281 USA. www.goldensoftware.com

Grünenbaum, N., Günther, T., Greskowiak, J., Vienken, T., Müller-Petke, M., Massmann, G. (2023). Salinity distribution in the subterranean estuary of a meso-tidal high-energy beach characterized by Electrical Resistivity Tomography and direct push

technology. Journal of Hydrology 617, 129074. https://doi.org/10.1016/j.jhydrol.2023.129074

Hoover, D.J., Odigie, K.O., Swarzenski, P.W., Barnard, P. (2017). Sea-level rise and coastal groundwater inundation and shoaling at select sites in California, USA. Journal of Hydrology: Regional Studies 11, 234-249. https://doi.org/10.1016/j.ejrh.2015.12.055

Hui, T.R., Park, E., Loc, H.H., Tien, P.D. (2022). Long-term hydrological alterations and the agricultural landscapes in the Mekong Delta: Insights from remote sensing and national statistics. Environmental Challenges 7, 100454. https://doi.org/10.1016/j.envc.2022.100454

Kang, H., Sridhar, V., Mainuddin, M., Trung, L.D. (2021). Future rice farming threatened by drought in the Lower Mekong Basin. Scientific Reports 11, 9383. https://doi.org/10.1038/s41598-021-88405-2

Loke, M.H., (2021) Tutorial: 2-D and 3-D Electrical Imaging Surveys, accessed 17 August 2022, https://www.researchgate.net/publication/264739285_Tutorial_2-D_and_3-D_Electrical_Imaging_Surveys

Mansaray, L., Huang, W., Zhang, D., Huang, J., Li, J. (2017). Mapping rice fields in urban Shanghai, Southeast China, using Sentinel-1A and Landsat 8 datasets. Remote Sensing 9(3), 257. https://doi.org/10.3390/rs9030257

Mastrocicco, M., Gervasio, M.P., Busico, G., Colombani, N. (2021). Natural and anthropogenic factors driving groundwater resources salinization for agriculture use in the Campania plains (Southern Italy). Science of the Total Environment 758, Article number https://doi.org/144033. 10.1016/j.scitotenv.2020.144033

Minderhoud, P.S.J., Coumou, L., Erkens, G., Middelkoop, H., Stouthamer, E. (2019). Mekong delta much lower than previously assumed in sea-level rise impact assessments. Nature Communications 10, art. no. 3847. https://doi.org/10.1038/s41467-019-11602-1

Nguyen, K.A., Liou, Y.A., Tran, H.P., Hoang, P.P., Nguyen, T.H. (2020). Soil salinity assessment by using near-infrared channel and Vegetation Soil Salinity Index derived from Landsat 8 OLI data: a case study in the Tra Vinh province, Mekong

Delta, Vietnam. Progress in Earth and Planetary Science 7, Article 1. https://doi.org/10.1186/s40645-019-0311-0

Nguyen, L.D., Nguyen, T.V.K., Nguyen, D.V., Tran, A.T., Nguyen, H.T., Heidbüchel, I., Merz, B., Apel, H. (2021). Groundwater dynamics in the Vietnamese Mekong Delta: Trends, memory effects, and response times. Journal of Hydrology: Regional Studies 33, 100746. https://doi.org/10.1016/j.ejrh.2020.100746

Nguyen, T.G., Tran, N.A., Vu, P.L., Nguyen, Q.H., Nguyen, H.D., Bui, Q.T. (2021). Salinity intrusion prediction using remote sensing and machine learning in data-limited regions: A case study in Vietnam's Mekong Delta. Geoderma Regional 27, Article e00424. https://doi.org/10.1016/j.geodrs.2021.e00424

Nguyen, V.H., Germer, J., Duong, N.V., Asch, F. (2023a). Soil resistivity measurements to evaluate subsoil salinity in rice production systems in the Vietnam Mekong Delta. Near Surface Geophysics. https://doi.org/10.1002/nsg.12260

Nguyen, V.H., Germer, J., Asch, F. (2023b). Evaluating topsoil salinity via geophysical methods in rice production systems in the Vietnam Mekong Delta. Journal of Agronomy and Crop Science (submitted).

Park, E., Loc, H.H., Van Binh, D., Kantoush, S. (2022). The worst 2020 saline water intrusion disaster of the past century in the Mekong Delta: Impacts, causes, and management implications. Ambio 51, 691–699. https://doi.org/10.1007/s13280-021-01577-z

Pauw, P., De Louw, P.G.B., Oude Essink, G.H.P. (2012). Groundwater salinisation in the Wadden Sea area of the Netherlands: Quantifying the effects of climate change, sea-level rise and anthropogenic interferences. Geologie en Mijnbouw/Netherlands Journal of Geosciences 91(3), 373-383. https://doi.org/10.1017/S0016774600000500

Rao, S., Lesparre, N., Flores-Orozco, A., Wagner, F., Kemna, A., Javaux, M. (2020). Imaging plant responses to water deficit using electrical resistivity tomography. Plant and Soil 454, 261-281. https://doi.org/10.1007/s11104-020-04653-7

Samouëlian, A., Cousin, I., Tabbagh, A., Bruand, A., Richard, G. (2005). Electrical resistivity survey in soil science: A review. Soil and Tillage Research 83, 173-193. https://doi.org/10.1016/j.still.2004.10.004

Schmitt, R.J.P., Rubin, Z., Kondolf, G.M. (2017). Losing ground - scenarios of land loss as consequence of shifting sediment budgets in the Mekong Delta. Geomorphology 294, 58-69. https://doi.org/10.1016/j.geomorph.2017.04.029

Schneider, P., Asch, F. (2020). Rice production and food security in Asian Mega deltas - A review on characteristics, vulnerabilities and agricultural adaptation options to cope with climate change. Journal of Agronomy and Crop Science 206, 491-503. https://doi.org/10.1111/jac.12415

Seladji, S., Cosenza, P., Tabbagh, A., Ranger, J., Richard, G. (2010). The effect of compaction on soil electrical resistivity: a laboratory investigation. European Journal of Soil Science 61(6), 1043-1055. https://doi.org/10.1111/j.1365-2389.2010.01309.x

SNAP - ESA Sentinel Application Platform, http://step.esa.int

Setiawan, I., Morgan, L., Doscher, C., Ng, K., Bosserelle, A. (2022). Mapping shallow groundwater salinity in a coastal urban setting to assess exposure of municipal assets. Journal of Hydrology: Regional Studies 40, 1-22. https://doi.org/10.1016/j.ejrh.2022.100999

Sharan, A., Lal, A., Datta, B. (2023). Evaluating the impacts of climate change and water over-abstraction on groundwater resources in Pacific island country of Tonga. Groundwater for Sustainable Development 20, 100890. https://doi.org/10.1016/j.gsd.2022.100890

Tran, D.A., Tsujimura, M., Pham, H.V., Nguyen, T.V., Ho, L.H., Le Vo, P., Ha, K.Q., Dang, T.D., Van Binh, D., Doan, Q.V. (2022). Intensified salinity intrusion in coastal aquifers due to groundwater over extraction: a case study in the Mekong Delta, Vietnam. Environmental Science and Pollution Research 29, 8996-9010. https:// doi.org/10.1007/s11356-021-16282-3

Tran, D.D, Dang, M.M., Duong, B.D., Sea, W., Vo, T.T. (2021). Livelihood vulnerability and adaptability of coastal communities to extreme drought and salinity intrusion in

the Vietnamese Mekong Delta. International Journal of Disaster Risk Reduction 57, 102183. https://doi.org/10.1016/j.ijdrr.2021.102183

Tran, P.H. (2020). Assessment of changes in the structure land use in Tra Vinh Province under the scenarios of climate change and sea level rise. Vietnam Journal of Science and Technology 58(1), 70-83. https://doi.org/10.15625/2525-2518/58/1/13982

Wassmann, R., Ngo, D.P., Tran, Q.T., Chu, T.H., Nguyen, H.K., Nguyen, X.H., Vo, T.B.T., To, P.T. (2019). High-resolution mapping of flood and salinity risks for rice production in the Vietnamese Mekong Delta. Field Crops Research 236, 111-120. https://doi.org/10.1016/j.fcr.2019.03.007

Zohdy, A.A.R., Martin, P.M., Bisdorf, R. J. (1993). A study of seawater intrusion using direct-current soundings in the southeastern part of the Oxnard Plain, California. Vol. 93. US Geological Survey. https://doi.org/10.3133/ofr93524

Chapter 5

General Discussion

5.1. Geo-physics investigation and soil salinity of agricultural land

In order to capture the variation in soil salinity, the Electro Magnetic Induction (EMI) and Electrical Resistivity Tomography (ERT) were integrated in a comprehensive approach. EMI was identified as a better choice than ERT for investigating topsoil salinity above 1 m depth. ERT, on the other hand, was found to be a powerful tool for providing detailed information on soil salinity in deeper soil layers. By combining these two tools, the variation in soil salinity over large areas of agricultural land was assessed in a case study in the VMD. In this study, we used the conductivity threshold of more than 4.5 mScm-1 as an indicator of topsoil salinity as suggested by FAO (2022). In the meantime, through validation with drilling data in Chapter 2, a resistivity of less than 3 Ωm is considered the threshold for saline water. This is consistent with previous studies that have shown that the threshold for saline water in the soil varies from <1 to 6 Ωm (Hodlur et al., 2006; Galazoulas et al., 2015).

It should be noted, however, that there are some technical issues that need to be taken into account when using this approach, including:

- Factors affecting geophysical results: Besides salt contamination in soil, soil properties also have an effect on the results of geophysical methods, such as soil type and soil moisture content (Samouëlian et al., 2005). In particular, clay content can also be mistaken with resistivity of less than 3 Ωm. Clay soil was shown to have low resistivity; however, it depends on types of clay that its resistivity can vary between 1 and 3 Ωm for Pusan clays in the coastal area of Korea (Giao et al., 2003) or in a wider range from 1 to 100 Ωm (Palacky et al., 1987; Galazoulas et al., 2015). Therefore, reference data such as present borehole data or geological information of the research area should be obtained in order to fully understand the results of geophysical methods.

- Interpretation of soil salinity maps produced by geophysical methods: The resistivity map can be used to interpret soil salinity by using a resistivity of less than 3 Ωm as an indication of soil salinity. According to the validation of ERT maps in Chapter 2, the low resistivity was found in the triple rice field, which was also observed in Chapter 4. Thus, in addition to soil type and geological information, it is important to know regional factors such as land use history of the study area to improve the interpretation of resistivity maps.

In general, there is no significant topsoil salinization in rice production systems in the VMD. Above all, the double-cropped rice fields were the only rice cultivation that tended to be slightly saline as classified by FAO (2022) with EC mainly higher than 3 $mScm^{-1}$. The slight salinity of the topsoil of double-cropped rice fields was probably caused by inappropriate irrigation with saline water, as it was mainly distributed in areas adjacent to the coast and canals. The single-cropped rice fields are also cultivated in the vicinity of the canals, but these fields are normally rainfed fields, where rice is only cultivated during the rainy season (Sakamoto et al., 2006; Chen et al., 2011), and therefore no salinity was observed in the topsoil.

In contrast to the topsoil, the shallow aquifer under the rice fields was found to be dominated by saline water at the relatively shallow depth of less than 2 m. According to Yang et al. (2011), this is a critical water table depth where saline water can move up to the root zone and accumulate salt in the topsoil, causing yield loss and affecting plant growth (Befus et al., 2020). Schneider and Asch (2020) argued that in the non-flooded state, such as with water saving techniques, saltwater has a higher chance of rising to the topsoil, while in the flooded state capillary rise from groundwater is not significant. However, the saline water table may become shallower than at present and the upwelling of saltwater to the topsoil may be exacerbated, especially in the double rice or single rice-cropped fields, in the context of ongoing sea level rise combined with severe land subsidence (Schmitt et al., 2017; Wassmann et al., 2019) and frequent droughts in the dry season (Phan et al., 2020).

5.2. Effects of land-use to soil salinity

This study attempted to establish the relationship between land-use based on rice production systems and salinity, and to investigate whether cropping types affect soil salinity by mapping topsoil salinity and near-surface saline groundwater. Ultimately, however, no clear relationship was found between land-use based rice production systems, including triple rice, double rice, triple/double rice and single rice, and soil salinity. It seems that double-cropped rice fields are most susceptible to saltwater intrusion, either from the topsoil or from the subsoil due to their proximity to saltwater sources. Thus, it can be argued that the salinity of the soil determines the types of cropping cycles associated with the rice production systems.

Recently, crop rotation has been introduced as an alternative to intensive monoculture rice in the VMD to improve soil quality (Tran et al., 2014) and to alleviate climate change induced sea level rise (Schneider and Asch, 2020). Rice-upland or rice-aquaculture has been proposed to replace the intensive monoculture rice with low yields, which are usually distributed in the saline water affected areas (Smajgl et al., 2015). Rice-upland rotation was found to improve soil quality (Tran et al., 2014), whereas rice-aquaculture rotation has been associated with salinization of the soil (Ali et al., 2006). After a period of time, rice-aquaculture rotation fields will be permanently converted to shrimp farms due to the increase of salt contamination in the soil (Loc et al., 2021). Increasing income will accelerate the conversion from intensive rice to rice aquaculture or even shrimp (Hoanh et al., 2014), and thus this type of land-use will affect soil salinity in the near future.

5.3. Outlook for the monitoring of soil salinization

In this section, I discuss several remaining issues that would need to be addressed in order to gain full insight into soil salinity management in agricultural areas, such as in rice production systems in the VMD.

Assessing soil salinity through geophysical methods can provide valuable information about the spatial distribution and severity of salinity in an area, and understand the extent of the situation help to select appropriate management practices for sustainable agriculture. However, in relation to subsurface salinity, in order to improve the quality of soil maps, the arrangement of ERT profiles should be carefully considered prior to field measurement to

obtain a better grid size, such as increasing the number of ERT profiles. In addition to increasing the number of geophysical measurements, their combination with methods based on remote sensing can be an alternative option to obtain a more comprehensive map of soil salinity in a short period of time, especially for topsoil salinity studies.

With regard to topsoil salinity, Hardie and Doyle (2012) suggested that it should be measured and observed in a repeatable manner to assess topsoil salinity variability in areas close to saltwater sources and more susceptible to salinity from irrigation, which in this study are double rice and single rice fields.

For subsoil salinity, the interaction of the near surface groundwater with the nearby rivers, may have caused the salinity of the shallow groundwater (Nguyen et al., 2021, Tran et al., 2022) oscillating with seasonal and tidal fluctuations. Therefore, long term persistent changes in salinity are likely to be most accurately reflected during the dry seasons when the freshwater availability is most limited and thus the actual extend of salinization becomes more apparent. Thus, the monitoring proposed here should be conducted annually towards the end of the dry season as a means to judge the potential threat of salinity to agricultural productivity.

REFERENCES

Acosta, J.A., Faz, A., Jansen, B., Kalbitz, K., Martínez-Martínez, S. (2011). Assessment of salinity status in intensively cultivated soils under semiarid climate, Murcia, SE Spain. *Journal of Arid Environments* 75(11), 1056-1066. https://doi.org/10.1016/j.jaridenv.2011.05.006

Ali, A.M.S. (2006). Rice to shrimp: Land use/land cover changes and soil degradation in Southwestern Bangladesh. *Land Use Policy* 23(4), 421-435. https://doi.org/10.1016/j.landusepol.2005.02.001

Befus, K.M., Barnard, P.L., Hoover, D.J., Finzi Hart, J.A., Voss, C.I. (2020). Increasing threat of coastal groundwater hazards from sea-level rise in California. *Nature Climate Change* 10, 946-952. https://doi.org/10.1038/s41558-020-0874-1

Chen, C., Nguyen, T.S., Chang, L., Chen, C. (2011). Monitoring of soil moisture variability in relation to rice cropping systems in the Vietnamese Mekong Delta using MODIS data. *Applied Geography* 31(2), 463-475. https://doi.org/10.1016/j.apgeog.2010.10.002

Darwish, T., Atallah, T., Moujabber, M.E., Khatib. N. (2005). Salinity evolution and crop response to secondary soil salinity in two agro-climatic zones in Lebanon. *Agricultural Water Management* 78(1-2), 152-164. https://doi.org/10.1016/j.agwat.2005.04.020

Flaherty, M., Vandergeest, P., Miller, P. (1999). Rice paddy or shrimp pond: Tough decisions in rural Thailand. World Development 27(12), 2045-2060. https://doi.org/10.1016/S0305-750X(99)00100-X

FAO, Food and Agriculture Organization of the United Nations. (2022). Saline soils and their management, accessed 24 November 2022. https://www.fao.org/3/x5871e/x5871e04.htm.

Galazoulas, E.C., Mertzanides, Y.C., Petalas, C.P., Kargiotis, E.K. (2015). Large Scale Electrical Resistivity Tomography Survey Correlated to Hydrogeological Data for Mapping Groundwater Salinization: A Case Study from a Multilayered Coastal Aquifer in Rhodope, Northeastern Greece. *Environmental Processes* 2, 19-35. https://doi.org/10.1007/s40710-015-0061-y

Giao, P.H., Chung, S.G., Kim, D.Y., Tanaka, H. (2003). Electric imaging and laboratory resistivity testing for geotechnical investigation of Pusan clay deposits. *Journal of Applied Geophysics* 52, 157-175. https://doi.org/10.1016/S0926-9851(03)00002-8

Hardie, M., Doyle, R.B. (2012). Measuring soil salinity. Methods in molecular biology (Clifton, N.J.) 913:415-25. https://doi.org/10.1007/978-1-61779-986-0_28

Hoanh, C.T., Suhardiman, D., Anh, L.T. (2014). Irrigation development in the Vietnamese Mekong Delta: Towards polycentric water governance? *International Journal of Water Governance* 2, 61–82. https://doi.org/10.7564/14-IJWG59

Hodlur, G., Dhakate, R., Andrade, R. (2006). Correlation of vertical electrical sounding and borehole-log data for delineation of saltwater and freshwater aquifers. Geophysics 71(1). https://doi.org/10.1190/1.2169847

Kotb, T.H.S., Watanabe, T., Ogino, Y., Tanji, K.K. (2000). Soil salinization in the Nile Delta and related policy issues in Egypt. *Agricultural water management* 43(2). https://doi.org/10.1016/S0378-3774(99)00052-9

Loc, H.H., Lixian, M.L., Park, E., Dung, T.D., Shrestha, S., Yoon, Y. (2021). How the saline water intrusion has reshaped the agricultural landscape of the Vietnamese Mekong Delta, a review. *Science of The Total Environment* 794, 148651. https://doi.org/10.1016/j.scitotenv.2021.148651

Nguyen, L.D., Nguyen, T.V.K., Nguyen, D.V., Tran, A.T., Nguyen, H.T., Heidbüchel, I., Merz, B., Apel, H. (2021). Groundwater dynamics in the Vietnamese Mekong Delta: Trends, memory effects, and response times. *Journal of Hydrology: Regional Studies* 33, 100746. https://doi.org/10.1016/j.ejrh.2020.100746

Palacky, G.J. (1987). Resistivity characteristics of geologic targets. *Electromagnetic Methods in Applied Geophysics* 1, 53-129. https://doi.org/10.1190/1.9781560802631.ch3

Phan, V.H., Dinh, V.T., Su, Z. (2020). Trends in Long-Term Drought Changes in the Mekong River Delta of Vietnam. *Remote sensing* 12(18). https://doi.org/10.3390/rs12182974

Sakamoto, T., Nguyen, N., V., Ohno, H., Ishitsuka, N., Yokozawa, M. (2006). Spatio-temporal distribution of rice phenology and cropping systems in the Mekong Delta

with special reference to the seasonal water flow of the Mekong and Bassac rivers. *Remote Sensing and Environment* 100(1), 1-16. https://doi.org/10.1016/j.rse.2005.09.007

Samouëlian, A., Cousin, I., Tabbagh, A., Bruand, A., Richard, G., (2005) Electrical resistivity survey in soil science: A review. *Soil and Tillage Research* 83, 173-193. https://doi.org/10.1016/j.still.2004.10.004

Schmitt, R.J.P., Rubin, Z., Kondolf, G.M. (2017). Losing ground - scenarios of land loss as consequence of shifting sediment budgets in the Mekong Delta. *Geomorphology* 294, 58-69. https://doi.org/10.1016/j.geomorph.2017.04.029

Schneider, P., Asch, F. (2020). Rice production and food security in Asian Mega deltas - A review on characteristics, vulnerabilities and agricultural adaptation options to cope with climate change. *Journal of Agronomy and Crop Science* 206, 491-503. https://doi.org/10.1111/jac.12415

Smajgl, A., Toan, T.Q., Nhan, D.K., Ward, J., Trung, N.H., Tri, L.Q., Vu, P.T. (2015). Responding to rising sea levels in the Mekong Delta. *Nature Climate Change* 5(2), 167– 174. https://doi.org/10.1038/nclimate2469

Tran, D.A., Tsujimura, M., Pham, H.V., Nguyen, T.V., Ho, L.H., Le Vo, P., Ha, K.Q., Dang, T.D., Van Binh, D., Doan, Q.V. (2022). Intensified salinity intrusion in coastal aquifers due to groundwater over extraction: a case study in the Mekong Delta, Vietnam. *Environmental Science and Pollution Research* 29, 8996-9010. https:// doi.org/10.1007/s11356-021-16282-3

Tran, L.B., Le, V.K., Elsacker, S.V., Cornelis, W.M. (2014). Effect of cropping system on physical properties of clay soil under intensive rice cultivation. *Land Degradation and Development* 27, 973-982. https://doi.org/10.1002/ldr.2321

Truong, Q.C., Nguyen, T.H., Tatsumi, K., Pham, V.T., Tri, V.P.D. (2022). A land-use change model to support land-use planning in the Mekong Delta (MEKOLUC). *Land* 11(2), 297. https://doi.org/10.3390/land11020297

Wassmann, R., Ngo, D.P., Tran, Q.T., Chu, T.H., Nguyen, H.K., Nguyen, X.H., Vo, T.B.T., To, P.T. (2019). High-resolution mapping of flood and salinity risks for rice

production in the Vietnamese Mekong Delta. *Field Crops Research* 236, 111-120. https://doi.org/10.1016/j.fcr.2019.03.007

Yang, F, Zhang, G., Yin, X., Liu, Z., Huang, Z. (2011). Study on capillary rise from shallow groundwater and critical water table depth of a saline-sodic soil in western Songnen plain of China. *Environmental Earth Sciences* 64, 2119–2126. https://doi.org/10.1007/s12665-011-1038-4

Yu, J., Li, Y., Han, G., Zhou, D., Fu, Y., Guan, B., Wang, G., Ning, K., Wu, H., Wang., J. (2014). The spatial distribution characteristics of soil salinity in coastal zone of the Yellow River Delta. *Environmental Earth Sciences* 72, 589–599. https://doi.org/10.1007/s12665-013-2980-0

Yu, J., Li, Y., Han, G., Zhou, D., Fu, Y., Guan, B., Wang, G., Ning, K., Wu, H., Wang, J. (2014). The spatial distribution characteristics of soil salinity in coastal zone of the Yellow River Delta. *Environmental Earth Sciences* 72, 589–599. https://doi.org/10.1007/s12665-013-2980-0

Chapter 6

General conclusions

In this study, geophysical methods, including ERT and EMI, were used for the first time to map soil salinity and in the effort to understand the relationship between salinity and rice farming systems in the VMD. The integration of these two methods was used to identify the potential salinity risk areas, where EMI was found to be a fast and robust tool for investigating the horizontal distribution of topsoil salinity at the scale of agricultural fields, while ERT was proved to be a powerful tool for detecting and mapping the vertical layers of near-surface aquifers under the rice fields. The proposed approach has been shown to be a promising method for mapping soil salinity at an agricultural or even landscape scale.

In addition, this approach opens up a potential tool for regular monitoring of soil salinity to assess the impact of saltwater intrusion on agricultural land. From a management perspective, it is a perfect tool due to its effectiveness in terms of time, labor and cost.

There is no clear relationship was observed between soil salinity and rice production systems; however, the attention for double-cropped rice crops must be taken into account. Compared to other rice crops, double-cropped rice fields are more likely affected by saltwater intrusion, resulting in high topsoil salinity. Therefore, in order to avoid inappropriate irrigation with saline water from rivers, a more careful water management is needed for this type of cultivation. In addition to the salinization of the topsoil, the double-cropped rice fields are also at higher risk of capillary rise of saline water from the near-surface aquifers than the triple-cropped rice fields due to the fallow period during the dry season and their proximity to the saline water sources. As the sea level continues to rise due to climate change and land subsidence, the swelling of the saline water table to the topsoil is likely to increase. Therefore, it is highly advisable that regular and temporal monitoring of the saline water table should be carried out to avoid salinization of the soil. This will contribute to sustainable agricultural development.